People's Democratic Republic of Algeria

Ministry of Higher Education and Scientific Research

University of El Oued

Faculty of Technology

Department of Hydraulic and Civil Engineering

Course

Hydration and structuring of cement paste

Intended for first-year Master's students in civil engineering

Option: Civil engineering materials

Developed by:

DJEDID Tarek

Doctor of Civil Engineering

Academic year : 2025-2026

Abstract :

This course provides a comprehensive overview of the physico-chemical mechanisms governing the hydration and microstructure of Portland cement pastes. It begins with clinker mineral formation, detailing the four main anhydrous phases (C_3S alite 45–65 %, C_2S belite 15–35 %, C_3A 4–14 %, C_4AF 10–18 %), their chemical composition via oxide analysis and Bogue calculations or X-ray diffraction, and the role of gypsum in controlling setting. The hydrated paste microstructure is then examined, highlighting dominant solid phases—C-S-H gel (50–60 % volume), portlandite (20–25 %), sulfoaluminates, and residual clinker—alongside voids (interlayer/gel pores, capillary pores 10 nm–5 µm, air voids) and four water types (capillary, adsorbed, interstitial, chemically bound). Hydration proceeds in four stages (initial dissolution, dormancy, acceleration with portlandite/C-S-H formation, slowdown via diffusion), with phase-specific reactions for C_3S, C_2S, C_3A (ettringite to monosulfoaluminate via gypsum), and C_4AF, influenced by composition, fineness, W/C ratio, temperature, and admixtures. Accompanying phenomena include electrical conductivity evolution, Vicat setting times, exothermic heat release (dominated by C_3S and C_3A), and Le Châtelier chemical shrinkage leading to endogenous shrinkage and self-desiccation. Overall, the material emphasizes how these processes control strength development, rheology, and long-term durability of cementitious systems.

Résumé :

Ce cours offre un aperçu complet des mécanismes physico-chimiques qui régissent l'hydratation et la microstructure des pâtes de ciment Portland. Il commence par la formation minérale du clinker, en détaillant les quatre principales phases anhydres (alite C_3S 45–65 %, bélite C_2S 15–35 %, C_3A 4–14 %, C_4AF 10–18 %), leur composition chimique par analyse des oxydes et calculs de Bogue ou diffraction des rayons X, ainsi que le rôle du gypse dans le contrôle de la prise. La microstructure de la pâte hydratée est ensuite examinée, en mettant en évidence les phases solides dominantes — gel C-S-H (50–60 % en volume), portlandite (20–25 %), les sulfoaluminates et le clinker résiduel — ainsi que les vides (pores intercouches/du gel, pores capillaires de 10 nm à 5 µm, vides d'air) et les quatre types d'eau (capillaire, adsorbée, interstitielle, chimiquement liée). L'hydratation se déroule en quatre étapes (dissolution initiale, dormance, accélération avec formation de portlandite/C-S-H, ralentissement par diffusion), avec des réactions spécifiques à chaque phase pour le C_3S, le C_2S, le C_3A (transition de l'ettringite en monosulfoaluminate via le gypse) et le C_4AF, influencées par la composition, la finesse, le rapport E/C, la température et les adjuvants. Les phénomènes associés comprennent l'évolution de la conductivité électrique, les temps de prise Vicat, le dégagement de chaleur exothermique (dominé par le C_3S et le C_3A) et le retrait chimique de Le Châtelier conduisant à un retrait endogène et à une autodésiccation. Dans l'ensemble, cet ouvrage met en évidence la manière dont ces processus contrôlent le développement de la résistance, la rhéologie et la durabilité à long terme des systèmes cimentaires.

الملخص

تقدم هذه الدروس نظرة عامة شاملة على الآليات الفيزيائية والكيميائية التي تحكم عملية الترطيب والبنية المجهرية لمعاجين الأسمنت البورتلاندي. تبدأ الدورة بتكوين معدن الكلنكر، مع تفصيل المراحل الأربع الرئيسية غير المائية(C_3S alite 45-65٪ ، C_2S belite 15–35٪، C_3A 4–14٪، C_4AF 10–18٪)، وتركيبها الكيميائي من خلال تحليل الأكسيد وحسابات بوغ أو حيود الأشعة السينية، ودور الجبس في التحكم في التصلب. ثم يتم فحص البنية المجهرية للمعجون المائي، مع تسليط الضوء على المراحل الصلبة السائدة — هلام C-S-H (50–60٪ من الحجم)، البورتلانديت (20–25٪)، والسلفو ألومينات، والكلنكر المتبقي — إلى جانب الفراغات (مسام بين الطبقات/مسام الهلام، مسام شعرية 10 نانومتر–5 ميكرومتر، فراغات هوائية) وأربعة أنواع من الماء (شعري، ممتص، بين الخلايا، مرتبط كيميائيًا). تتم عملية الترطيب على أربع مراحل) الذوبان الأولي، السكون، التسارع مع تكوين البورتلانديت/ C-S-H ، التباطؤ عبر الانتشار، مع تفاعلات خاصة بكل مرحلة لـC_3S ، C_2S، C_3A من الإيترينجيت إلى أحادي سلفو ألومينات عبر الجبس، وC_4AF ، متأثرة بالتركيب، والنعومة، ونسبة الماء إلى الأسمنت، ودرجة الحرارة، والمواد المضافة. وتشمل الظواهر المصاحبة تطور الموصلية الكهربائية، وأوقات التصلب وفقًا لمقياس فيكا، وإطلاق الحرارة الطاردة التي يهيمن عليها C_3S وC_3A ، والانكماش الكيميائي وفقًا لمبدأ لو شاتيلييه الذي يؤدي إلى الانكماش الداخلي والتجفيف الذاتي. وبشكل عام، يركز هذا المادة على كيفية تحكم هذه العمليات في تطور القوة، وخصائص الريولوجيا، والمتانة طويلة الأمد للأنظمة الأسمنتية.

Foreword

This handout presents the module dedicated to the hydration and structuring of cement pastes, an essential field in construction materials science. It aims to provide an in-depth understanding of the physicochemical processes involved in the formation of hydrates and the development of the mechanical properties of cements and concretes.

The main objectives of this module are to enable learners to understand and explain the mechanisms of hydrate formation and structuring, as well as the origin of the mechanical strength of cements and concretes. This includes the analysis of chemical reactions, microstructural changes, and factors influencing durability.

The content is structured into six main chapters:

- Chapter 1: Formation of clinker minerals, which explores the synthesis processes of the anhydrous phases of cement.
- Chapter 2: Structure of materials, addressing the crystallographic and microstructural aspects of the components.
- Chapter 3: Hydraulicity and hydration theories, presenting the principles of water reactivity and theoretical models.
- Chapter 4: Phenomena accompanying hydration, analyzing thermal, volumetric, and rheological changes.
- Chapter 5: Origin of mechanical strength, explaining the links between microstructure and macroscopic properties.
- Chapter 6: Sophisticated analytical techniques for investigation the microstructure of cements

At the end of this document, we present comprehension questions and exercises designed to deepen understanding of hydration phenomena, a process directly linked to the durability of cementitious structures.

This module is intended for first-year master's students in civil engineering materials or professionals with prior knowledge of mineral binders, mineral chemistry, and physical chemistry, in order to facilitate the assimilation of advanced concepts.

In short, this handout is a comprehensive educational tool for mastering the fundamentals of cement hydration, promoting practical application in civil engineering and materials.

TABLE OF CONTENTS

Chapter 4: Phenomena accompanying hydration

Chapter 5: Origin of concrete's mechanical strength

Chapter 1 - Clinker mineral formation

1.1 introduction

Cement is an omnipresent material in our daily lives, often perceived as familiar due to its massive use in the manufacture of concrete, the world's most widespread building material. Its success is due to its low cost, ease of use and almost universal availability. Simply mixing cement powder with water, sand and gravel produces a solid, durable material at room temperature in just a few hours. Yet, despite the annual production of almost two billion tonnes of concrete, the physico-chemical mechanisms underlying this transformation are not yet fully elucidated and continue to be the subject of extensive research.

In what follows, we will focus primarily on the chemical aspect of these transformations, commonly referred to as hydration. Although simple, this term actually covers a complex set of physico-chemical processes governed by the fundamental laws of thermodynamics and kinetics. The complexity of cement hydration lies not in the nature of the elementary reactions, often well described for other materials, but in the very nature of the cement paste. Indeed:

Cement is a multiphase material, with each constituent phase reacting separately;

Reactions take place in a small, confined volume of aqueous solution;

The hydrated phases formed are often difficult to characterize due to their amorphous or nanocrystalline structure;

The hydration of each phase modifies the composition of the solution, thus influencing the reactions of the other phases.

To understand this complexity, a common approach is to study each of the cement's constituent phases separately. This is the method we adopt in this chapter, in order to better understand the individual mechanisms before considering their interaction within the overall system.

1.2 .Portland cement composition

The constituent phases of cement are mainly oxides, designated by an abbreviated notation based on the oxidized element: C for CaO (lime), A for Al_2O_3 (alumina), S for SiO_2 (silica) and H for H_2O (water). Portland cement is an anhydrous material composed essentially of calcium silicates and aluminates. It is obtained by combining lime (CaO), silica (SiO_2), alumina (Al_2O_3) and iron oxide (Fe_2O_3). Lime is generally supplied by carbonate rocks, while the other components come from clays. In the presence of water, these anhydrous phases react by hydration, a process that involves the dissolution of anhydrous compounds followed by the precipitation of hydrates, either crystallized or amorphous. These reactions give cement its mechanical properties and make it an effective hydraulic binder.

Clinker, an intermediate product in cement manufacture, is obtained by firing at over 1400°C an intimate mixture of limestone and clays (in a ratio of around 80/20%), sometimes enriched with pyrite or bauxite ash to adjust the iron content. After firing, clinker is rapidly cooled (quenching), freezing metastable mineral species. It is composed of four main phases:

Alite (C_3S): tricalcium silicate ($3CaO\text{-}SiO_2$), responsible for the cement's initial strength.

Belite (C_2S): Dicalcium silicate ($2CaO\text{-}SiO_2$), contributing to long-term strength.

Celite (C_3A): Tricalcium aluminate ($3CaO\text{-}Al_2O_3$), reactive but often regulated to avoid setting too quickly.

Ferrite (C_4AF): Tetracalcium ferro-aluminate ($4CaO\text{-}Al_2O_3\text{-}Fe_2O_3$), playing a role in color and resistance to chemical agents.

To control hydration kinetics, calcium sulfate (gypsum) is added at 2-4% by mass. Sulfate ions react with C_3A (and to a lesser extent with C_4AF) to form layers of primary ettringite and tricalcium sulfo-aluminate on the surface of cement grains. These low-permeability layers slow down the hydration of C_3A, thus preventing over-rapid setting. However, an excess of sulfate (in the cement or mixing water) can cause a false set, characterized by immediate solidification without development of the expected mechanical properties.

Hydration reactions are exothermic, which explains the rise in temperature observed during cement setting. This rise can vary between 40 and 60°C for standard structures, and can reach 50 to 80°C at the heart of massive structures, depending on cement formulation, part geometry and processing conditions. These thermal phenomena must be taken into account to avoid disorders such as cracking due to temperature gradients.

The duration of this thermal phase varies considerably between cement formulations (usually a few hours) and can be adjusted by adding specific additives.

For cement hydration to continue optimally, it is essential that the relative humidity of the storage environment be maintained above 75%. This is referred to as wet curing, a period during which hygrometric conditions favor continued hydration of the cement. The cure period refers to the time interval during which the cementitious material is left to rest in order to fully develop its mechanical properties and performance in the hardened state.

In standardized tests, the curing period is generally set at 28 days (four weeks), although in some cases it can be extended to three months for specific evaluations. On site, however, practical constraints often lead to this period being shortened. Cure times are then limited to the strict minimum, generally not exceeding three days. The main objective here is to avoid early dessiccation, which could compromise the quality and durability of the material. It is therefore crucial to balance these considerations with the operational realities and imperatives of cementitious materials use in the field.

The average chemical composition of Portland cement clinker is shown in Table 1.1. The heterogeneity of this artificial stone is shown in the figure below.

Table 1.1: Typical chemical composition of ordinary Portland cement

oxides	Content (%)
CaO	60-67
SiO_2	17-25
Al_2O_3	3-8
Fe_2O_3	0.5-0.6
MgO	0.1- 4
Alkaline (N_2O,K_2O)	0.4 -1.3
SO_3	1.3-3

In addition to the main compounds listed in Table 1.1, Portland cement clinker also contains minor compounds such as MgO, TiO_2, Mn_2O_3 and K_2O, the quantity of which generally only exceeds a few percent of the cement's total mass.

Among these minor oxides, sodium oxide (Na_2O) and potassium oxide (K_2O), grouped together under the term alkalis - although other alkalis are also present in cement - are of particular importance. Indeed, they have been shown to react with certain types of aggregate, leading to concrete degradation and influencing the rate at which cement strength develops.

The term “minor” refers to their low proportion and not to their impact on cement quality.

During curing, four main minerals are formed in Portland cement, with varying contents presented in table 1.2.

Table 1.2: Typical average mineralogical composition of Portland cement clinker

Compound	Composition	Abbreviation Phase	Composition (%)
Tricalcium silicate	$3CaO.SiO_2$	C_3S	45-65
Dicalcium silicate	$2CaO.SiO_2$	C_2S	15-35
Tricalcium aluminate	$3CaO.Al_2O_3$	C_3A	4-14
Tetracalcium aluminoferrite	$4CaO.Al_2O_3.Fe_2O_3$	C_4AF	10-18

These four components can be determined either by the Bogue method or by X-ray, SEM , ATG..... as an example or a sulfate-resistant Portland cement (CRS) whose chemical composition is given below.

Table1.3: Chemical composition of cement (CRS)

Oxide	**Quantity (%)**
Al_2O_3	4,55
SiO_2	20,9
Fe_2O_3	5,03
CaO	63,69
SO_3	2,08
K_2O	0,33
Cl	0,001
Na_2O	0,18
PAF	0,7
RI	0,75
CaO Libre	0,75

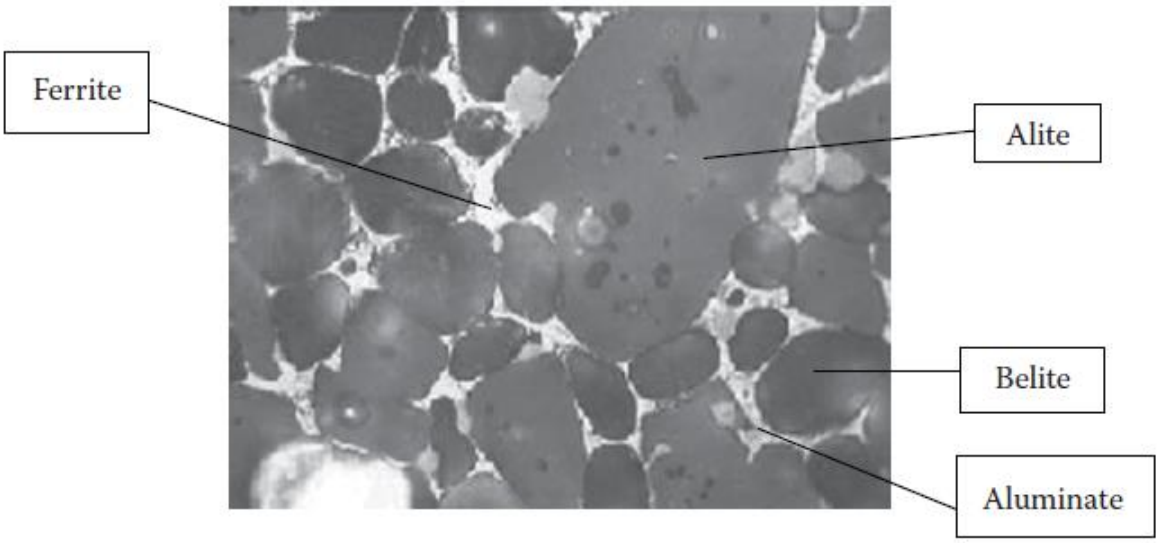

Figure 1.1: Portland cement clinker.
Reflected-light micrograph of clinker showing alite, belite, ferrite and aluminate phases.

Note: Alite occurs as subhedral (partially crystallized, with some faces well defined and others granular) to anhedral (with no distinct outer shape) crystals, around 25 µm in size.

Belite appears in large clusters, with crystals around 15 µm in size. Belite occurs in large clusters, with crystals around 15 µm in size. The interstitial constituents are ferrite, which takes the form of medium- to fine-grained laths, and aluminate, which fills the spaces between these laths. Field width: 250 µm (Adapted from Stutzman, P.E., and Leigh, S., Compositional analysis of NIST reference clinker 8486, in "Accuracy of Powder Diffraction III", Proceedings, National Institute of Standards and Technology, Poster No. 2, Gaithersburg, MD, April 22-25, 2001).

The mineralogical composition of this cement, calculated according to Bogue's formulas and using the quantitative X-ray diffraction (AQDX) technique, is as follows

1.3 Calculation of the percentage of cement minerals

1.3.1 Bogue formulas

Bogue's formulas are used to calculate the theoretical proportions of clinker phases from the oxide composition, based on the following assumptions:

-The four main phases are C_3S, C_2S, C_3A and C_4AF;

-All iron is in the form of C4AF

-Remaining Al2O3 is in the form of C3A

-Remaining CaO and SiO2 combine as C3S and C2S;

-The combination between the various constituents is complete, and the minor elements present in the clinker are not involved.

The formulas originally established by Bogue (1950) greatly overestimate the C3S content and correspondingly underestimate the C2S content.

Terms in brackets represent the percentage of different oxides in terms of total cement weight.

C3S= 4.07(CaO) - 7.60 (SiO2) - 6.72 (Al2O3) - 1.43 (Fe2O3) - 2.85 (SO3)

C2S = 2.87 (SiO2) - 0.75 (3CaO.SiO2)

C3A= 2.65 (Al2O3) - 1.69 (Fe2O3)

C4AF= 3.04 (Fe2O3)

1.3.2 x-ray

The composition of cement can also be obtained using the X-ray diffraction method.

The results obtained by the two methods are shown in table (1.4). The Bogue method overestimates tricalcium silicate (C3S) and underestimates dicalcium silicate (C2S), due to the replacement of calcium oxides in tricalcium silicate.

Figure (1.2) shows the X-ray diffraction spectrum of Portland cement (Portland Cement Third edition) with the composition as follows:

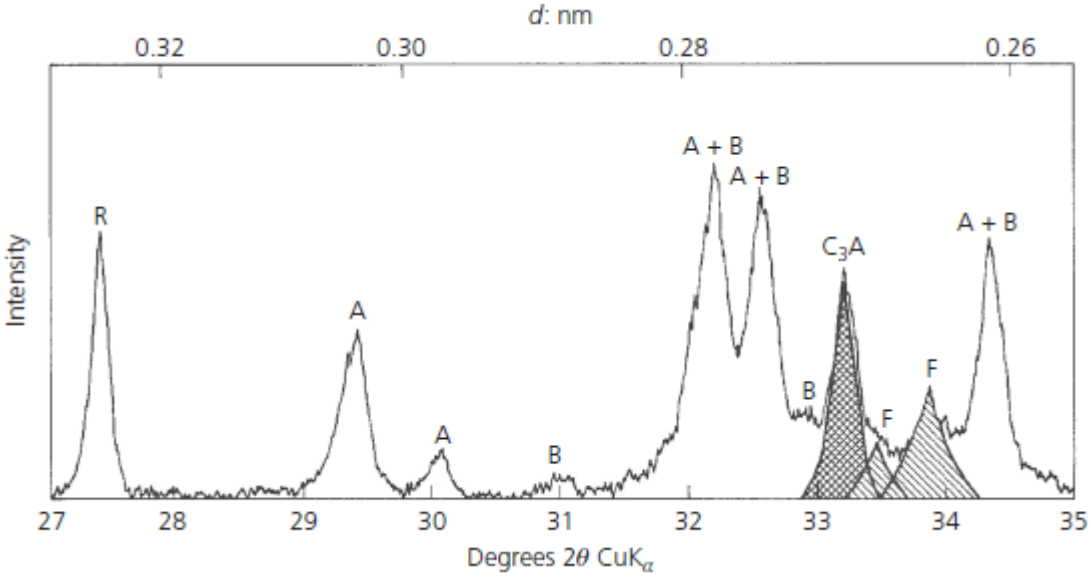

Figure(1.2) X-ray diffraction pattern of ground clinker with rutile (R) as internal standard: A - alite; B - belite; F - ferrite phase (idealized peak areas are hatched to indicate overlap)

Table (1.4) Mineralogical composition of ordinary Portland cement by Bogue and AQDX methods

Components	AQDX(%)	Bogue (%)
C_3S	52.79	61
C_2S	24.64	11
C_4AF	7.22	9
C_3A	4.16	4
$CaSO_4$	1.31	-

Chapter 2: Material structure

2.1 Microstructure of hydrated cement paste

The term "hydrated cement paste" pertains to pastes created from Portland cement, typically composed of anhydrous Portland cement powder made of various compounds. The powder consists of angular particles ranging in size from 1 to 50 µm, produced by grinding clinker mixed with a small amount of calcium sulfate. Clinker is a heterogeneous mixture of compounds resulting from high-temperature reactions involving calcium oxide, silica, alumina, and iron oxide. The primary compounds found in clinker are represented by the chemical formulas C3S, C2S, C3A, and C4AF. When water is added to Portland cement, the calcium sulfate and high-temperature-formed calcium compounds dissolve, saturating the liquid phase with various ionic species. Initially, during cement hydration, the interaction of calcium, sulfate, aluminate, and hydroxyl ions leads to the creation of needle-shaped crystals known as ettringite, specifically hydrated calcium trisulfoaluminate. As hydration progresses, larger prismatic calcium hydroxide crystals and fine fibrous calcium silicate hydrate crystals occupy the spaces initially filled with water and dissolved cement particles. After a few days, depending on the alumina/sulfate ratio, ettringite may transform into hydrated monosulfoaluminate, displaying a hexagonal plate shape. This unique hexagonal morphology is characteristic of hydrated calcium aluminate, which forms in cement pastes with high C3A content. An electron micrograph in Figure 2-1 illustrates the typical morphology of phases resulting from mixing calcium aluminate and calcium sulfate solution.

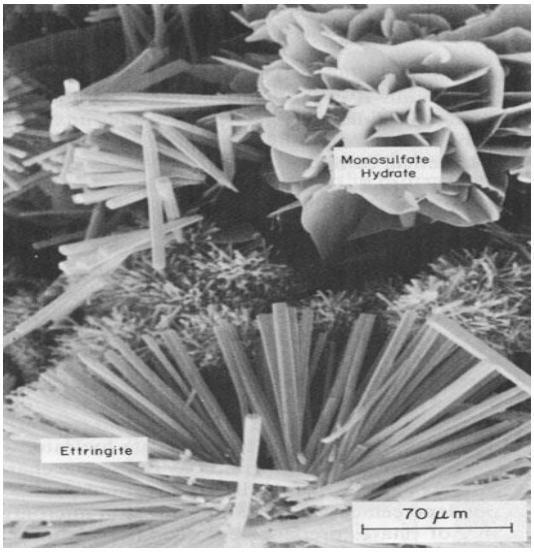

Figure 2-1 Scanning electron micrograph of typical hexagonal crystals of hydrated monosulphate and needle-like ettringite crystals formed by mixing calcium aluminate and calcium sulphate solutions.

An example of the essential phases present in the microstructure of a well-hydrated Portland cement paste is shown in Figure 2-2.

It is useful to note that the various phases are not uniformly reconstituted in terms of size and morphology based on the microstructural model of the hydrated cement paste shown in Figure 2-6. In solids, microstructural alterations can have serious effects on resistance and other mechanical properties. In addition to the microstructure's evolution due to chemical changes that occur after the cement comes into contact with water, it is useful to pay attention to some rhéological characteristics of freshly mixed cement paste, which also affect the microstructure of the resin's durability. For instance, anhydrous cement particles have a tendency to attract one another and form flocons, which traps large amounts of mixed water. It is obvious that the primary source of evolution in heterogeneous systems would be local differences in the water/cement ratio. The crystalline products of hydration would differ from those of a well-dispersed system in addition to the size and shape of the pores in a highly flocculated cement paste system.

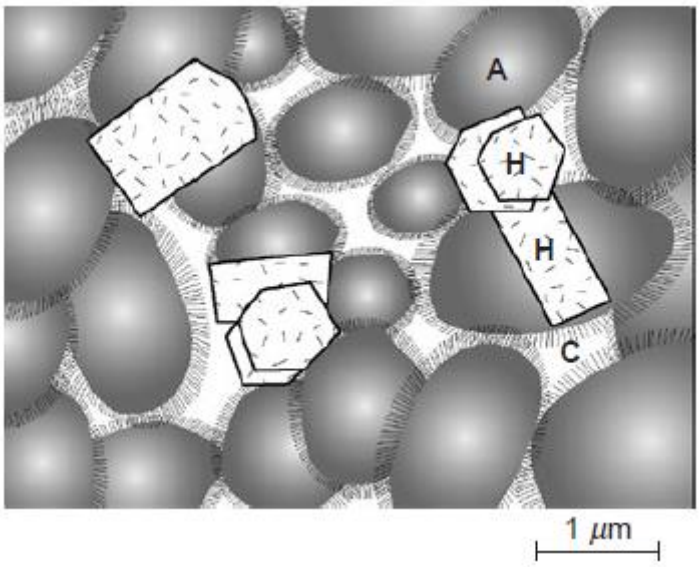

Figure 2-2 An example of Portland cement paste that has been properly hydrated. Aggregation of weakly crystalline C-S-H particles with at least one colloidal dimension (1 to 100 nm) is denoted by the letter "A." An aggregation's particle spacing ranges from 0.5 to 3.0 nm, with an average of 1.5 nm. Hexagonal crystalline products like CH, C4AH19, and C4ASH18 are represented by the letter H. Large crystals, usually 1 µm wide, are formed by them. C stands for cavities or capillary voids that form when cement hydration products do not fully fill the spaces that were initially occupied by water. Capillary voids range in size from 10 nm to 1 µm, but in well-hydrated pastes with a low water/cement content, they are less than 100 nm.

2.2 Hydrated cement paste solids

The four primary solid phases of hydrated cement paste that can be identified by electron microscopy are as follows, along with their types, amounts, and properties:

2.2.1 Hydrated calcium silicate.

The most crucial phase in determining the properties of a fully hydrated Portland cement paste is the hydrated calcium silicate phase, or C-S-H for short, which makes up 50–60% of the solid volume. C-S-H is not a well-defined compound because it is a hyphenated term; the structural water content varies even more, and the C/S ratio ranges from 1.5 to 2.0. Additionally, the morphology of C-S-H varies, ranging from reticular networks to poorly crystalline fibers. Only with the development of electron microscopy was it possible to resolve C-S-H crystals because of their colloidal size and propensity to aggregate. The substance is frequently referred to as C-S-H gel in earlier literature. The internal crystal structure of C-S-H is still unclear; previously, it was thought that it resembled naturally occurring tobermorite, which is why it was occasionally referred to as "tobermorite gel."

Several models have been put forth to explain the properties of the materials, despite the fact that the precise structure of C-S-H is unknown. The Powers-Brunauer model indicates that the material has a very large surface area and a layered structure. Surface areas for C-S-H have been suggested to range from 100 to 700 m2/g, depending on the measurement method, and van der Waals forces are primarily responsible for the material's strength. It is estimated that the gel's pore size, or the distance between solids, is approximately 18 Å. The C-S-H structure is represented by the Feldman-Sereda model as consisting of a collection of irregular or folded layers that are haphazardly arranged to form interlayer spaces of various sizes and shapes (5 to 25 Å).

2.2.2 Calcium hydroxide

Crystals of calcium hydroxide, sometimes referred to as portlandite, make up 20–25% of the hydrated paste's solids volume. In contrast to C-S-H, calcium hydroxide has a specific stoichiometry, $Ca(OH)_2$. It frequently forms large crystals with a recognizable hexagonal prism shape. The available space, hydration temperature, and impurities in the system all have an impact on the morphology, which typically varies from indeterminate to large plate stacking. Because calcium hydroxide has a much smaller surface area than C-S-H, its potential contribution to strength is constrained.

2.2.3 Hydrated calcium sulfoaluminates

Since they only make up 15–20% of the hydrated paste's solid volume, hydrated calcium sulfoaluminates have a negligible impact on the microstructure of concrete. a small part in the relationships between microstructure and properties. The sulfate/alumina ion ratio of the solution phase during the early stages of hydration has already been shown to favor the formation of hydrated trisulfate, C6AS3H32, also referred to as ettringite, which forms needle-shaped prismatic crystals. Ettringite eventually changes into hydrated monosulfate, C4ASH18, which crystallizes into hexagonal plate crystals in regular Portland cement pastes. Portland cement concrete is susceptible to sulfate attack due to the presence of hydrated

monosulfate. It should be mentioned that trace amounts of iron found in both ettringite and monosulfate can substitute aluminum ions in the crystal structure.

2.2.4 Unhydrated clinker grains

Even long after hydration, unhydrated clinker grains may be present in the microstructure of hydrated cement pastes, depending on the degree of hydration and the size of the anhydrous cement particles. Modern Portland cement typically contains clinker particles that range in size from 1 to 50 μm, as was previously mentioned. The smallest particles dissolve and leave the system first, followed by the larger particles, which get smaller, as the hydration process goes on. Because there isn't much room between the particles, hydration products often crystallize near the hydrating clinker particles, creating the illusion that a coating is forming around them. The in situ hydration of clinker particles results in the formation of a very dense hydration product at more advanced ages, which may resemble the original clinker particle in morphology due to the lack of available space.

2. 3 Voids in hydrated cement paste

A variety of void types, in addition to solids, are present in hydrated cement paste and significantly impact its characteristics. Fig. 2-3a shows the typical sizes of the solid phases and voids in hydrated cement paste. The following section discusses the various kinds of voids, their numbers, and their importance. Fig. 2.3b shows the size of a number of objects for comparison, ranging from human height to the diameter of Mars.

2.3.1 C-S-H interlayer space

Although Feldman and Sereda proposed that the interlayer space could range from 5 to 25 Å, Powers assumed that the width of the space was 18 Å and concluded that it represented a porosity of 28% in solid C-S-H. This void size is too tiny to negatively impact the hydrated cement paste's permeability and strength. Water in these tiny spaces, however, can be retained by hydrogen bonding, as explained below, and its removal under specific circumstances may exacerbate drying shrinkage and creep.

The spaces between the solid layers of C-S-H were referred to as "gel pores" in some earlier publications. They are commonly referred to as intercalation spaces in contemporary literature.

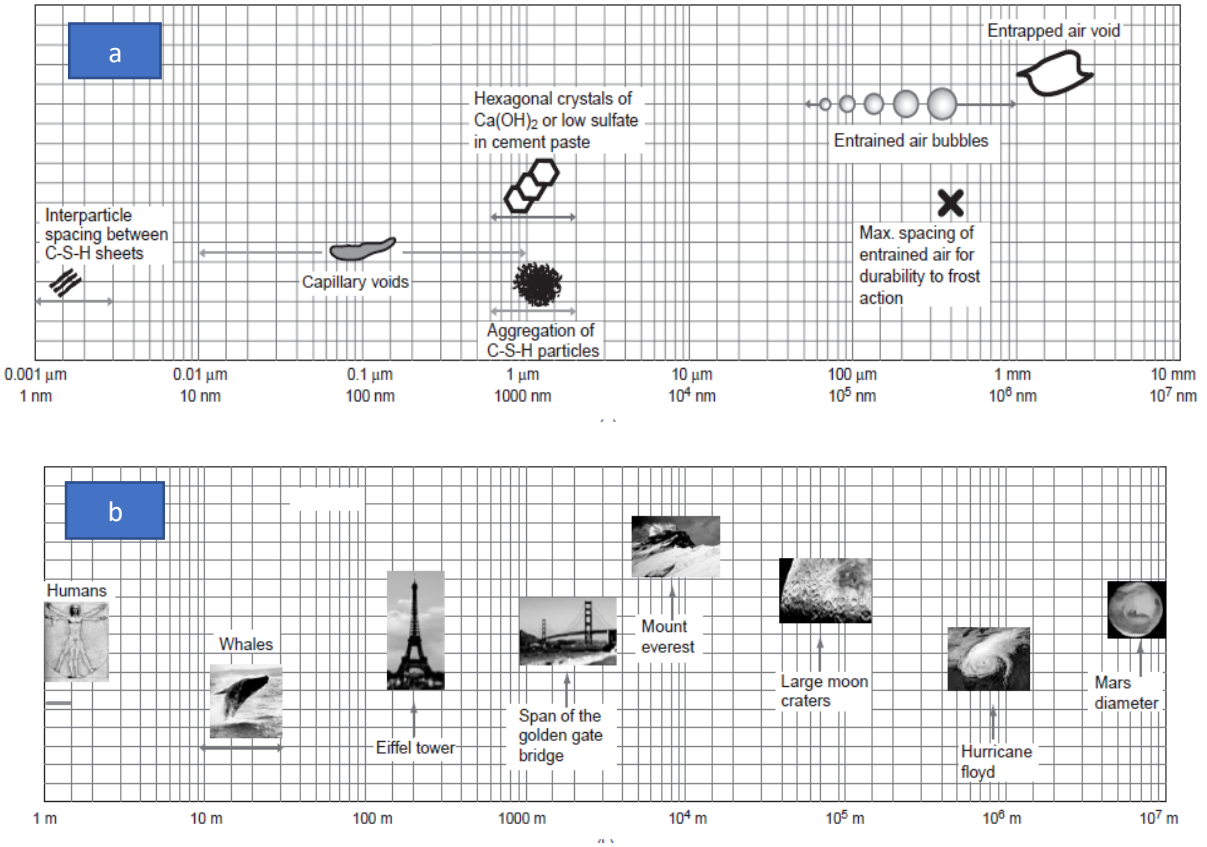

Figure 2-3: (a) Range of sizes of solids and pores in hydrated cement paste, (b) illustrates a similar range using the height of a human being as the starting point and the planet Mars as the end point.

2.3.2 Capillary voids

The space left empty by the solid ingredients of the hydrated cement paste is known as a capillary void. Throughout the hydration process, the overall volume of a normal cement-water mixture essentially stays the same. Compared to anhydrous Portland cement, the average bulk density of hydration products is significantly lower; 1 cm^3 of fully hydrated cement is thought to require about 2 cm3 of space to hold the hydration products. Therefore, cement hydration can be thought of as a process where space filled with hydration products gradually replaces the space initially occupied by cement and water. The initial distance between the anhydrous cement particles in the freshly mixed cement paste (i.e., the water ratio) and the degree of cement hydration determine the volume and size of the capillary voids, which make up the space not occupied by cement or hydration products. Later on, we will discuss a technique for determining the total volume of capillary voids, also known as porosity, in Portland cement pastes with varying water-to-cement ratios or levels of hydration.

Capillary voids can be anywhere between 10 and 50 nm in well-hydrated pastes with a low water-to-cement ratio, and they can reach 3 to 5 µm in pastes with a high water-to-cement ratio in the early stages of hydration. Typical pore size distribution curves for a number of hydrated cement paste samples examined using the mercury intrusion technique are displayed in Figure

2-4. Pore size distribution has been proposed as a more appropriate criterion for assessing the properties of hydrated cement paste than total capillary porosity. While capillary voids smaller than 50 nm, known as micropores, are crucial for drying shrinkage and creep, capillary voids larger than 50 nm, known as macropores in contemporary literature, most likely have a more significant influence on strength and impermeability properties.

2.3.3 Air voids (air bubbles)

Air voids are typically spherical in shape, whereas capillary voids are irregular. When mixing concrete, a tiny quantity of air is typically trapped in the cement paste. Admixtures may be added to concrete to purposefully create tiny voids for a variety of reasons. Entrained air voids typically range from 50 to 200 µm, while trapped air voids can reach 3 mm. Because they are larger than capillary voids, trapped and entrained air voids in hydrated cement paste can have a negative impact on strength.

2.4 Water in hydrated cement paste

The voids in hydrated cement paste appear to be empty when viewed under an electron microscope. This is because the sample must be dried under a high vacuum as part of the sample preparation procedure. In actuality, untreated cement paste can contain a significant amount of water, depending on the porosity of the paste and the ambient humidity. Hydrated cement paste comes in a variety of forms, just like the solid and void phases mentioned above. Water is categorized into various types based on how easy or difficult it is to remove from the hydrated cement paste. The boundary between the various water states is not strict since a saturated cement paste continuously loses water when the environment's relative humidity drops. In spite of this, the classification helps to explain the characteristics of hydrated cement paste. Hydrated cement paste contains water in the following states in addition to vapor in voids or partially filled with water:

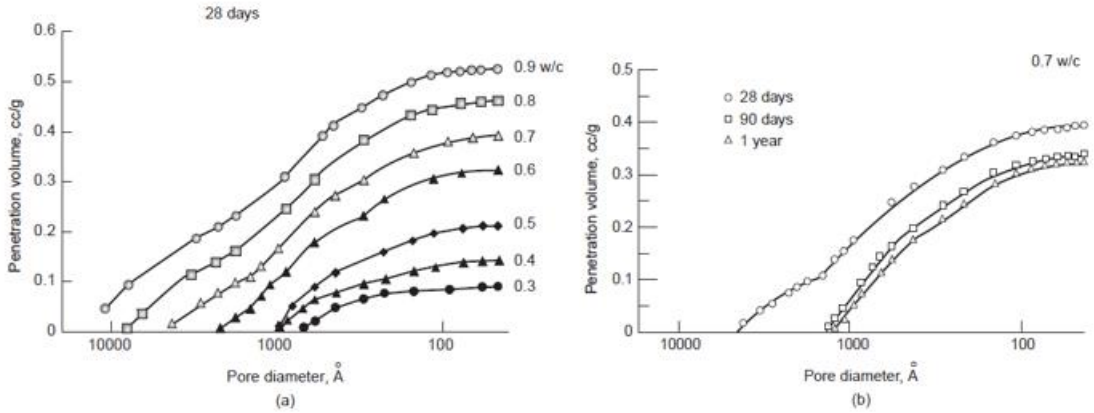

Figure 2-4: Distribution of pore size in hydrated cement pastes.

Strength, permeability, and volume changes in hardened cement paste are actually controlled by the distribution of pore sizes rather than total porosity. The ratio of cement to water and the age (degree) of cement hydration determine the distribution of pore sizes. Small pores primarily affect drying shrinkage and creep, while large pores primarily affect compressive strength and permeability.

2.4.1 Capillary water

This is water found in spaces bigger than roughly 50 Å. It can be defined as the mass of water that is unaffected by the solid surface's attractive forces. From the perspective of how capillary water behaves in hydrated cement paste, it is actually preferable to separate capillary water into two groups: water in large voids of the order of > 50 nm (0.05 μm), which is also known as free water because its removal does not alter the volume, and water held in small capillaries (5 to 50 nm) by capillary tension, which can cause the system to shrink if removed.

2.4.2 Adsorbed water

This water is near the solid surface. Water molecules are physically adsorbed onto the solids' surface in the hydrated cement paste due to attractive forces. It has been proposed that hydrogen bonding can physically retain up to six molecular layers of water (15 Å). When the hydrated cement paste is dried to 30% relative humidity, a considerable amount of the adsorbed water may be lost because the binding energies of individual water molecules decrease with distance from the solid surface. The hydrated cement paste shrinks as a result of the loss of adsorbed water.

2.4.3 Interstitial water

This water is connected to the C-S-H structure. It has been proposed that hydrogen bonds firmly hold a monomolecular layer of water between the C-S-H layers. Only when there is substantial drying (i.e., below 11% relative humidity) is interstitial water lost. When interstitial water is lost, the C-S-H structure significantly deteriorates.

2.4.4 Chemically bound water

This water is a crucial component of the microstructure of different cement hydration products. When the hydrates break down when heated, this water is released rather than lost during drying. Fig. 2-5 shows the various types of water related to C-S-H based on the Feldman-Sereda model.

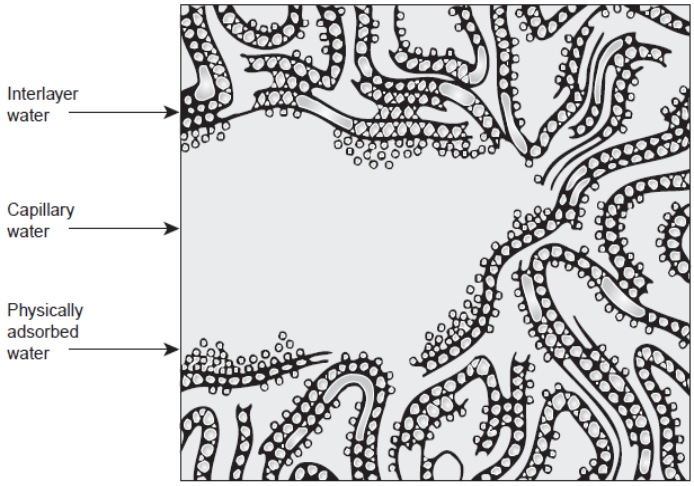

Figure 2-5 Schematic model of the types of water associated with hydrated calcium silicate.

Water can take many different forms in hydrated cement paste. These can be categorized based on how easily the water can be extracted. Understanding the volume changes related to water contained in tiny pores is made easier with the help of this classification.

Chapter 3: Hydraulicity and theories of hydration

3.1 Introduction

When cement and water undergo a chemical reaction, the end product is hydrated cement paste (hydration reaction). The primary ingredients of cement undergo a complex chemical reaction to create new insoluble compounds that solidify over time. Strength is mostly developed by the hydration of C_3S and C_2S, which results in the production of calcium silicate hydrate (C-S-H) and portlandite ($Ca(OH)_2$). The cement paste stays workable while the reactions proceed gradually over the course of one to several hours. After that, the paste thickens, marking the start of setting. The pores gradually fill with the entwined crystals of calcium silicate and portlandite. The substance solidifies and becomes denser. In the following, we will detail the hydration process of each mineral in the clinker.

3.2 Hydration mechanism of Portland cement .

There are four stages in the hydration mechanism, which are shown in Figure 3.1.

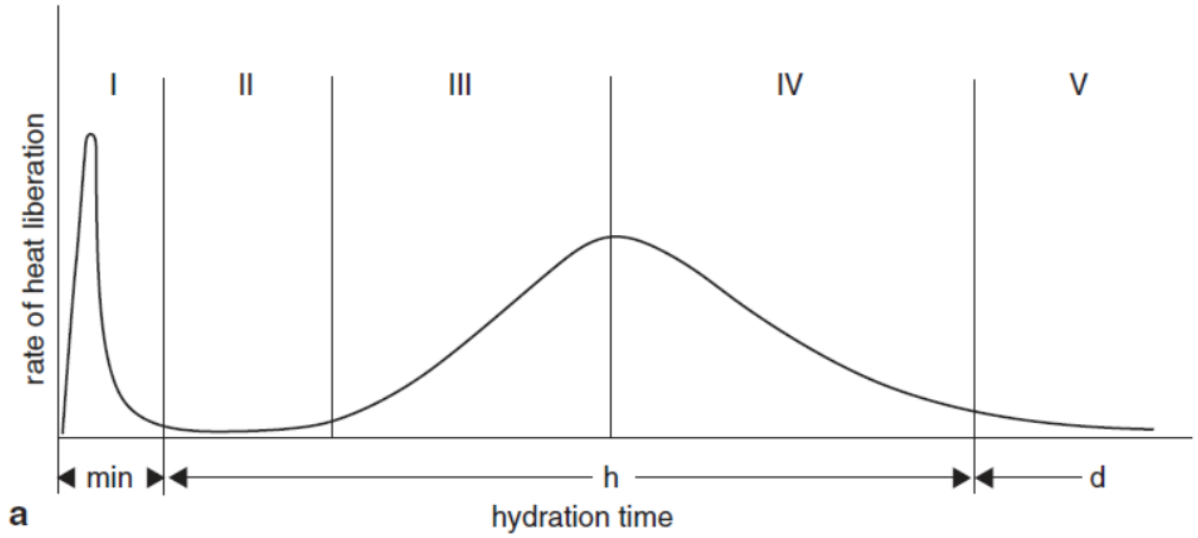

Figure 3.1. Typical isothermal calorimetry curve for cement paste

Period 1: Initial reactions

This period begins as soon as the water comes into contact with the cement and lasts a few minutes. The C_3S and C_3A in the cement grains react immediately with the water, forming ettringite and C-S-H. A dissolution phase is indicated by this. Ions start to dissolve.

Period 2: Dormancy period

Ions such as Ca^{2+} and OH- are released during this time. This causes the solution's pH to rise, which slows down the constituents' dissolution. There is then little heat release. This time frame is the same as the phase in which the material is workable.

Period 3: Acceleration period

This phase starts when the solution's electrical conductivity reaches its maximum and the concentration of Ca^{2+} and OH^- ions in the solution reaches a critical value. Portlandite precipitates as a result of this supersaturation. The processes of the various phases' dissolution, nucleation, and precipitation that enable the formation of hydrates (ettringite, portlandite, C-S-H) come next. The material's temperature rises as a result of the high level of chemical activity. A stiff solid is produced as the hydrates start to mix together. During this time, the concrete solidifies. This is the point at which the cement paste transitions from a liquid to a solid state, meaning that a continuous stream of particles that are mechanically bonded moves through the solid.

Period 4: Slowdown period

A thickening layer of hydrates covers the anhydrous grains. Water must permeate the gel pores in order for hydration to continue. As a result, the curve shows a drop in the amount of heat released during this time. A portion of the cement will never be hydrated if the porous network is closed off. Furthermore, the critical value is $(W/C)_{crit} = 0.4$ because the initial water must be enough to hydrate all of the cement. Ettringite dissolves and changes into monosulfoaluminate during this time as well.

3.2.1 Hydration of tricalcium silicate (C_3S)

Tricalcium silicate is hydrated by three primary reactions :

the dissolution of C_3S (exothermic reaction) ,

the precipitation of C-S-H (endothermic reaction) ,

the precipitation of portlandite (endothermic reaction).

Grain dissolution of tricalcium silicate

As soon as the cement is wetted, this initial stage starts. An extremely basic environment is produced when calcium silicate grains dissolve on their surface. One way to express the dissolution reaction is:

$$Ca_3SiO_5 + 3H_2O \longrightarrow 3Ca^{2+} + 4OH^- + H_2(SiO_4)^{2-}$$

Rapid growth of C-S-H gel

This second stage lasts for several hours and starts a few minutes after hydration. The C-S-H gel will nucleate and then grow based on the concentrations of calcium ions from the first stage, silicate ions [$H_2(SiO_4)^{2-}$], and hydroxyl ions (i.e., pH). This intricate precipitation can be expressed as follows:

$$x\ Ca^{2+} + H_2(SiO_4)^{2-} + 2\ (x-1)\ OH^- + 2(y-x)\ H_2O \longrightarrow (CaO)x(SiO_2)(H_2O)y$$

Precipitation of portlandite

After a few hours, this phase starts. Portlandite naturally precipitates when the pH is extremely high (between 12.4 and 13.5) and the concentration of calcium ions in the solution rises to a level that exceeds the solubility of portlandite in water, which is 22 mmol/l at 25°C.

$$Ca^{2+} + 2OH^- \longrightarrow Ca\ (OH)_2$$

C-S-H appears as a gel under the scanning electron microscope (SEM) and lacks any distinct crystalline form (Figure 3.2). Conversely, Portlandite is visible as hexagon-shaped platelets that are stacked in between the cement grains (3.3).

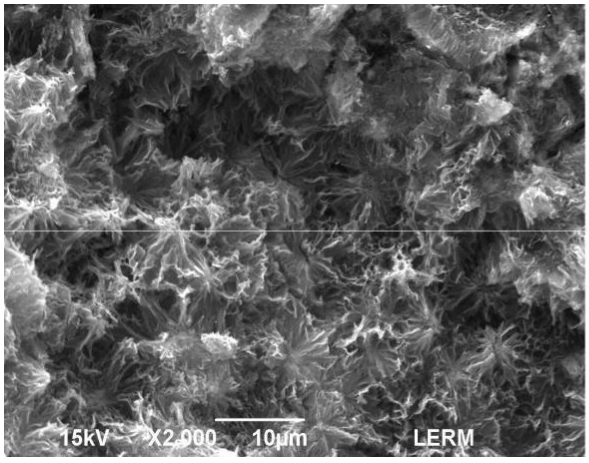

Figure 3.2. C-S-H under SEM

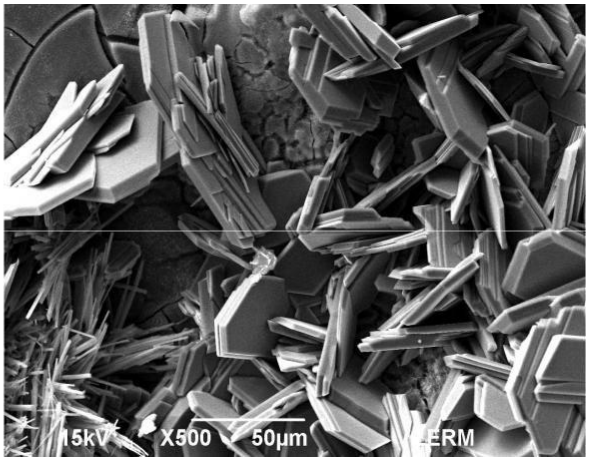

Figure 3.3. Portlandite under SEM

3.2.2 Hydration of dicalcium silicate (C_2S)

C_2S does not contribute significantly to the early stages of cement property development because its hydration rate is lower than that of C_3S. The following is its hydration reaction:

$$2(2CaO.SiO_2) + 4H_2O \longrightarrow 3CaO.2SiO_2.3H_2O + Ca(OH)_2$$

3.2.3 Hydration of tricalcium aluminates (C_3A)

After a few minutes, the paste quickly stiffens due to the extremely quick kinetics caused by the hydration of C_3A during mixing. The other clinker components, especially C_3S, would not be able to hydrate if aluminates were prepared right away. Because the resulting paste lacks mechanical strength characteristics but is not malleable, this phenomenon is known as "rapid setting."
The hydration kinetics of tricalcium aluminate are controlled by adding roughly 5% gypsum ($CaSO_4.2H_2O$) in order to prevent this undesirable phenomenon. A slow reaction with kinetics similar to the hydration of C_3S takes place in place of a rapid one.

The following sequential reactions show that C_3A and gypsum dissolve quickly when combined with water during mixing:

$$Ca_3Al_2O_6 + 2H_2O \longrightarrow 3Ca^{2+} + 4OH^- + 2AlO_2$$

$$CaSO_4.2H_2O \longrightarrow Ca^{2+} + SO_4^{2-} + 2H_2O$$

A solution that is supersaturated with regard to hydrates is produced as a result of these exothermic reactions. According to the reaction, the ions come together almost instantly to form crystals of calcium trisulfoaluminate hydrate (TSA), also referred to as ettringite, which resemble needles (Figure 3.4):

$$6Ca^{2+} + 2AlO^{2-} + 3SO_4^{2-} + 30H_2O + 4OH^- \longrightarrow 3CaSO_4.Al_2O_3.3CaSO_4.32H_2O$$

For simplicity's sake:

$$C_3A + 3CaSO_4.2H_2O + 26H_2O \longrightarrow C_6AS_3H_{32}$$

The gypsum is totally consumed and excess C_3A is left over after 10 to 24 hours (long after the cement has set, which takes 2 to 6 hours). The C_3A that hasn't been consumed yet will then get its sulfate from ettringite. According to the reaction, the ettringite will change and combine with the extra C_3A and water to create hydrated calcium monosulfoaluminate, which will have a plate-like hexagonal structure (Figure 3.5):

$$\underset{\text{(Ettringite)}}{C_3A.3CaSO_4.32H_2O} + 2C_3A + 4H_2O \longrightarrow \underset{\text{(Monosulfoaluminate)}}{3(C_3A.CaSO_4.12H_2O)}$$

For simplicity's sake:

$$C_6AS_3H_{32} + 2\ C_3A \longrightarrow 3\ C_4ASH_{12}$$

This reaction causes rapid dissolution of the excess anhydrous aluminate.

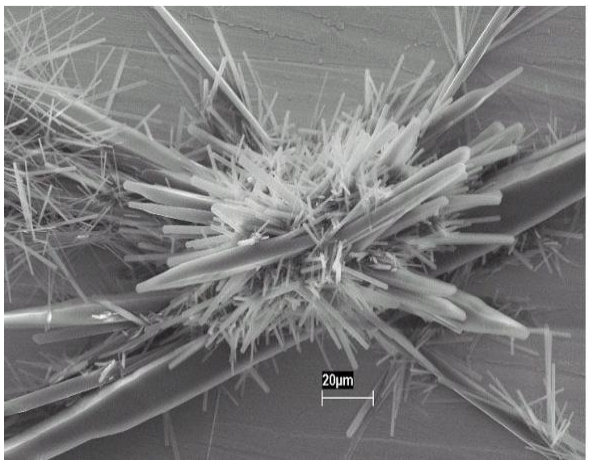

Figure 3.4. Ettringite in SEM

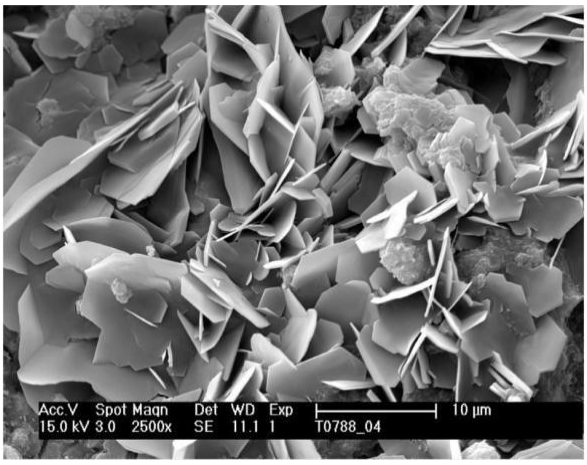

Figure 3.5. Monosulfoaluminate in SEM

3.2.4 Hydration of tetracalcium aluminoferrite (C_4AF)

It is unclear how the ferrite phase is hydrated. However, a number of investigations have revealed parallels between C_4AF and C_3A's hydration products. In the presence of gypsum, C4AF produces iron, portlandite, ettringite, and monosulfoaluminate (after gypsum depletion),

$$C_4AF + 3(CaSO_4.2H_2O) + 2Ca(OH)_2 + 34H \longrightarrow (C_3A.(CaSO_4)_3.32H_2O) + (FH_3) + Ca(OH)_2$$

(Gypse) (Ettringite) (Portlandite)

$$2C_4AF + C_3A.3(CaSO_4).32H_2O + 12H \longrightarrow 3(C_3A.CaSO_4.12H_2O) + 2(FH_3) + Ca(OH)2$$

(Ettringite) (Monosulfoaluminate) (Portlandite)

3.3 Factors affecting cement hydration

Several factors influence the hydration of Portland cement, including (Odler, 1988).

•The cement's composition,

• The amount of gypsum it contains,

• The presence of foreign ions in specific compounds,

• The distribution of cement fineness particle size

• The mixture's water to cement ratio;

• The ambient temperature;

• The amount and presence of admixtures and/or additives.

Because of their interactions with one another and with other minor phases like free CaO, MgO, alkali sulfates, etc., the hydration mechanism and kinetics of Portland cement are significantly more complex than those of the individual phases. Figure 3.6 shows the typical progression of hydration in terms of the hydration products formed.

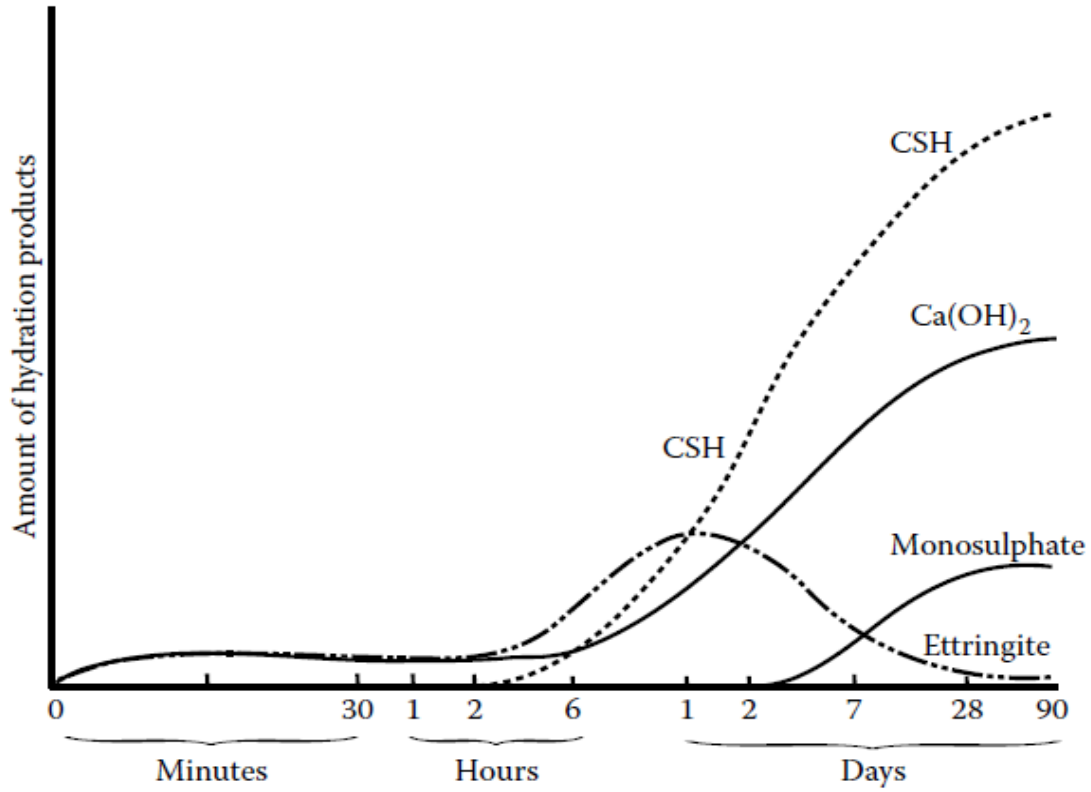

Figure 3.6 Rate of hydration product formation in Portland cement.

3.4 Techniques used to study hydration

The following methods are used to examine cement hydration:

- Thermal analysis

- X-ray diffraction

- Scanning electron microscopy

The study of hydrated cement requires the removal of free water and the stopping of the hydration process. This step is usually performed by immersing the sample in acetone and then drying it at a low temperature (<50°C) under partial vacuum.

3.4.1 Thermal study

The most widely used method is thermogravimetric analysis. A small sample of hydrated cement is placed in a thermobalance, where its weight is measured during gradual heating, at a controlled rate, from room temperature to approximately 1000°C. This approach allows for accurate quantification of the content of certain hydrates, such as ettringite and $Ca(OH)_2$.

3.4.2 X-ray diffraction analysis

This method is fast, but its results are limited because several hydrates, such as C–S–H gel and calcium aluminate monosulfate, have low crystallinity, resulting in unclear diffraction patterns.

3.4.3 Scanning electron microscopy (SEM)

This method is particularly effective, especially when using a microscope equipped with an analytical microprobe. It relies on techniques similar to X-ray fluorescence to analyze the chemical composition of the hydrates observed. Thanks to its high resolution, SEM can be used to explore the microstructure of hydrated cement paste in concrete or mortar. However, caution should be exercised when analyzing the images, as sample preparation and the vacuum required in most microscopes can create artifacts that are not present in the wet paste.

Chapter 4:

Phenomena accompanying hydration

By keeping an eye on specific phenomena that are happening concurrently in the hydrating cement paste, one can track the effects of the hydration reaction, including:

• modifications to the interstitial solution's electrical conductivity;

• paste setting;

• heat development;

• volumetric changes;

• rise in compressive strength and modulus of elasticity.

4.1 Variation in electrical conductivity

This measurement, which monitors the rate at which ions are released or combined during the hydration process, is incredibly straightforward and easy. A characteristic curve that depicts the change in electrical conductivity over time is shown in Figure 4.1. There are various components to this curve. The ascending section that comes after the Portland cement particles come into contact with water is represented by the first part, A. It results from the dissolution of the different chemical species found in Portland cement, which is caused by intense chemical activity. The pH rises quickly and sharply, but this chemical activity is only surface-level and does not result in the formation of large crystals that could stiffen the matrix. A peak (P) and a slight decline (C) mark its conclusion. When the interstitial solution reaches a point of supersaturation in Ca^{2+} ions, the first portlandite crystals precipitate almost instantly, as indicated by this tiny drop.

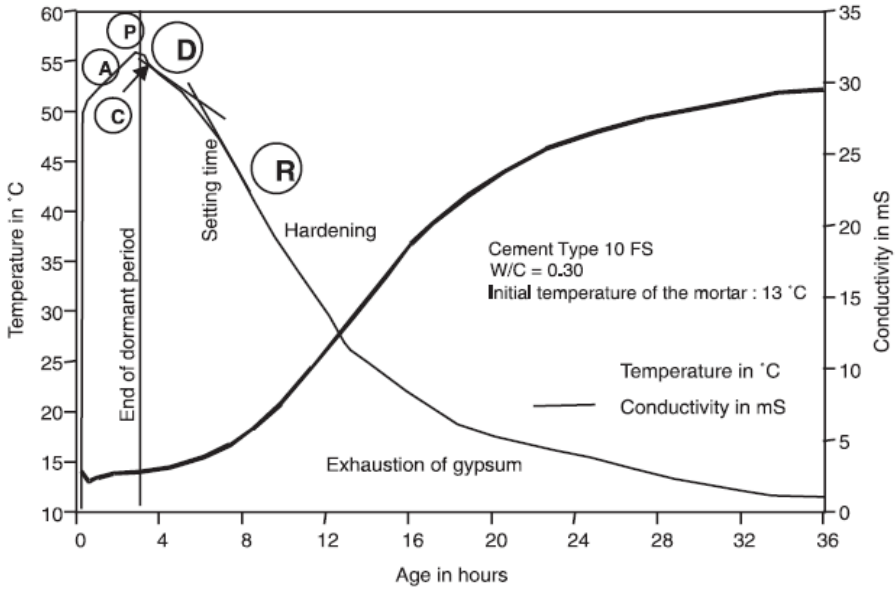

Figure 4.1 Electrical conductivity and heat release of a blended cement containing 8% silica fume.

Short-term conductivity (D) decreases more gradually after this minor decrease (C), and part R decreases more quickly after that.
The "structuring" of the hydrated cement paste is represented by this rather quick drop in part R of the curve.
The first hydrates at this stage of the hydration process bridge the cement particles, making it harder for ions to move through the interstitial solution because of the tortuosity of their path. Additionally, because some of the water has been combined in hydrated products, there is less water available in the interstitial solution.

It is simple to track the impact of a specific parameter on the hydration of Portland cement when measuring the electrical conductivity of various cement pastes. Examples of these parameters include the effect of an admixture, a mineral component, a specific clinker component, the type of sulfate, etc.

4.2 Setting of Portland cement

Vicat created a straightforward test to track the setting of Portland cement. When a standard load is applied to a standard needle, the penetration is measured. Initial and final setting times are identified and determined to be more or less arbitrary in relation to cement hydration. These two setting times, which correspond to two distinct levels of structure formation attained by the hydrated cement paste, come after the portlandite precipitation and the acceleration of C_3S hydration.

Since these two setting times are a reliable indicator of production consistency, they can be used to control the production of Portland cement. Furthermore, it provides a clear understanding of the extent of control over the cement paste's rheology (initial setting) and initial hardening rate (final setting).

4.3 Development of hydration heat

It is possible to track the amount of heat generated during the hydration process, or more accurately, the rate of heat release (the variation in heat rate over time). Figure 4.2 displays a typical curve.

It is better to examine the development of the heat rate of C_3S and C_3A pastes before attempting to directly interpret such a curve. Figures 4.3 and 4.4 display these curves.

Five distinct stages, denoted 1 through 5, can be distinguished in the curve that depicts the heat release rate of C_3S (Figure 4.3). Stage 1 is the brief heat release that occurs after C_3S and water make their initial contact. The dissolution of the most active ionic species on the C3S particles' surface is linked to this heat release. As a result, the C_3S particles develop a thin layer of C-S-H. Further hydration of the C_3S is prevented or at least markedly slowed down by this thin layer of C-S-H.

The duration of this initial phase is roughly fifteen minutes.

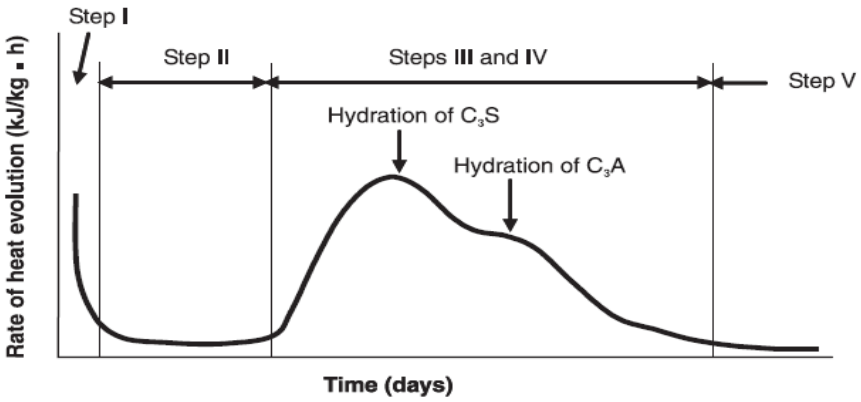

Figure 4.2: Heat release rate during Portland cement hydration.

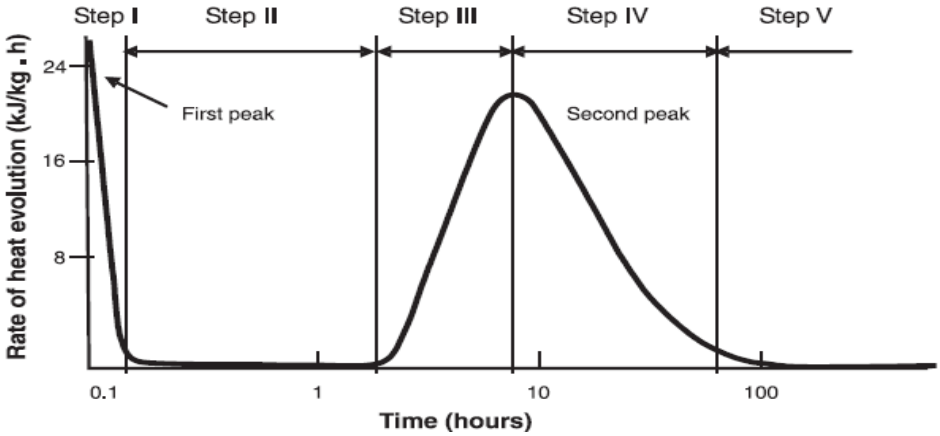

Figure 4.3: Heat release rate during hydration of C_3S.

The so-called dormant period is correlated with the second stage. This is not a time when "nothing" occurs because the C_3S paste stiffens a little and the pH and electrical conductivity rise. The duration of this stage is roughly one or one and a half hours.

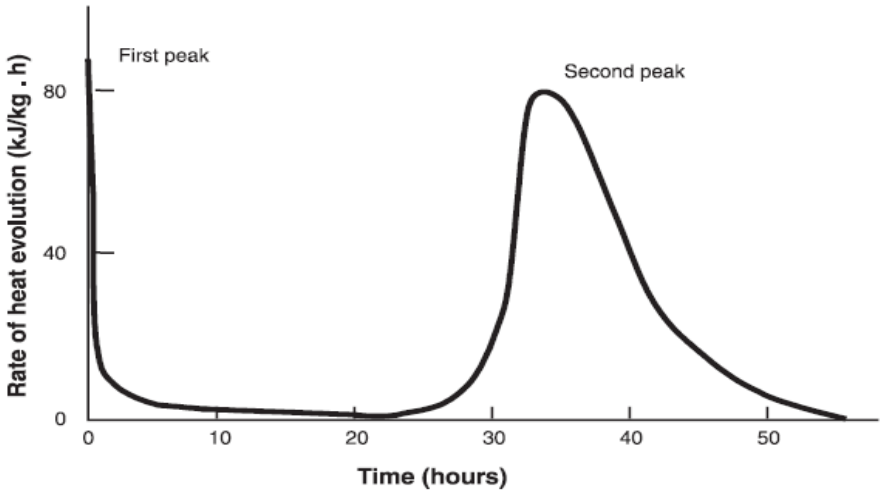

Figure 4.4: Heat release rate during C_3A hydration.

After the first portlandite crystals precipitate, C_3S hydrates quickly, resulting in the third stage, which is associated with rapid heat release. After reaching a peak, the rate of heat release starts to fall as quickly as it had increased. Because the initial hydrates that form on the surface of the C_3S particles through a dissolution/precipitation process obstruct the migration of water to the interior of the C_3S particles, this decrease is indicative of a slowdown in the hydration reaction. Instead of proceeding as a dissolution/precipitation process as in the ascending portion of the peak, the hydration reaction then proceeds as a diffusion process.

Part 5, the last stage of heat release, exhibits a slight decrease in heat release over time. The hydration reaction continues, albeit very slowly.

Although the shape of the heat release rate of C_3A and C_3S is similar, Figure 4.4 demonstrates that the heat release rate of C_3A is significantly higher on the y-axis. Additionally, we can observe that the second peak on the x-axis happens later than in the case of C_3S.

Ettringite's initial formation on the C3A crystals is represented by the first peak in the C_3A curve. Similar to how the first layer of tiny C-S-H crystals prevented the hydration of C3S, this first layer of ettringite momentarily prevents the hydration of C_3A. The duration of this initial peak is roughly fifteen minutes. Later, when the ettringite starts to change into monosulfoaluminate, the protection offered by this initial layer of ettringite stops, and C_3A's hydration resumes. A second peak represents this quick release of heat. The second peak is a little later in cements with high gypsum content. After the concrete has been in the formwork for a few hours and the hydrated cement paste has solidified, this second peak usually happens between 10 and 15 hours. The rate of heat release for C_2S and C_4AF demonstrates that these two compounds are significantly less reactive than C_3A and C_4AF, and their impact on Portland cement's heat release rate is minimal.

Considering that there is five to ten times more C_3S than C_3A in Portland cement, we can see that this curve can be obtained by combining the curves obtained for C_3S and C_3A in Figure 4.2, which depicts the evolution of the heat rate over time. Thus, in the curve showing the heat release rate of Portland cement, the heat developed by C_3S is predominant even though C_3A develops three times as much heat as the same mass of C_3S.

However, a closer look at Portland cement hydration reveals that, as synergies form during hydration, the curve showing the rate of heat evolution of Portland cement is not precisely the sum of the corresponding curves for C_3S, C_3A, C_2S, and C_4AF. For instance, C_3A and C_4AF directly compete for sulfate ions, but C_3A consumes SO_4^{2-} ions faster than C_4AF due to its higher reactivity. Calcium sulfate dissolves more readily as a result, indirectly initiating C_4AF's hydration.

Furthermore, some SO_4^{2-} ions may be trapped in the C-S-H formed during the hydration of C_3S and C_2S, and gypsum is known to speed up this process. Portland cement typically contains half as much monosulfoaluminate as is theoretically expected, according to Mindess and Young (1981) and Bensted (2001).

The amount of gypsum added to Portland cement is always optimized by cement manufacturers. In actuality, too little ettringite leads to the early formation of

monosulfoaluminate, while too much causes the paste to swell and microcrack. This quick monosulfoaluminate formation slows down the hydration of C_3S and consumes some lime. According to some researchers, the presence of an ideal gypsum dosage is caused by the acceleration of C_3S hydration and, concurrently, the weakening of the C-S-H formed because of the presence of sulfate ions trapped within the C-S-H.

It is possible to measure each phase's heat of hydration independently. The compound that releases the most heat per unit mass is undoubtedly C_3A (900 kJ/kg), followed by C_3S (500 kJ/kg), C_4AF (400 kJ/kg), and C_2S (250 kJ/kg). Given that the average Portland cement has 50–60% C_3S, 20–30% C_2S, and 5–10% C_3A and C_4AF, the primary factor influencing the heat of hydration of Portland cement is undoubtedly the heat released during the hydration of C_3S. C_3A, C_2S, and C_4AF all make much smaller contributions. Naturally, the content of C_2S and C_4AF must be increased while the amounts of C_3S and C_3A must be decreased when making Portland cement for mass concrete.

4.4 Volumetric variations associated with the hydration reaction

LeChâtelier demonstrated that a decrease in volume accompanied cement hydration as early as 1900.

LeChâtelier recorded variations in the water level in cement and water-filled capillary tubes (Fig. 4.5). But only extremely high W/C ratios (>1) can use this method. About 8.7% of the volume of the hydrates formed is equivalent to the **LeChâtelier contraction**. Additionally, it is equivalent to roughly 5.8 milliliters per 100 grams of hydrated cement.

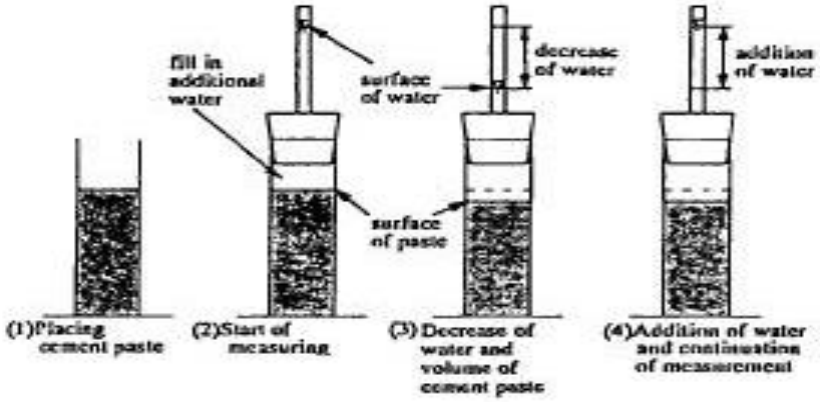

Fig. 4.5 - Measurement of chemical shrinkage in cement paste.

Le Châtelier's contraction results in only a minor reduction in apparent external volume prior to the formation of a rigid mineral skeleton (setting) (Figs. 4.6 and 4.7). Following setting, the volume loss brought on by hydration is incompatible with the amount of deformation that the mineral skeleton can withstand.

The porosity of the paste, which was first saturated with water, then shows a gas volume (water vapor) (Figs. 4.6 and 4.7).

The volume of gas voids rises with increasing hydration. The degree of hydration and the W/C ratio affect the ratio of gas volume to total pore volume.

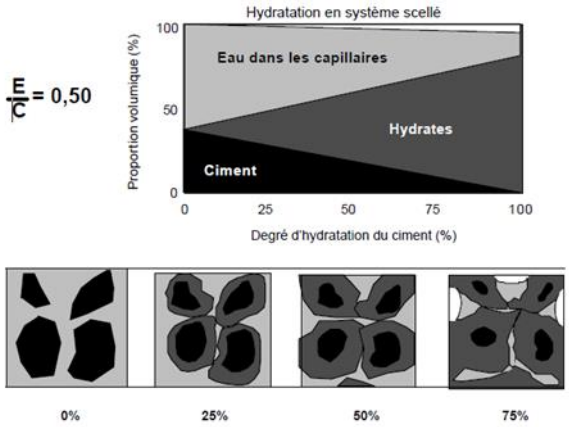

Fig. 4.6 - Schematic evolution of the hydration of cement paste (W/C=0.50) in a sealed system.

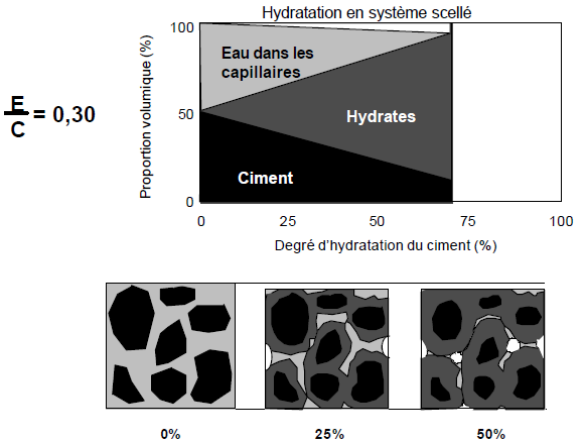

Fig. 4.7 - Schematic evolution of the hydration of cement paste (E/C=0.30) in a sealed system.

Gas voids (menisci) initially form in the largest capillaries in concrete when Le Châtelier contraction causes the volume of free water to decrease in relation to the total volume of capillary pores (Figs. 4.6 and 4.7).

As a result, capillary pores with a diameter less than ro contain the full volume of capillary water at any given time.

We can determine the liquid phase depression using Laplace's equation (Tab 4.1 and Fig. 4.8). The relative humidity in the concrete can be determined using Kelvin's equation (Tab 4.1 and Fig. 4.8).

Kelvin's law **DP = RT/Mv . ln h**

DP: pressure gradient between the gas phase and the liquid phase

R: ideal gas constant

T: capillary water temperature

M: mass of one mole of water

v: specific volume of water

h: relative humidity in the capillary pore

Laplace's law **DP = 2s/r . cos a**

DP: pressure gradient between the gas phase and the liquid phase

s: surface tension of water

r: radius of a capillary pore where the meniscus exists

a: wetting angle

Tab 4.1 - Calculated values of relative humidity and capillary depression for different capillary pore radii.

r (nm)	50	25	10	5
h (%)	98	95	90	80
ΔP (MPa)	3	6	15	3

Fig. 4.8 Schematic representation of a meniscus in a capillary.

The depression caused by Le Châteleir contraction in the liquid phase is generally compensated for by compression in the solid phase of the paste, which causes shrinkage known as endogenous shrinkage.

• Endogenous shrinkage depends in particular on:

The E/C ratio

The fineness of the cement

4.4.1 Influence of the W/C ratio

As the W/C ratio falls, endogenous shrinkage rises quickly (Fig. 4.9).
In the case of BHP, this is a significant phenomenon. Strong capillary depressions form early on due to the extremely fine capillary porosity of these concretes, which forces the formation of highly curved menisci.
As the W/C ratio falls, the internal relative humidity rapidly drops as well (Fig. 4.10).

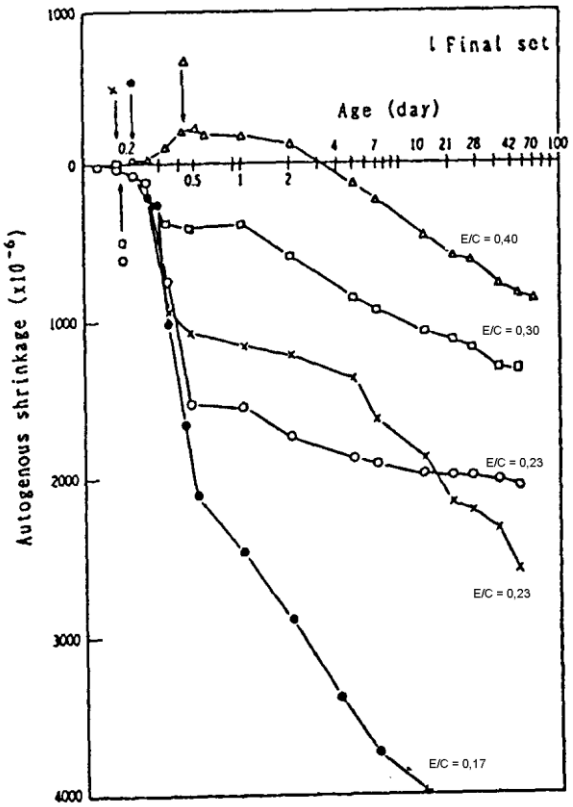

Fig. 4.9 - Influence of the W/C ratio on the endogenous shrinkage of the paste.

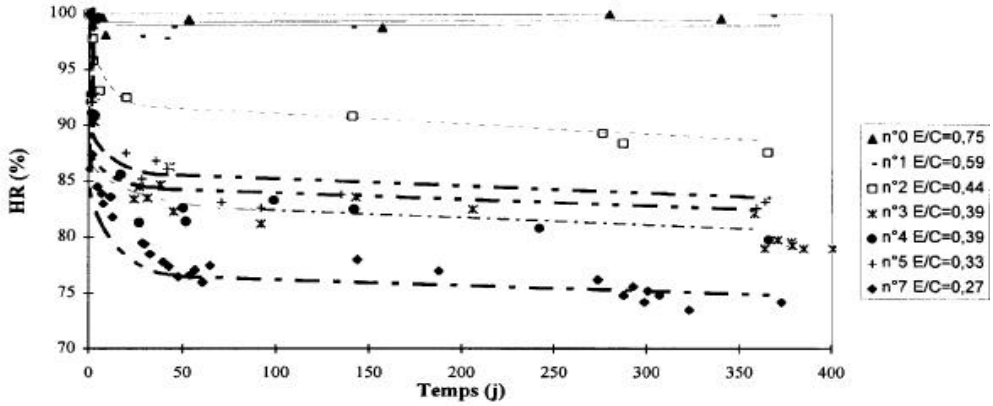

Fig. 4.10 - Influence of the W/C ratio on the internal relative humidity of concrete.

4.4.2 Influence of cement fineness

Concrete's endogenous shrinkage increases with increasing cement fineness (Fig. 4.11). As fineness rises, endogenous shrinkage starts earlier.

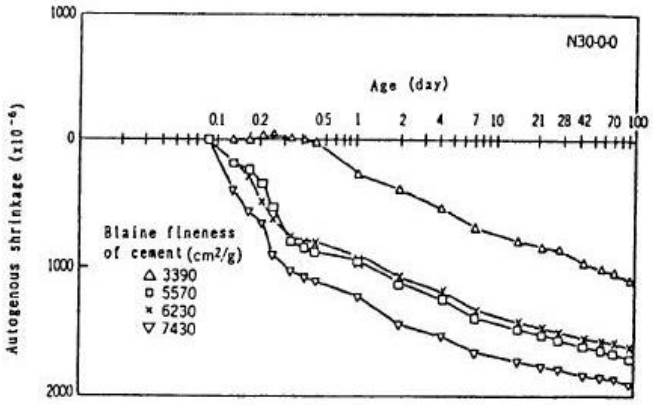

Fig. 4.11 - Influence of cement fineness on the endogenous shrinkage of a paste (W/C=0.30).

4.4.3 Influence of silica fume

When silica fume is used in place of cement, internal relative humidity decreases and endogenous shrinkage increases (Fig. 4.12).
More capillary depressions result from pore refinement brought on by silica fume.

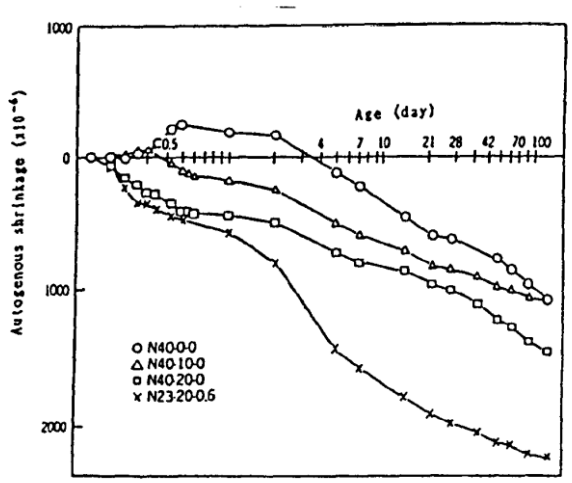

Fig. 4.12- Influence of silica fume (0-10-20%) on the endogenous shrinkage of the paste (W/C=0.40 and W/C=0.23).

Chapter 5

Origin of concrete's mechanical strength

5.1 Overview:

The quality that engineers and designers value the most in concrete is its strength. Porosity, or the volume fraction of voids, and strength are fundamentally inversely related in solids. As a result, the porosity of each microstructure component can restrict strength in multiphase materials like concrete. Because natural aggregates are typically dense and robust, the strength properties of concrete are typically determined by the porosity of the cement paste matrix and the interfacial transition zone between the matrix and the coarse aggregate.

While the water-to-cement ratio plays a significant role in determining the interfacial transition zone and matrix porosity, and consequently the concrete's strength, other elements like compaction and curing conditions (the degree of cement hydration), aggregate size and mineralogy, admixture types, Strength can also be significantly impacted by the specimen's geometry, moisture content, stress type, and loading rate. This chapter looks closely at how different factors affect the strength of concrete. The connections between uniaxial compressive strength and other forms of strength, including tensile, flexural, shear, and biaxial strength, are examined because uniaxial compressive strength is widely recognized as a general indicator of concrete strength.

5.2. Definition:

The capacity of a material to withstand stress without failing is known as its strength. Cracks can occasionally be used to identify failure. Ordinary concrete, on the other hand, has numerous tiny cracks even before it is exposed to external stress, according to microstructural studies. This is in contrast to most structural materials. Therefore, strength in concrete is defined as the highest stress that a concrete sample can tolerate and is correlated with the stress necessary to cause failure. Failure of the specimen usually indicates failure in tensile tests. Even if there are no outward indications of fracture, the specimen is deemed to have failed in compression if the internal cracking has progressed to the point where the sample cannot support a greater load.

5.3. Meaning:

Strength is the characteristic that is typically specified in concrete design and quality control. This is due to the fact that strength testing is comparatively simple in comparison to the majority of other properties. Furthermore, strength data can be used to infer many of the properties of concrete, including its modulus of elasticity, impermeability, and resistance to aggressive waters and other atmospheric agents. The majority of concrete components are made to capitalize on the material's higher compressive strength, which is several times higher

than that of other materials. In reality, though, the majority of concrete is simultaneously exposed to a mix of tensile, shear, and compressive stresses in two or more directions.

There is typically a fundamentally inverse relationship between a solid's porosity and resistance. For simple and homogeneous materials, it can be described as follows:

$$S = S_0 e^{-kp} \qquad (5.1)$$

Where S= strength of material with a given porosity p

S0 = intrinsic strength at zero porosity k = constant

Plotting the S/S0 ratio against porosity yields a similar curve for a variety of materials. For instance, the information in Fig. 5-1 shows a range of aggregates, autoclaved cements, and normally hardened cements. Iron, plaster of Paris, zirconia, and sintered alumina are just a few of the materials that exhibit the same strength-porosity relationship (Fig. 5-1b).

$$f_{c_{28}} = a.x^3 \qquad (5.2)$$

where x is the solid-to-space ratio, or the amount of solid fraction in the system, which is equal to 1 -p, and an is the material's intrinsic strength at zero porosity, p. Figure 5-1c displays Powers' data; he determined that the value of a was 234 MPa. The strength-porosity relationship in solids is generally valid, as shown by the similarity of the three curves in Fig. 5-1.

Porosity and strength are related in hardened cement paste or mortar, but not in concrete. Concrete is too complex to predict strength using exact strength-porosity relationships because of the microcracks in the interfacial transition zone between the coarse aggregate and the matrix. However, because the porosities of the concrete's constituent phases, including the interfacial transition zone, do in fact become limiting in terms of strength, the general validity of the strength-porosity relationship must be respected. Both the matrix's and the interfacial transition zone's strengths will determine the material's strength in concrete with traditional low-porosity or high-strength grids.

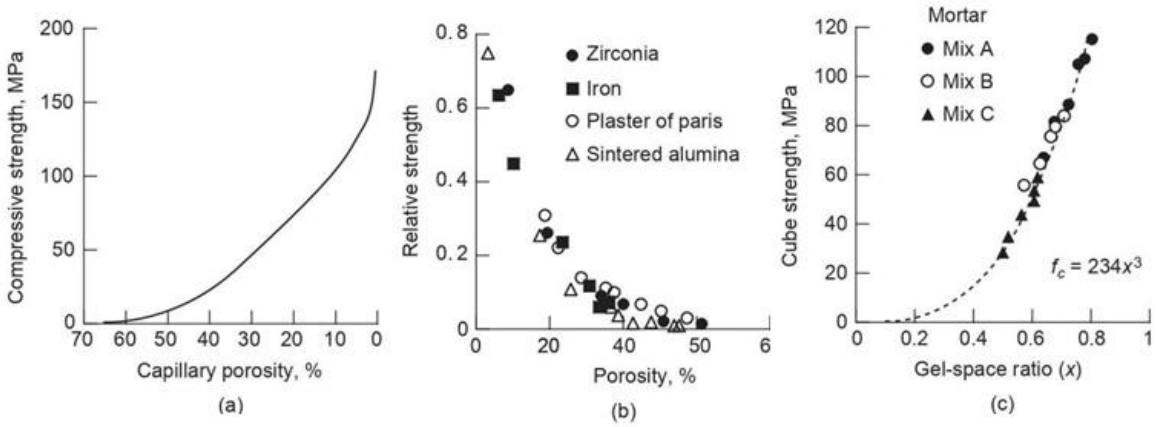

Figure 5-1 : Relation porosité-résistance dans les solides: (a) ciments, ciments auto-clavés et agrégats normalement durcis; b) fer, plâtre de Paris, alumine frittée et zircone; (c) mortiers de ciment Portland avec différentes proportions de mélange.

Porosity and strength have an inverse relationship that generally holds true for a wide range of materials, not just cement-based products.

5.4. Compressive strength and factors affecting it:

The response of concrete to applied stress depends not only on the type of stress, but also on how a combination of various factors affects the porosity of the different structural components of concrete. These factors include the properties and proportions of the materials that make up the concrete mix, the degree of compaction, and the curing conditions. From a strength perspective, the relationship between the water-cement ratio and porosity is undoubtedly the most important factor because, regardless of other factors, it affects the porosity of both the cement mortar matrixes and the interfacial transition zone between the matrix and the coarse aggregate.

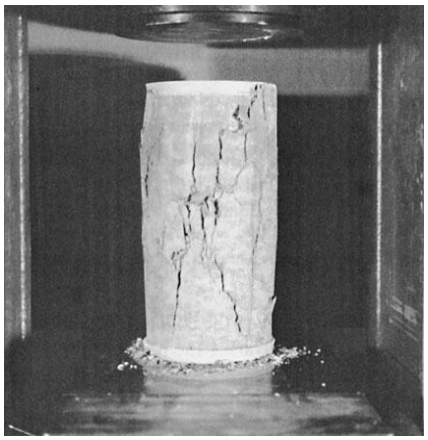

Figure 4-2: Typical failure mode of concrete under compression.

Since it is not feasible to directly determine the porosity of the matrix and the interfacial transition zone, two structural components of concrete, reliable models for forecasting concrete strength cannot be created. Though compressive strength is frequently used as an index of all other types of strength, numerous practical empirical relationships have been discovered over time that offer adequate indirect information on the influence of numerous factors on compressive strength. However, the precise way that concrete reacts to applied stress depends on a number of intricate interactions.

To facilitate a clear understanding of these factors, they can be discussed separately under three categories:

1) Characteristics and proportions of materials.
2) Hardening conditions
3) Test parameters.

5.4.1 Characteristics and proportions of materials:

The first step in producing concrete that satisfies the required strength is choosing the right ingredients and their ratios before mixing. Nonetheless, this article looks at a few of the crucial elements from the perspective of concrete strength. It should be underlined once more that many mix design parameters are interdependent in practice, making it impossible to fully isolate their influences.

5.4.1.1 Water-cement ratio:

Duff Abrams discovered a connection between the strength of concrete and the water-to-cement ratio in 1918 after conducting a number of tests at the Lewis Institute, University of Illinois. The expression for this inverse relationship is commonly referred to as Abrams' water-cement ratio rule.

$$fc = k_1/k_2^{\,w/c} \qquad (5.3)$$

Where w/c represents the water-cement ratio of the concrete mix and k_1 and k_2 are empirical constants. Typical curves illustrating the relationship between the water-cement ratio and strength at a given wet curing age are shown in Figure 5-3.

The w/c-strength relationship in concrete can be readily explained as the inevitable result of a progressive weakening of the matrix caused by the increase in porosity with the increase in water-cement ratio, in light of the factors that determine the strength of hydrated cement paste and the effect of increasing the water-cement ratio on porosity at a given degree of cement hydration.

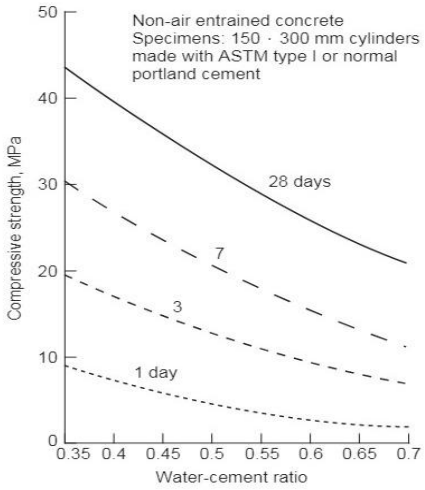

Figure 5.3. Influence of water-cement ratio and wet curing age on concrete strength.

However, the impact of the water-to-cement ratio on the interfacial transition zone's strength is not taken into account in this explanation. In low- and medium-strength concrete made with normal aggregates, the porosity of the interfacial transition zone and the porosity of the matrix determine strength, and a direct relationship between water-cement ratio and concrete strength holds. For high-strength concrete mixes (i.e., with very low water-cement ratios), this no longer appears to be the case.

For water-cement ratios below 0.3, disproportionately high increases in compressive strength can be achieved with very small reductions in the water-cement ratio. The phenomenon is mainly attributed to a significant improvement in the strength of the interfacial transition zone at very low water-cement ratios. Furthermore, the surface area of hydration products is proportionally larger and their crystal size is significantly smaller at low water-to-cement ratios.

5.4.1.2 Air entrainment.

Essentially, the porosity of the cement paste matrix at a particular degree of hydration is determined by the water-to-cement ratio; however, air voids can also increase porosity and decrease system strength when they are introduced into the system, either through the use of an air-entraining mix or as a result of insufficient compaction.

The curves in Fig. 5-4a show how increasing the volume of entrained air affects the compressive strength of concrete at a specific water-to-cement ratio. It has been noted that the amount of strength loss resulting from entrained air is dependent on both the cement content and the concrete mix's water-to-cement ratio (Fig. 5-4a). To put it briefly, the general strength level of the concrete can be roughly linked to the strength loss caused by entrained air.

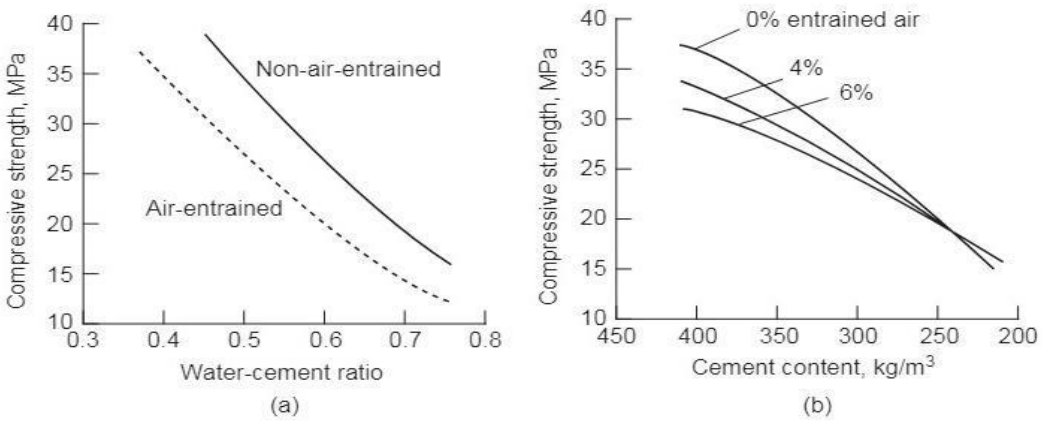

Figure 5-4 :Influence of water-cement ratio, entrained air and cement content on concrete strength.

Entrained air typically weakens concrete at a specific cement content or water-to-cement ratio. In fact, entrained air can boost strength for very low cement contents. According to the data in Fig. 5-4b, high-strength concretes (those with a high cement content) lose strength significantly as entrained air levels rise, while low-strength concretes (those with a low cement content) typically only lose strength slightly or even gain strength as a result of entrained air. This point is of great importance in concrete mix design.

The two conflicting effects of adding air to concrete can be used to explain how the cement content and water-to-cement ratio affect how concrete reacts to applied stresses. Entrained air will reduce the strength of the composite material by increasing matrix porosity. Conversely, entrained air tends to increase the strength of the interfacial transition zone (especially in mixes with very low water and cement content) by making the mix more workable and compactible, which in turn increases the strength of the concrete. With low-cement concrete mixes, it appears that the positive impact on the interfacial transition zone more than outweighs the negative impact on matrix strength when air entrainment is combined with a notable decrease in water content.

5.4.1.3 Type of cement:

Keep in mind that porosity and, in turn, strength are directly impacted by the degree of cement hydration. Because ASTM Type III Portland cement has a higher fineness and hydrates more quickly than other types at normal temperatures, concrete containing Type III Portland cement will have lower porosity and, as a result, higher strength at early hydration ages (such as 1, 3, and 7 days) and at a specific water-to-cement ratio. However, the rates of hydration and strength development with Type IV and Type V cements, as well as with portland-slag and portland-pouzzolan cements, are slower for up to 28 days when compared to ASTM Type I, Type II, and Type III portland cements. However, once they have attained a comparable level of hydration, the differences usually vanish.

5.4.1.4 Aggregate

Numerous issues have arisen in concrete technology as a result of an overemphasis on the connection between strength and the water-to-cement ratio. For instance, most people are unaware of how aggregates affect the strength of concrete. Since the aggregate particle is many times stronger than the matrix and interfacial transition zone of concrete, except for lightweight aggregates, aggregate strength is typically not a factor in normal-strength concrete. To put it another way, the other two phases determine failure, so aggregate strength is rarely used with most natural aggregates.

Concrete strength is known to be influenced to varied degrees by aggregate properties other than strength, such as size, shape, surface texture, grading (particle size distribution), and mineralogy. Changes in the water-to-cement ratio are frequently the cause of aggregate characteristics' impact on concrete strength. However, the published literature contains enough proof that this isn't always the case. Furthermore, it is predicted from theoretical considerations that the size, shape, surface texture, and mineralogy of aggregate particles will influence the characteristics of the interfacial transition zone and, consequently, affect concrete strength, regardless of the water-to-cement ratio.

Two opposing effects on concrete strength can result from a change in the maximum size of a well-graded coarse aggregate of a particular mineralogy. Concrete mixes with larger aggregate particles use less water to mix than those with smaller aggregates, even when the cement content and consistency are the same. Conversely, a weaker interfacial transition zone with more microcracks is typically formed by larger aggregates. Depending on the type of stress applied and the concrete's water-to-cement ratio, the overall effect will change. In the mesh range of 5 to 75 mm, Cordon and Gillispie (Fig. 5-5) demonstrated that the impact of increasing the maximum aggregate size on the 28-day compressive strengths of concrete was more noticeable for high-strength (water-cement ratio 0.4) and moderate-strength (water-cement ratio 0.55) concrete than for low-strength (water-cement ratio 0.7) concrete. In fact, the decreased porosity of the interfacial transition zone starts to significantly affect concrete strength at lower water-to-cement ratios. Furthermore, any change in the coarse aggregates' properties will likely affect the material's tensile-compressive strength ratio because the interfacial transition zone's characteristics have a greater impact on concrete's tensile strength than its compressive strength.

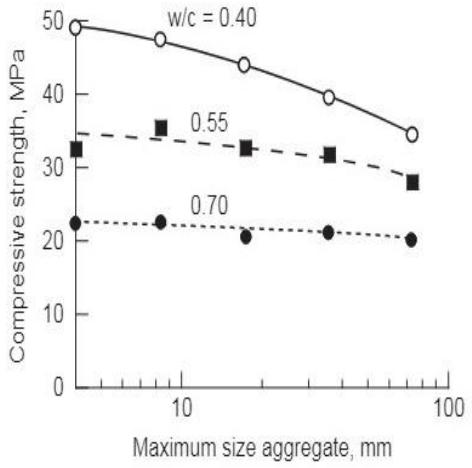

Figure 5-5: Influence of aggregate size and water/cement ratio on concrete strength.

The tensile strength-compression ratio will rise with a decrease in coarse aggregate size at a specific water-to-cement ratio.

When a change in aggregate gradation causes a corresponding change in the consistency and bleeding properties of the concrete mix, it can affect the strength of the concrete without affecting the maximum coarse aggregate size and while maintaining a constant water-to-cement ratio. In a laboratory experiment, the average 7-day compressive strength decreased by about 12% when the cement content and the proportion of coarse/fine aggregates in a concrete mix were gradually increased to increase the consistency of (50 to 150 mm) slump, while maintaining a constant water-cement ratio of 0.6. Fig. 5-6 shows how concrete mix strength and cost are affected by greater consistency.

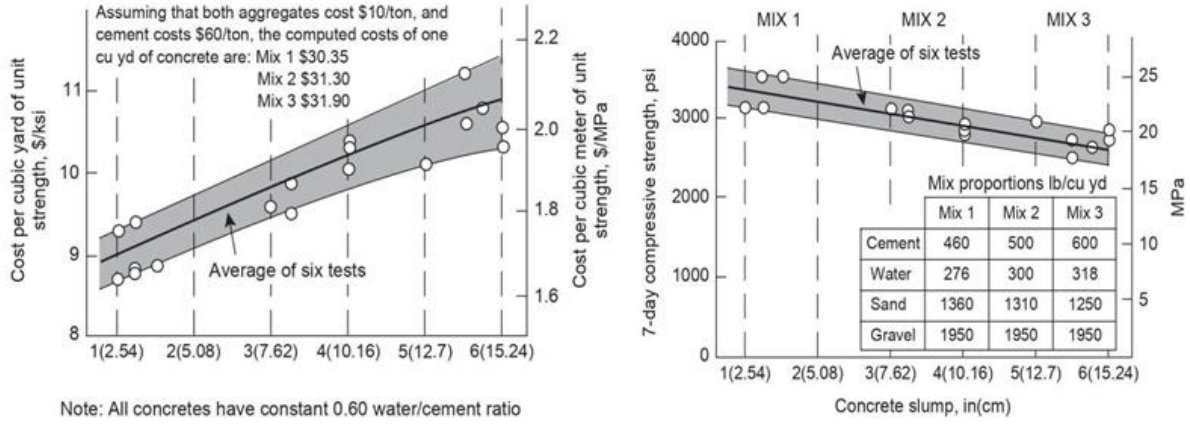

Figure 5-6: Influence of concrete slump on compressive strength and cost.

Concrete mixes with higher slumps typically provide less strength for a given water-to-cement ratio. Producing concrete mixes with higher slumps than required is not economical.

A concrete mix with a crushed or rough-textured aggregate has been found to show somewhat greater strength (especially tensile strength) at an earlier age than a corresponding concrete mix with a smooth or weathered aggregate of comparable mineralogy. This is believed to be caused by a stronger physical bond between the aggregate and the hydrated cement paste. The impact of aggregate surface texture on strength may diminish as the cement paste and aggregate start to interact chemically. Under a microscope, a smooth piece of weathered gravel seems to have sufficient roughness and surface from the perspective of the physical bond with the cement paste. Moreover, with a given cement content, a little extra mixing water is generally required to achieve the desired workability in a concrete mix containing rough-textured aggregates; thus, the small advantage due to better physical bonding may be lost in terms of overall strength.

Concrete strength is also known to be impacted by variations in aggregates' mineralogical composition. Reports show that, with identical mix proportions, substitution of a limestone by a siliceous aggregate can result in improved strength. For instance, Fig. 5.7 shows that concrete strength at 56 days was greatly increased by both a reduction in the maximum size of coarse aggregate (Fig. 5.7a) and a substitution of limestone for sandstone (Fig. 5.7b). The increased interfacial bond strength with the limestone aggregate at an advanced age could be the cause of this.

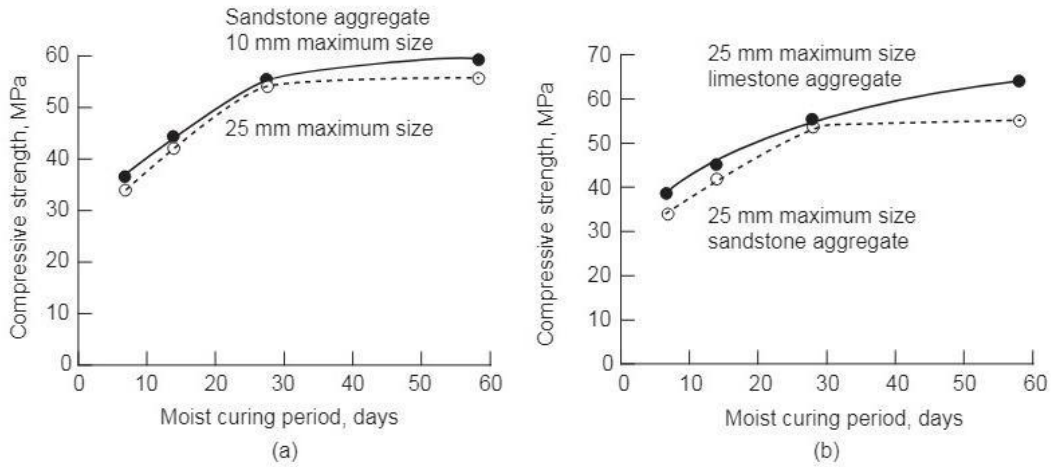

Figure 5-7: Influence of aggregate size and mineralogy on the compressive strength of concrete.

The choice of aggregate size and type can have a significant impact on concrete strength for a given cement content and water-to-cement ratio.

5.4.1.5 Water mixing:

Excessive impurities in the water used to mix concrete can impact not only the strength of the concrete but also its setting time, corrosion of the reinforcement and prestressing steels, and efflorescence, which are white salt deposits on the concrete surface. Since many specifications for the production of concrete mixes require the water used to be fit for consumption and municipal drinking water rarely contains dissolved solids in excess of 1000 ppm (parts per million), mixing water is generally rarely a factor in concrete strength.

Generally speaking, water that is unfit for human consumption is not always unfit for mixing concrete. It is not necessary to completely reject water that is slightly acidic, alkaline, salty, brackish, colored, or malodorous. Given the scarcity of water in many regions of the world, this is crucial. Additionally, recycled water from mines, cities, and numerous industrial processes can be used to mix concrete in a safe manner. The most effective method for assessing whether unknown water is suitable.

The process for making concrete involves comparing the cement take-time and resistance of mortar cubes made with unconverted water to a reference water that is owned. The cubes made using the questionable water should have compression resistances of 7 and 28 days that are equal to or 90% equal to the resistance of reference products made with their own water; additionally, the quality of the gâchage water shouldn't have an unacceptable impact on the cement's take-time.

The strength of regular concrete is unaffected by seawater, which has about 35,000 parts per million of dissolved salts. The use of seawater as concrete mixing water should be avoided in these situations because it raises the risk of steel corrosion with reinforced and prestressed concrete. Generally speaking, excessive amounts of algae, oil, salt, or sugar in the mixing water should raise red flags from the perspective of concrete strength.

5.4.1.6 Admixtures:

As was previously mentioned, air-entraining admixtures have a negative impact on the strength of concrete. Water-reducing admixtures can increase the initial and final strength of concrete by lowering the water content of a concrete mix at a specific consistency. The presence of water-reducing admixtures in concrete typically has a positive impact on cement hydration rates and early strength development at a specific water-to-cement ratio. The rate of strength gain would obviously be greatly impacted by additives that could speed up or slow down cement hydration, but final strengths might not be greatly impacted. Numerous researchers have noted that when the rate of strength gain at early ages is postponed, concrete tends to have higher ultimate strengths.

The use of cementitious and pozzolanic by-products as mineral admixtures in concrete is steadily growing for both economic and environmental reasons. Mineral admixtures typically have a delaying effect on early-age strength when used as a partial substitute for Portland cement. The porosity of the matrix and the interfacial transition zone can be significantly decreased, though, if a mineral admixture has the capacity to react with calcium hydroxide (found in hydrated Portland cement paste) at room temperature and produce an extra calcium silicate hydrate. As a result, adding mineral admixtures to concrete can significantly increase its ultimate strength and watertightness. It should be mentioned that adding mineral admixtures to concrete is a particularly good way to increase its tensile strength.

5.4.2 Hardening conditions

The phrase "concrete hardening" refers to a confluence of factors that promote cement hydration, specifically the time, temperature, and humidity levels immediately following the placement of a concrete mix in formwork.
The degree of cement hydration determines the porosity of a hydrated cement paste at a specific water-to-cement ratio. Certain Portland cement ingredients start to hydrate as soon as water is added at room temperature, but hydration reactions significantly slow down once the hydration products cover the anhydrous cement grains. Actually, hydration can only continue in a saturated state; when the capillaries' water vapor pressure drops below 80% of saturation humidity, it nearly stops. Therefore, time and humidity play a significant role in the water diffusion-controlled hydration process. Furthermore, hydration reactions are accelerated by temperature, just like all other chemical reactions.

5.4.2.1 Time:

It should be noted that time-strength relationships in concrete technology generally assume wet curing conditions and normal temperatures. At a given water-cement ratio, the longer the wet curing period, the higher the strength (Fig 5.3), assuming hydration of the anhydrous cement particles continues. In thin concrete elements, if water is lost through capillary evaporation, air-curing conditions prevail and strength will not increase over time (Fig. 5.8). The evaluation of compressive strength over time is a major concern for structural engineers. ACI Committee 209 recommends the following relationship for wet-hardened concrete made with normal Portland cement (ASTM Type I):

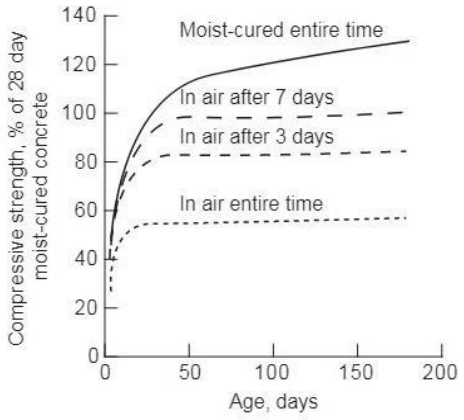

Influence of curing conditions on strength.

Unless curing occurred in the presence of moisture, the curing age would not improve the strength of the concrete.
The CEB-FIP (1990) model code proposes the following relationship for concrete specimens hardened at 20°C:

$$f_{cm}(t) = \exp\left\{ s\left(1 - \sqrt{\frac{28}{t/t_1}}\right)\right\} f_{cm}$$

Where: $f_{cm}(t)$= average compressive strength at age t days
f_{cm} = average compressive strength over 28 days
s = coefficient depending on cement type, such as s = 0.20 for high early strength cements, s = 0.25 for normal hardening cements; s = 0.38 for slow hardening cements.
t_1 = One day

5.4.2.2 Humidity

The data presented in Figure 5.8 clearly illustrates the impact of curing moisture on concrete strength. At a specific water-to-cement ratio, the strength of continuously moisture-cured concrete was three times higher than that of continuously air-cured concrete after 180 days. Additionally, thin moisture-hardened concrete elements experience a slight regression in strength when exposed to air-drying, most likely as a result of drying shrinkage-induced microcracking in the interfacial transition zone. In addition to the concrete element's surface-to-volume ratio, temperature, relative humidity, and ambient air velocity all affect how quickly water evaporates from concrete after placement.

For concrete that contains regular Portland cement, a minimum of 7 days of wet curing time is advised; naturally, a longer curing time is preferred for concrete mixtures that contain blended Portland cement or mineral admixture in order to guarantee the strength contribution of the pozzolanic reaction. Spraying, ponding, or covering the concrete surface with moist sand, sawdust, or cotton mats are methods for achieving moisture curing. The proper application of an impermeable membrane soon after concrete placement offers a suitable way to maintain strength development at a satisfactory rate because the amount of mixing water used in a concrete mix is typically more than necessary for the hydration of port cement (estimated at around 30 percent by weight of cement).

5.4.2.3 Temperature:

The time-temperature history of casting and hardening determines how temperature affects strength in wet-hardened concrete. Three scenarios—concrete poured and hardened at the same temperature, concrete poured at a different temperature but hardened at a normal temperature, and concrete poured at a normal temperature but hardened at a different temperature—can be used to demonstrate this.

When concrete is cast and cured at a specific constant temperature between 5 and 46°C, it is typically found that, for up to 28 days, the higher the temperature, the faster the cement hydrates

and gains strength. It is clear from the data in Figure 5-9 that specimens cast and cured at 5°C had a 28-day strength that was about 80% of those cast and cured between 21°C and 46°C. Differences in concrete strength eventually vanish along with variations in the degree of cement hydration. However, as will be discussed below, it has been found that the ultimate strength decreases with increasing pouring and curing temperatures.

A distinct pouring and curing time-temperature history is depicted in Figure 5-9b. All concrete mixes were wet-hardened at a consistent temperature of 21°C after the pouring temperature, or the temperature in the first two hours following the manufacture of the concrete, fluctuated between 10 and 46°C. According to the data, concrete cast at 5°C or 13°C had higher ultimate strengths (180 days) than concrete cast at 21, 30, 38, or 46°C. Numerous researchers have deduced from microscopic analyses that the higher strength of low-temperature casting is due to a comparatively more homogeneous microstructure of the hydrated cement paste, specifically the distribution of pore sizes. Figure 5-9c illustrates how the curing temperature affects strength using concrete mixes that were cast at 21°C and then cured at different temperatures ranging from below zero to 21°C. In general, the lower the curing temperature, the higher the strength up to 28 days. At temperatures close to freezing, concrete's strength at 28 days was roughly half that of concrete cured at 21°C; at temperatures below freezing, almost no strength developed. It appears that sufficient temperature levels must be maintained for a long enough period of time to provide the activation energy required for the reactions to start, given the slow hydration reactions of Portland cement compounds. This permits unhindered progress in the strength development process linked to the gradual filling of voids with hydration products.

The influence of time-temperature history on concrete strength has several important applications in concrete construction practice. Since curing temperature is far more important for strength than placing temperature, ordinary concrete mixes that are placed in cold weather must be kept above a certain minimum temperature for a sufficient length of time. Concrete cured in summer or tropical climates can be expected to have higher initial strength but lower ultimate strength than the same concrete cured in winter or colder climates. In the precast concrete industry, steam curing is used to accelerate strength development for faster demolding. In solid elements, when no temperature control measures are taken, the concrete temperature will remain at a much higher level than the ambient temperature for a long time. Consequently, compared with the strength of samples treated at normal laboratory temperature.

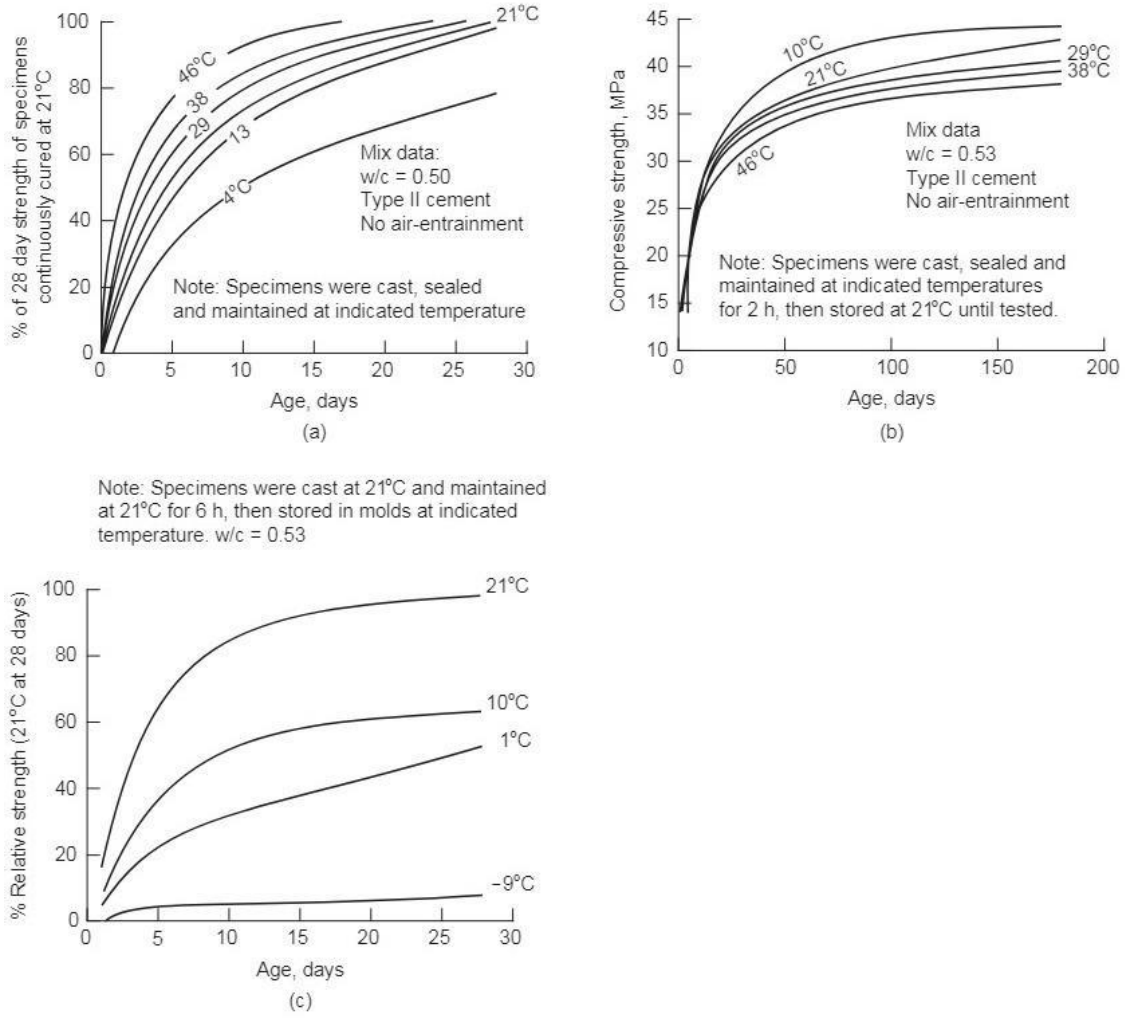

Figure 5-9: Influence of pouring and curing temperatures on concrete strength.

Temperatures at which concrete is poured and cured regulate the degree of cement hydration, which has a significant impact on the strength development rate and final strength.

5.4.3 Test parameters

It is sometimes overlooked that specimen and loading condition parameters have a big impact on concrete strength test results. The impact of concrete's size, shape, and moisture content are examples of specimen parameters; the amount, duration, and rate of stress application are examples of loading parameters.

5.4.3.1 Sample parameters

A 15 x 30 cm cylinder is the typical specimen used in the USA to test the compressive strength of concrete. When a concrete mix is tested in compression using cylindrical specimens of different diameters, the greater the diameter, the lower the strength, provided that the height/diameter ratio remains at 2. According to the data in figure 5-10, the average strength

of the cylindrical specimens measuring 5 x 10 cm and 7.5 x 15 cm was 106 and 108 percent, respectively, when compared to standard specimens. A significantly smaller decrease in resistance is seen when the diameter is increased above 45 cm.

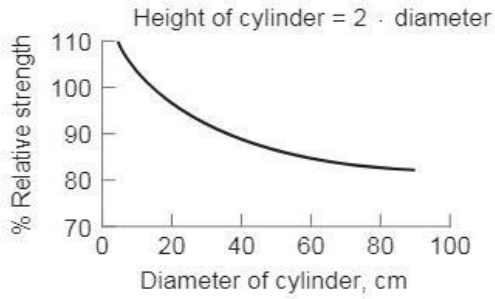

Figure 5-10: Influence of specimen diameter on concrete strength the height-to-diameter ratio is equal to 2

Specimen geometry can affect laboratory test data on concrete strength. Size effects do not significantly affect the strength of cylindrical specimens with a diameter greater than 30 cm or a slenderness ratio (H / D) greater than 2.

Fig. 5.11 shows how altering the specimen geometry (height/diameter ratio) affects the compressive strength of concrete. Generally speaking, strength decreases with increasing specimen height/diameter ratio. For instance, specimens with a height/diameter ratio of 1 demonstrated strength that was roughly 15% higher than that of standard specimens (height/diameter ratio equal to 2). It might be worthwhile to note that concrete strength tests using the common 15 cm cube used in Europe would yield a strength that is 10 to 15% greater than that of the same concrete mix tested using standard American procedure.

Standard procedure stipulates that specimens must remain moist during testing due to the impact of moisture state on concrete strength. Air-dried specimens have been found to have a strength that is 20 to 25 percent greater than corresponding specimens tested in a saturated state in compression tests. The disjunction pressure in the cement paste is the cause of saturated concrete's decreased strength.

5.4.3.2 Loading conditions

A uniaxial compression test (ASTM C 469) is used in laboratories to measure the compressive strength of concrete. The specimen is dropped in two to three minutes after the load is gradually increased.

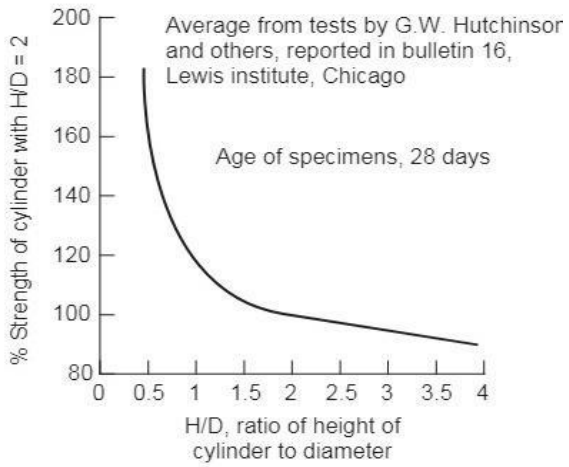

Figure 5.11: Influence of length/diameter ratio variation on concrete strength

In actuality, the majority of structural components endure an indefinite dead load as well as sporadic impact or repeated loads. Therefore, understanding the relationship between concrete strength under laboratory test conditions and actual load conditions is desirable. The next section describes how concrete behaves under various stress conditions. This description leads us to the conclusion that strength is significantly impacted by the loading condition. Fig. 5.12 provides a summary to help visualize the intricate network of numerous factors affecting concrete strength.

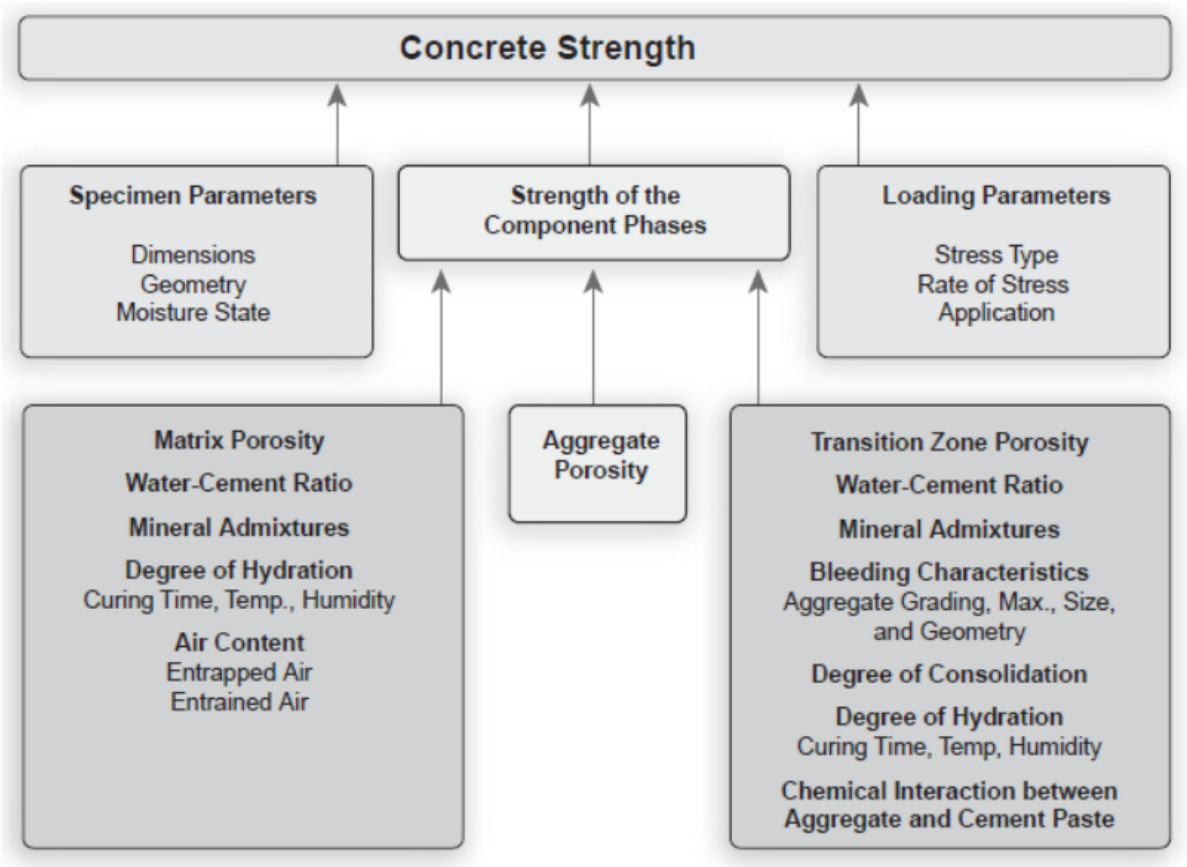

Figure 5-12 Interplay of factors influencing the concrete strength.

Chapter 6:

Sophisticated analytical techniques for investigation the microstructure of cements

6.1 SCANNING ELECTRON MICROSCOPE (SEM)

6.1.1 Introduction

The first microscopes were made with the view of the small things i.e. magnifying small things and seeing them clearly (high resolution) as their main features.1630, the invention of light-based simple microscopes that are capable of resolving 1 micron (μm). Still, looking at such small magnifications was not popular until the idea of using an electron source for magnification was developed and this eventually led to the electron microscopy. The widespread use of electron microscopes is due to their enormous high zoom and high quality; they even allow scientists to see things that are below the size of an atom. Since the electron size is much smaller than that of the atom, one cannot actually see electrons used as a source for magnification with the naked eye. Hence, electron microscopy has a monitor that can transform the strength of electrons into the strength of light for taking pictures or looking at. Lately, due to the rapid development in technology, imaging can also be done through television detectors.

All natural substances consist of atoms; each atom is composed of a center and electrons. In the electron microscope technique used for imaging a material, electrons will have a strong interaction with the sample. The interaction will be of such nature that the electrons situated in one of the shells around the nucleus can be released. This event leads to the generation of various electron signals from the specimen being examined. These electron signals can be taken as a means to analyze and know the material. The various types of signals that come out during the interaction are:

1. Backscattered electrons (BSE)
2. Auger electrons
3. Secondary electrons (SE)
4. Characteristic X-rays
5. Visible light
6. Elastically scattered electrons
7. Bremsstrahlung X-rays
8. Inelastically scattered electrons

X-rays are one of the main secondary signals generated during the interaction, and their production is through each element present in the sample. Each of these X-rays has a specific wavelength and is indicative of a certain element. The quantification and analysis of materials can be done through energy dispersive spectroscopy (EDS), which takes advantage of this fact.

6.1.2 Apparatus Required and Their Usage

The scanning electron microscope (SEM) should be thought of as a mapping tool, not as an imaging device. The sample to be analyzed is positioned and hit by a beam of electrons through an electron column. Electrons that scan the surface of the sample produce images of the sample. The electron column basically includes an electron gun (cathode and the related electrodes), which is Situated in a very well vacuum and connected to a high voltage output source (30–40 kV) (Anwar, 2018). The electron's speed and density can be altered by controlling the voltage across the gun. The pressure at which the electrons from the electron gun strikes the sample surface is determined by the accelerating voltage (usually adjusted between 2 kV and 30 kV). The brightness and current density are the key factors determining the performance of the electrons coming from the electron gun. With the movement of the electron source closer to the sample in the electron column, the current density of the source electron changes. This occurs because various parts within the electron column block the flow of electrons, thus the current density is reduced. However, one can also look upon the brightness as an indicator of the electron gun's performance. Brightness can be described as the amount of electrons the source outputs in a particular area along with the solid angle that the emitted electrons cover. Therefore, the angular speed of the beam while moving is very important as well. Thus, the electron column has a uniform brightness all over its length. Besides, the brightness has a direct relationship with the voltage that is applied at the output source. Hence, the glowing of source (filament in electron gun) gets stronger when the applied voltage gets higher. The characterization of brightness is crucial in this case. The current (the electrons, in this case) coming from the probe of a specific diameter is very much dependent on the brightness. Therefore, the brightness will control how many electrons can strike a certain area on the sample within 1 second. Consequently, this will have an impact on the detail of the image produced.

Another factor that will influence the quality of the image obtained is the size of the source (i.e.; the size of the electron released from the probe (tip of the source)). If the tip of the electron source is very small then the diameter of the released source will be less; this leads to high spatial resolution. Hence the electron source from where it is released should be of the least possible diameter. This will lessen the work of de-magnifying the electron source. Hence, a high current will be present in the probe to image the sample, which will ultimately result in excellent imaging. Similarly, many electromagnetic lenses (consisting of copper coils and iron shields) and the voltage applied to them should be controlled extremely well to achieve the desired focal length. Therefore, the focus of the electron on the sample can be very accurately

controlled for better brightness and proper resolution by a powerful condenser lens, which has a bigger demagnification. Similar to the lenses, the apertures are a small rectangular strip made up of molybdenum. They are employed to regulate the convergence angle of the electrons that are travel through the column. A scanning electron microscope is depicted in Figure 6.1.

6.1.3 Working Principle

The SEM is equipped with a source of electrons, the best resolution of the SEM is achieved by regulating the opening of the last electron beam that comes from the source. A cathode is usually employed as the electron emitter. The cathode that is often utilized is thermionic tungsten. But the use of tungsten due to its relatively short life has been replaced by a sintered polycrystalline material made of lanthanum hexaboride (LaB6), which is infinitely brighter and has a long-life span. The electron source requires enlarging and reducing it through a series of electron lens systems. Normally, the electrons when emitted from the cathode or electron gun have a diameter of 10-50 μm. This is de-magnified to a size of 1 nm to 1 μm. Reducing lenses or condenser lenses (primarily a magnetic field outside the electron gun) are utilized for the electron beam de-magnifying from the source in such a manner that the final spot on the sample is covered by 1-2 nm. An objective lens is then used as the final lens in controlling the movement of the probe to focus the image of the sample.

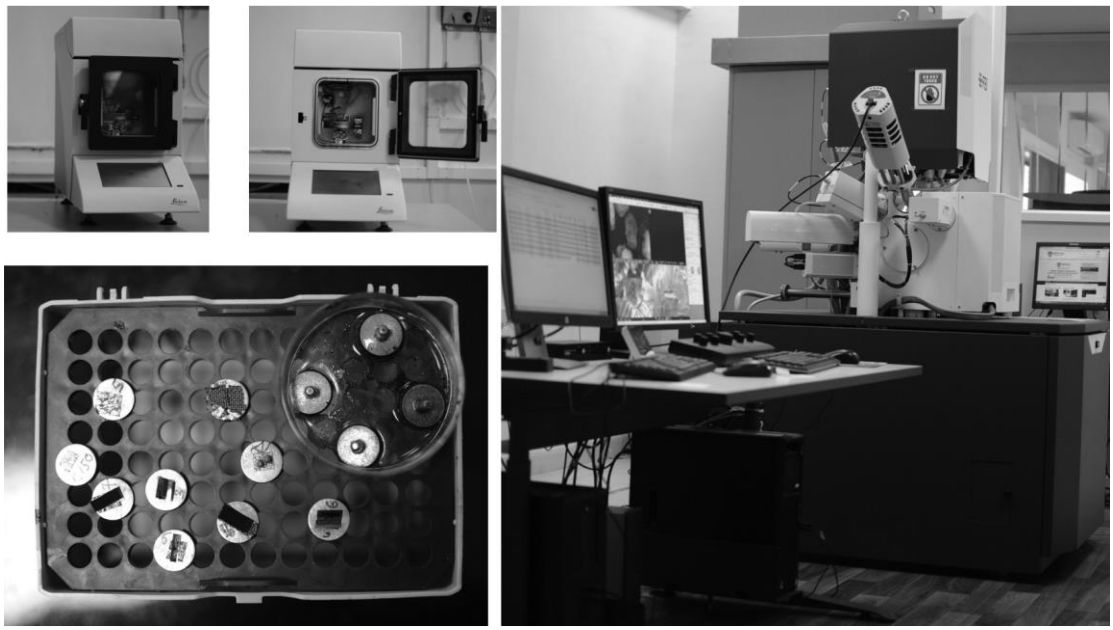

FIGURE 6.1 Scanning electron microscope.

When the electron beam collides with the surface of the sample, various electrons are ejected from the sample. The two major types of electrons that leave the sample are backscattered

electrons (BSEs) and secondary electrons (SEs). BSEs are produced as a result of elastic scattering while SEs are produced due to inelastic scattering. The selective detection and collection of these electrons are the key factors in successful observation. To that end, the SEM is designed with different electron collectors to capture BSEs and SEs emitted from the sample. The electrons are the ones that form the SEM images. BSEs are energetic in nature and can even come out from a few micrometres below the sample. They go straight through and carry very crucial information such as the average atomic number and the chemical background of the sample being examined. The SEs, on the other hand, mainly carry the topographic features of the sample. After collection, the SEs and BSEs can be used separately or together to generate a signal, and this signal is further transformed into an image.

Backscattered Electrons (BSE)

Electrons emitted from a subsurface depth of a few micrometres are the ones mentioned here. The overall atomic number of the elements in the sample being studied-on, that is compositional image, is the main information transported by these electrons. A detector made from solid-state photodiodes is utilized to gather BSEs. An increase in the mean atomic number results in a corresponding increase in the intensity of the image.

Secondary Electrons (SE)

The electron collectors (Everhart-Thornley (ET-detectors)) are responsible for detecting the secondary electrons and collecting them. The scheme of the sample is revealed by the image produced from the SEs collected. These electrons are ejected from the superficial layer of the sample that is being studied. The morphological features of the specimen can be revealed with SE mode.

6.1.4 Steps Involved in Sample Preparation Specific to Cement-Based Materials

Step 1. Cast samples (hard cement paste/mortar/concrete) are sliced into proper dimensions. To cease the hydration, the samples that are ready are immersed in iso-propanol. The iso-propanol solution is changed every 1 hour during the first 5 hours and then it is changed once every 24 hours. Most of the time, the samples are kept for one day in order to stop the hydration. Some studies such as microstructure development with respect to time; then the samples are placed in iso-propanol after the specified time in which the microstructure needs to be studied.

Step 2. Among the important and essential requirements during the preparation of the sample for SEM analysis, coarse grinding and polishing of the surface of the sample to be studied are included.

Step 3. A silicon carbide sheet is chosen for initial manual grinding and thus the sample preparation is done. The grinding has to be continued for a long time until the surface of the sample becomes glossy or shiny when the sample is held against the light.

Step 4. Once the grinding of the surface has been completed to the desired level, the surface is cleaned with compressed air to get rid of the remaining powders. After the surface is verified to be at the required level, it is put in the desiccator. The process of lowering the pressure is done in such a way that the desiccator has no air at all.

Step 5. SEM analysis requires the sample to undergo the process of being impregnated in resin epoxy. The impregnation is carried out using a tiny custom-made mould crafted from a polyvinyl chloride (PVC) pipe or a silicone mould or a mould, which is capable of performing the impregnation task efficiently.

Step 6. Clean and flat arrangement of the sample is the first step. Next, position the mould and centre it around the sample. According to the instructions given by the producer, pour the mixed resin into the mould while making sure that the sample is right at the centre. Very carefully, make sure that no resin is going under the sample.

Step 7. During the impregnation of the sample into the resin, it is necessary to avoid the occurrence of any air bubbles; this can be done by putting the impregnated sample in a desiccator under low pressure for 4–8 hours. The duration varies with the amount of air bubbles to be removed in the process.

Step 8. The grinding in advance that was done in steps 3 and 4 was performed only to guarantee that the sample's surface was evenly and smoothly prepared for the subsequent operation of grinding and polishing.

Step 9. After successfully impregnating the sample in the epoxy resin, the samples are then subjected to fine grinding and polishing. The grinding and polishing machine is used to grind and smoothen the surface of the sample to be diagnosed. Initially, the samples are ground to get rid of the resin layer over the sample.

Step 10. Polishing is then performed after the resin has been completely removed from the surface of the sample (which can be verified by light exposure and checking for glossy or shiny surface). The necessary amount of polishing can be determined by the sample's observation through an optical microscope.

Step 11. The polishing process is carried out using a diamond grinder that is specially made for this purpose. The lubricant used is either petrol or iso-propanol or any other solvent that is not reactive with the sample. The solvent used should be non-hazardous and should not react with the sample, thus preventing the formation of new or additional hydration products.

Step 12. The specimen, after being ground and polished to the desired finish, receives a thin layer of conductive material which allows it to be used for the SEM trial and subsequent analysis.

Step 13. The whole sample preparation procedure from step 2 to step 11 mentioned above is only preferred if the intention is to get the SE images, BSE images as well as the FDXM (characteristic X-ray of the elements that are excited).

Step 14. The following steps can be taken for a very basic understanding of the images obtained from the SEM experiment.

1. Chemical composition analysis should be done at least twice for each place. To get the right quantification for C-S-H, at least 200 places should be analyzed.

2. For different phases in the system with very close chemical compositions (like: C3S, C2S), elemental ratios can be calculated and then used to find the variation. For example, in C3S there are 3 calcium for every silicate and in C2S there are 2 calcium for every silicate; therefore, the difference in amount obtained during imaging can lead to each phase being identified.

3. A thorough comprehension can be achieved by analyzing the phases via ratios. The chart of Al/Ca ratio versus Ca/Si ratio, for instance, can provide a considerable amount of information on the present phases.

4. One of the primary disadvantages of the method discussed above is its ineffectiveness in the case of less-heavy metals detection such as hydrogen.

5. When it comes to calcium hydroxide (Ca (OH)2) and free lime (CaO), differentiation can be made through the hydration time and compositional ratios.

i. In such cases, the oxygen from Ca (OH)2 would be larger than the oxygen from free lime.

ii. Sample hydration time: If the hydration time is three days, then, more or less, free lime will have been consumed by then due to its higher reactivity.

6. SEM images are capable of revealing the phase of the material and the extent of its crystallinity after processing so that the reactivity of the material can be understood. 7. The combined action of BSEs and SEs is advantageous in most instances for determining the phases and the morphology of the hydration products.

8. SEM pictures can be divided into point detection and phase mapping when FDXM is used for compositional analysis.

9. The mapping of the phases obtained by this procedure is more advantageous than the results from other techniques.

It's important to point out that in the process of sample preparation water must be eliminated from the sample to prevent the development of static electricity on the sample surface that might cause images to be distorted.

6.1.5 Experimentation and Interpretation of Obtained Results

Electrons that are generated from the electron gun move like a beam over the surface of the sample. In this action, the electrons are participating in an atomic scale interaction with the sample. Atoms are the smallest units of an element and these elements can be put together to make different kinds of materials. Cement is one such material, which is the result of processing different compounds. The chemical reaction of cement with water leads to the formation of hydration products. When a cement sample is prepared by the methods specified in sample preparation, then the material is put under the electron source in the SEM, a high contrast image can be produced by the detection of BSEs and SEs. The two main kinds of scattering occurring due to the electron beam hitting the sample surface are elastic and inelastic scattering.

Elastic Scattering and Inelastic Scattering

If the electrons coming from the sample are the ones already in the beam (from the electron gun), the scattering is called as elastic scattering when the kinetic energy of the electrons (negatively charged) does not vary much because of the deflection of the nucleus (positively charged). Backscattered electrons (BSE) are those electrons emerging from the sample. The latter is the case where scattering has the highest probability in heavy-element materials due to their nucleus being very strong and positively charged. The higher the energy of the electron, the less its tendency to scatter elastically. This happens because the electrons will have enough kinetic energy to overcome the attractive forces of the nucleus which results in less elastic scattering. The BSEs generate backscattered electron images that are usually referred to as such. These images can reveal compositional or atomic number contrast.

Conversely, inelastic scattering occurs when the incoming electrons are attracted to the atomic nuclei and, as a consequence, lose part of their kinetic energy. Here, the electrons eject the weakly bound orbital electron from the atom, thus vacating the atom's orbiting shell. The electrons are turned at minor angles (since their accelerating energy is greater). The electrons emitted from the elemental shells are referred to as secondary electrons (SE). These are associated with the atoms of the sample under examination. The pictures generated by these electrons are referred to as secondary electron images. These images are helpful for revealing morphological details.

The main distinguishing factor between BSEs and SEs is the energy level in which they occur. SEs are characterized by an extremely low energy level (50 eV or less). This energy level is considered as a dividing line between the two types of electrons, separating SEs from BSEs.

Backscattered Electron Image or Compositional Contrast or Z-Contrast

The compositional and atomic number contrast that occurred during the collection of BSEs was caused by differences in the atomic number for the elements in the sample being analyzed. With high atomic number elements, elastic collision will be the main process. The result is that there will be a more BSE. This can be represented by a coefficient known as the backscatter coefficient. This coefficient is the outcome of the ratio between the number of backscattered electrons and the number of incident beam electrons. For high atomic number elements in the sample, the backscattered coefficient ratio will be at its maximum. This is because the attractive forces of the nucleus of high atomic number elements also will be higher. Thus, their electrons will undergo the highest elastic scattering. Besides, those electrons can be drawn back from the sample surface without losing much of their kinetic energy. This leads to an increase in signal strength because of the higher backscatter coefficient and as the BSEs have the maximum energy. Hence, in the case of the sample, the resulting contrast will be the brightest for the high atomic number (high density) element and darkest for the low atomic number (low density) one. As a result, the passage of the electron source through the voids will cause the obtained compositional image to show a dark contrast. This is also the case with cement samples. Meanwhile, at low beam energy (less than 5 keV from the source) the backscatter coefficient will behave vice versa (i.e. the backscatter coefficient for elements with low atomic number (less than 30) will increase and for those with high atomic number (more than 30) it will decrease). This makes matters complicat.

Overall, to summarize, the compositional contrast will be brighter (i.e. strong contrast) for the phases with high atomic number and will be dark (i.e. weak contrast) for the phases with low atomic number. Moreover, to differentiate two phases with low atomic numbers, compositional contrast (z-contrast) can be used if the difference in obtained contrast is more than 10%. Since SEM can differentiate a compositional contrast equal to or more than 10%. On the other hand, using compositional contrast to discern between phases of high atomic number is difficult. As the percentage difference in their compositional contrast is very low (less than 1%), it cannot be differentiated by SEM. Backscattering coefficient can be calculated by the following empirical equation

$$\eta = - 0.0254 + 0.016\, Z - 1.86\times10^{-4}\, Z^2 + 8.3\times10^{-7}\, Z^3$$

In this equation, η being a backscattering coefficient, Z referring to the atomic number of the atom under observation.

Z-contrast (Cz) is the term used to describe the difference between two points in a sample. The following is a definition of z-contrast between two locations in the sample.

$$Cz = \frac{\eta 2 - \eta 1}{\eta 2}$$

Where, η1 and η2 are different backscattering coefficients at different locations The BSEs method not only provides compositional contrasts, but also reveals topographical contrasts through directionality component of BSEs. The roughness of the sample surface affects the directionality component, which in turn changes the emitted BSE trajectories. Hence, the separation of directionality component from z-contrast can provide topographical images in isolation.

Secondary Electron Image or Topographical Contrast

Just like BSEs the SEs have a secondary electron coefficient (δ) in case of the SEs. It is a ratio of the secondary electrons produced from the sample to the number of the incident beam electrons. Typically, the exhalation depth of SEs is smaller than that of BSEs. This happens because the secondary electrons come out of the surface of the sample after the inelastic collision. So, SEs do not bear very high energy as opposed to BSEs, which are electrons from an electron gun. When the SEs are coming out of the surface of the sample through inelastic collision, then the energy level of these electrons will be very low. With a low energy level (<50 eV) their ability to escape from the surface will be tough because this will not be enough to go beyond the work potential of the sample surface. Likewise, the depth from which these electrons come out is of a few nanometres (nm) as compared to BSEs which can be a few μm.

One of the main factors that contribute to the emission of secondary electrons from shallow depths is the high energy levels of the inner shell electrons of the atom, which are very hard to extract. Once the inner electrons are taken out, they will not have enough energy to leave the sample surface due to numerous inelastic collisions with other electrons. As a consequence, the SEs are emitted from a few nanometres of the sample surface. It is noteworthy that the emanation depth will be even smaller for conductive samples in comparison with insulating materials. The SEs will possess very low kinetic energy of less than 50 eV. It is estimated that around 90% of the SEs will have energy below 10 eV.

Metals during the process of secondary electron (SE) emission release SEs with different characteristics: SE1 coming from the point of electron interaction where the electron beam from the gun hits and SE2 originating at a farther distance away from the source of the electron. SE2 are mainly produced by the inelastic scattering of BSEs that can collide with some electrons in the orbiting shells of the atoms leading to the production of SE2 electrons. The SE2 signal is much stronger than the SE1 signal. But the current density distribution of SE1 is higher; thus, the resolution at high magnification is determined by SE1 electrons, while SE2 electrons contribute to the background. In the case of light elements, SE1 will take priority; this is because the inelastic scattering of BSEs will be less as the number of BSEs available will be smaller. On the other hand, in the case of heavy elements, SE2 will be favored due to the larger number of inelastic scattering events involving BSEs. In the case of heavy elements, the attraction of the nucleus will be stronger leading to more BSEs and thus more inelastic scattering which in turn results in more SE2 electrons being emitted from the surface of heavy-element-containing samples. At low beam energy, the depth of penetration of the source

electron becomes slim. Hence, the secondary electron (SE) coefficient will be correspondingly high. The reason for this is the fact that these electrons are emitted at a low energy from a shallow depth of the surface. SEs emitted from the sample surface are not related to the atomic number of the sample elements; however, surface contaminations do significantly influence SE emission.

SEs are utilized for determining the size, shape, and surface texture of the samples (topographical features, in other words). In this respect, secondary electron microscopy is the main technique used to assess the sample's surface properties. The Everhart-Thornley (ET-detectors) detectors are the ones collecting the SEs when the ET-detectors have a positive bias (+200–300 V). A phenomenon called edge effect brings about the increase of brightness in certain parts of the sample. This is because those parts of the sample emit more secondary electrons. This usually occurs on raised areas, steep surfaces, protrusions, edges of thin surfaces, and holes. The flat areas around these mentioned areas will look less bright. Likewise, spherical particles will be very bright because of the grazing effect.

When the beam hits the surface of the spherical particles at an angle, a greater number of SEs come up from the surface layer. But, as one goes deeper into the surface, smaller number of SEs will be produced, and this also occurs when the beams hit the surface at a right angle of 90°. The electron beam continuously loses energy until it reaches a point where the remaining energy is just a few eV when it finally stops. The depth of penetration of electrons in the sample is influenced by various factors, such as the specimen's density, the atomic number of the atoms, the energy of the incident beam, and the stopping power of the sample being studied. The approximate decrease in the electron energy is about 1–10 eV for each nanometer (nm) of penetration by the electrons. In general, when electrons pass through heavy elements, they get stopped faster compared to when they pass through light elements (i.e., for a greater depth of penetration in heavy elements, higher-energy electrons are needed compared to lighter elements). However, in the case of light elements, because of the high number of electrons per unit volume, the source of the electrons loses energy rapidly through a large number of inelastic collisions with the electrons in the sample (thus higher SEs are emitted from the surface of the sample).

This clearly indicates that the electron source does not hit the sample at a predetermined convergence site and the electrons do not follow straight paths. On the contrary, they go through a wider area and greater depth. As a general rule, secondary electrons (SEs) are released from a depth of 100 nm, while backscattered electrons (BSEs) can reach a depth of 1 μm and characteristic X-rays can go as deep as 5 μm.

6.2 THERMO-GRAVIMETRIC ANALYSIS (TGA)

6.2.1 Introduction

Temperature reactions and some of the most common ones are dehydration, oxidation, dehydroxylation, decomposition, de-carbonation, etc. Mass and heat transfer, on the other hand, are some of the results brought about by the thermal reaction. Consequently, TGA has been established as the foremost technique for the analysis of mass change with respect to the increase in temperature; moreover, the change in mass at a certain temperature indicates a specific mineral that is experiencing one of the above-mentioned thermal reactions. The thermo-gravimetric analysis is one among the widely used techniques in the field of cement chemistry to follow the reactivity of cementitious materials (Lothenbach, Durdziński, & Weerdt, 2016). This method is used widely to supplement interesting facts obtained from other methods such as SEM and XRD. Primarily, in the case of cementitious materials, this method is used to study the bound water and the amount of portlandite (Ca(OH)2) formed or consumed during the reaction. Often, this is used as a method to understand the reactivity of supplementary cementitious materials (SCM's). In a typical TGA, the sample is heated, and the weight loss of the sample is recorded. Figure 6.2 shows a thermo-gravimetric analyser.

6.2.2 Factors That Influence TGA

The choice of device significantly settles the thermal analysis. Below are some of the primary conditions that influence the thermal analysis. These include the heating rate, the type of container, purging gas (O2, N2, argon, helium, etc.), particle size, purging rate, sample weight, sample pre-treatment method, etc. It is, therefore, not generally accepted to compare results from two different devices. As a result, if a certain measurement protocol is used for one sample, it is better to use the same protocol for the whole experiment. The subsequent section discusses the important factors that influence the results obtained.

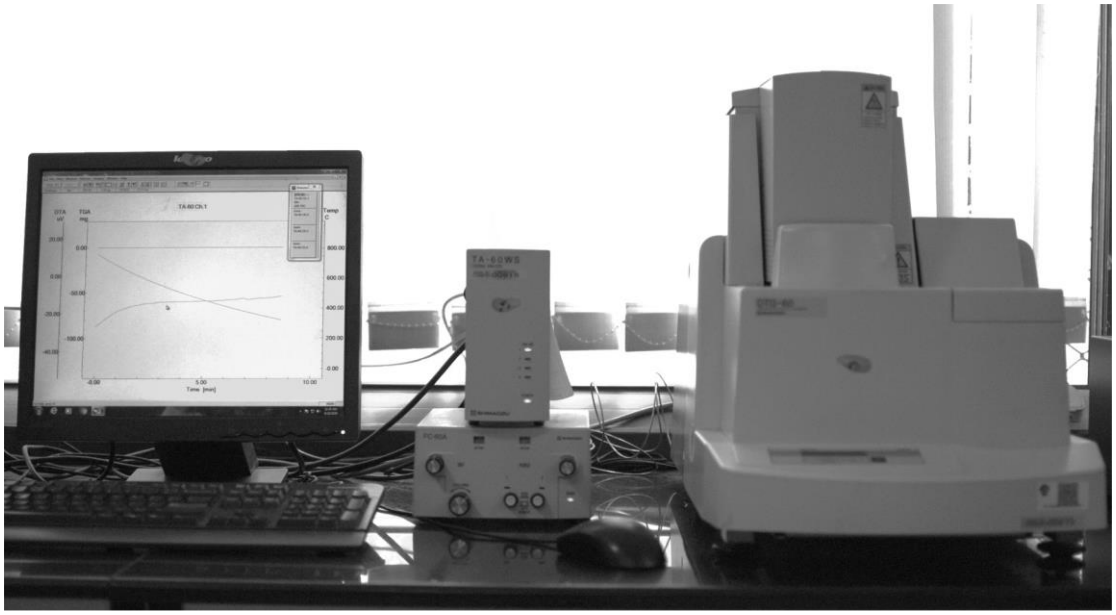

FIGURE 6.2 Thermo-gravimetric analyzer.

Rate of Heating

The rate of heating plays a significant role in determining the peaks seen in thermal analysis. When the heating is at a high rate, it generates narrower and more definite peaks, but it may also contribute to the rapid accumulation of vapor pressure in the chamber. This pressure will subsequently lead to an increase in the temperature of dehydration and dehydroxylation. In contrast, if the heating is done at a low rate, the vapor pressure developed will be lower, and this could possibly allow dehydration to occur at a much lower temperature.

Typically, the case in the majority of situations is that dehydration of gypsum (CaSO4.2H2O) to anhydrite (CaSO4) occurs at around 140°C (Hudson-Lamb, Strydom, & Potgieter, 1996). The dehydration process is distinct when gypsum (CaSO4.2H2O) is converted to hemihydrate (CaSO4.1/2H2O) and then to anhydrate (CaSO4) at a higher than normal temperature due to the increased vapor pressure from rapid heating in the closed chamber (Paulik, Paulik, & Arnold, 1992).

Rate of Gas Purging

Just as the heating rate, the gas flow has an effect on the temperature at which a certain mineral is decomposed. Generally, a high flow rate can lead to a temperature shift downwards. Besides, no good distinction between different peaks can be seen. Similarly, the kind and the size of the pan are also influencing the vapor pressure that is produced; thus the temperature level at which the dehydration or dehydroxylation is detected (Paulik et al., 1992).

Weight of the Sample

The sample weight for thermal analysis is one of the major factors that impact the results. The more the sample weight, the more the temperature at which the dehuhydration happens will be. Besides, the peak that is formed will be less sharp. Therefore, to ensure that different samples are properly compared, the results are escalated to 100% of the total weight of the sample at the beginning.

If the sample contains a mere trace of gypsum, the principal peak corresponding to mass loss will take place in the very beginning around 115°C. The turning into gas of anhydride will occur during the range of over 135°C. In case the gypsum is present in the sample to a higher extent, then the peak will be moved to a higher temperature. The main peak for the removal of waters of hydration from gypsum to hemi-hydride will be at about 145°C, followed by the change of hemi-hydride to anhydride at around 180°C. This is because the increased amount of gypsum results in the higher release of water vapor during the process of dehydration. Thus, it is creating a higher vapor pressure in the closed chamber, thus making the peak to be observed at the higher temperature (Paulik et al., 1992).

6.2.3 Methods Involved in Pre-treating the Sample for TGA and Their Details Specific to Cement-Based Materials

1. The pre-treatment of the samples is a very significant variable that impacts the thermal analysis. Pre-treatment is usually done by quenching in either nitrogen or solvent exchange (Zhang & Scherer, 2011) to stop the moisture absorption at a certain time. This is afterwards done by freeze-drying, vacuum drying or any other means to take away the water (free water). However, every different treatment has its own impact on the thermal analysis results obtained.

2. It has been observed that methanol, ethanol, and iso-propyl alcohol solvent exchange technique has interactions with the hydration products C-S-H, portlandite, ettringite, and AFm phases. In case of prolonged solvent exchange exposure, the interlayer water

of ettringite and AFm phases gets completely replaced by the solvents. Notably, monosulfate phases undergo complete dehydration during the solvent exchange process. Furthermore, it has been reported that solvents intercalated in the layers are very hard to be eliminated from the layers even by using vacuum drying techniques (Khoshnazar, Beaudoin, Raki, & Alizadeh, 2013a, 2013b).

3. The methanol acting as a solvent was very energetic in disrupting the ettringite and AFm phases created during the hydration process. Additionally, methanol and acetone caused portlandite to interact during TGA, producing calcium carbonates. The latter is indicated by the increased mass loss above 600°C. The aforementioned interactions are responsible for the alteration in the mass loss signal during TGA.

4. In order to keep the hydrated phases free from organic solvents, other methods through immersion in liquid nitrogen or with diethyl ether, which is a less sorbing organic solvent, can be used. To stop the hydration reaction by diethyl ether is a 2-step process (Deschner et al., 2012; Schöler, Lothenbach, Winnefeld, & Zajac, 2015).

a. The first step is iso-propanol immersion where the pore water is substituted with iso-propanol and then diethyl ether immersion takes place.

b. This is followed by drying at 40°C for the removal of diethyl ether that is remaining in the pores. c. Following the above-mentioned 2-step procedure could lead to a lower disturbance of portlandite or possibly no evidenced carbonation of portlandite compared to freeze-drying method.

One more method that could be used instead of stopping hydration is freeze-drying, provided that such reactions have very little influence. First, the sample is cooled with liquid nitrogen to the needed temperature. Next, the sample is put in a vacuum and carbonation free environment where the ice will sublime thus water vapour will be produced from the direct melting of ice. However, if ettringite is the target for the study, this method requires special attention as the freezing and thus dying of waters in ettringite may cause the suppression of associated signal in TGA due to their evaporation. In addition, other hydrates might also get rid of their water that was not tightly held in the crystals and which was present between the layers.

6.2.4 Typically Observed TGAData for Cementitious Materials

Table 6.1 gives a general idea about the decomposition temperature of different hydration products obtained in a TGA

6.2.5 Experimentation and Interpretation of Obtained Results

Generally, experimentation is done under the following boundary conditions.

1. Aluminium crucibles are used having a volume of 150 µL (which is ample for 50 mg of paste sample). Direct testing of other powder sample is also done.

2. Heating rate is usually selected at 10–20°C per minute.

3. Temperature is set between 40°C and 1,000°C.

4. The selective purging gas and the purging rate: N2 with a flow between 30 mL/minute and 50 mL/minute is the purging gas.

5. Prior to the experiments, a blank curve is generated using the selected crucible at a corresponding heating rate together with the same purging gas and rate.

6. The samples are after the time set for hydration, smashed and pulverized in a mortar and pestle. Take all necessary precautions to keep carbonation during this process to a minimum.

TABLE 6.1:

Temperature Range at which the Cementitious Materials Are Decomposed by Thermal Reactions (Lothenbach et al., 2016)

Cementitious materials or hydration products	Particulars	Decomposition or dehydration or dehydroxylation temperature range (°C)
Gypsum	Two-step dehydration process	Closed vessel with a small hole should be used for a distinct difference
	Gypsum to hemihydrate	100–140
	Hemihydrate to anhydride	140–150
Portlandite	Dehydroxylation [$CaO + H_2O$]	460
Magnesium hydroxide or Brucite	Dehydroxylation [$MgO + H_2O$]	420
Calcium carbonate or Calcite	De-carbonation [$CaO + CO_2$]	600–800
Coarser calcite	Un-hydrated cement	720
Mono or hemi-carbonates	From carbonation of portlandite or C-S-H	600–650
Magnesium carbonate or Magnesite	De-carbonation [$MgO + CO_2$]	500–600
Aragonite and Vaterite (polymorphs of calcium carbonate)	Re-crystallization without any weight change	450 (approx.)
Amorphous calcium carbonate	De-carbonates partially [CaO + Calcite]	400–600
Dolomite (carbonates of calcium and magnesium with a trace of iron)	MgO + Calcite	650
	Calcite decomposes to $CaO + CO_2$	600–800
C-S-H	loss of water over a wide range of temperature (dehydration or dehydroxylation)	50–600
	C-S-H to wollastonite	800
AF^t	Lose of water	100
AF^t	Water loses from dehydroxylation of aluminium hydroxide	200–400
AF^m	Mono-carbonates (loss of 5 inter-layer water)	60– 200
AF^m	Mono-carbonates (loss of 6 inter-layer water)	200–300
AF^m	Loss of CO_2	650
AF^m	Mono-sulphates (loss of water from interlayers)	250–350
AF^m	Chlorides (Friedel's salt) (loss of water from interlayers)	140
Calcium aluminium hydrates	Loses its water	270
Calcium aluminium hydrates	Katoite	320
Calcium aluminium hydrates	Hydrogarnets	340

7. A pre-treatment procedure is then selected depending on the analysis, which will cause the hydration to stop. Either a solvent exchange or a freeze-drying method can be employed.

a. Solvent exchange method, iso-propanol is the solvent of choice. Approximately 5 grams of ground cement paste is put into a vessel containing iso-propanol for 10–15 minutes. This duration is enough for the iso-propanol to take the place of the free water.

b. The filtrate is separated using a Büchner funnel and a vacuum pump, thus the excess iso-propanol in the filtrate is removed.

c. The powdered material is now treated once again with diethyl ether (5–10 mL) to extract the surplus iso-propanol and then vacuum dried until the sample turns light in colour. This is verified by the pressure gauge of the vacuum pump (the pressure increases).

d. The resulting powder is now placed in a petri dish and dried in an air oven at 40°C or in the vacuum desiccator for 8–10 minutes.

e. Sample should be analyzed right away if it is possible. Otherwise, the sample can be kept in a closed vessel for a few days under light vacuum.

f. Freeze-drying is another option and can also be applied. Place the sample in liquid nitrogen for 15 minutes.

g. The freeze-dried sample is passed through a mortar and pestle to get crushed.

8. As soon as the sample has been prepared, carefully measure about 50 mg of the sample and then put it in the crucible. Additionally, detect the blank before the experiment is initiated.

9. In this manner, the amounts of gypsum, portlandite and calcite are to be quantified based on the measured weight loss during TGA, which is as follows. The temperature range of approximately 400-500°C is the interval when portlandite gets converted into CaO and water. The weight loss during this time is a sign of the decomposition of portlandite occurring. The amount of portlandite in the sample can be calculated based on the weight loss (WL (Ca(OH)2)) at this temperature. We also know that the molecular weight of portlandite is 74 g/mol and of water is 18 g/mol. Hence, the amount of portlandite present is given by the following calculation

$$\mathrm{Ca(OH)_{2\,measured}} = \mathrm{WL\left(Ca(OH)_2\right)} \times \frac{\text{molecular weight of portlandite}}{\text{molecular weight of water}}$$

$$= \mathrm{WL\left(Ca(OH)_2\right)} \times \frac{74}{18}$$

10. Just like that, calcium carbonate undergoes decomposition at a temperature of more than 600°C producing CaO and CO2. The loss in weight at this particular temperature can be the indicator to determine the amount of calcium hydroxide carbonated over a definite period as explained below.

$$Ca(CO)_{3\,measured} = WL(CaCO_3) \times \frac{\text{molecular weight of } CaCO_3}{\text{molecular weight of } CO_2}$$

$$= WL(CaCO_3) \times \frac{100}{44}$$

11. The TGA process involves frequent changes in the mass of the sample throughout the entire duration of the experiment. A correction must therefore be applied to the analysis in order to take into consideration the continuous mass loss of the sample. Thus, for every 100 grams of paste, the amount of portlandite and calcite will be required to be changed as follows.

$$Ca(OH)_{2\ paste} = \frac{Ca(OH)_{2\ measured}}{1 - H_2O_{bound} \times \left(1 + \frac{Water}{Cement}\right)}$$

$$Ca(OH)_{2\ paste} = \frac{Ca(OH)_{2\ measured}}{\text{weight at } 600°C \times \left(1 + \frac{Water}{Cement}\right)}$$

$$Ca(OH)_{2\ anhydrous} = \frac{Ca(OH)_{2\ measured}}{\text{weight at } 600°C}$$

12. The quantification of other compounds can be performed through the weight loss at the specified temperatures. However, the high overlap of the TG curves between different compounds makes it difficult to de-convolute TGA outputs.

13. Generally, two main methods are employed for the purpose of estimating the area underweight loss in TGA curves. The selection of these methods is determined by the software in use. The quantification of calcite, on the other hand, is rather uncomplicated since the de-carbonation occurs above 600°C. The impact of other hydration products is minimal at this elevated temperature.

14. Nonetheless, there is still a problem for the quantification of portlandite to be considered, as the weight loss caused by C-S-H overlaps the dehydration of portlandite. To avoid that, the tangential method or stepwise method is applied to erase those effects. Usually, the step-wise method over-estimates portlandite content since the curve can include the weight loss due to C-S-H, as well. Conversely, the tangential method presumes a correction for other hydrates, particularly for C-S-H, whereby a linear increase in weight loss in the specified temperature range is inferred. Besides, to achieve more accurate quantification, manual integration of the area under the curve can also be an option.

In the scenario wherein blast furnace slags are incorporated in the cement during TGA, there is a decrease in weight as a result of H2S gas being released. This occurs at temperatures roughly below 700°C. Conversely, weight gain can be noted above this point. This is mainly owing to the transformation of sulphur into sulphate (to a certain extent, 1.996 g per g of S^{2-}) (Montes-Morán et al., 2012). Moreover, the oxidation of metallic iron and manganese might also contribute to the increase of slag samples' weight. The degree to which an oxidizable product is formed depends heavily on the kind of gas supplied in the chamber and the temperature increment rate.

6.3 X-RAY DIFFRACTION TECHNIQUE (XRD)

6.3.1 Introduction

The German physicist Rontgen made the first discovery of X-rays. However, the use of X-rays for material characterization by diffraction was only discovered later, in 1912, by which time the concept of wave-particle duality had already been established. X-rays are very short wave radiation like that of the electromagnetic spectrum (EM) with a wavelength ranging from 0.1 to 100 Ångstrom. They are produced whenever rapidly moving electrons, directed towards a target (copper (Cu) or molybdenum (Mo)), are suddenly slowed down by the application of a voltage difference. In the usual crystallographic method, a cathode (tungsten filament (W)) is heated to give off electrons. These electrons strike an anode that is capable of being rotated about its axis. Upon striking the anode, the electrons scatter many times; as a consequence, a large amount of heat is generated. About 10% of the emitting source electrons are converted into and used for X-rays which can be performed through crystallographic investigation. The basic layout of the sealed X-ray tube is depicted in Figure 6.3.

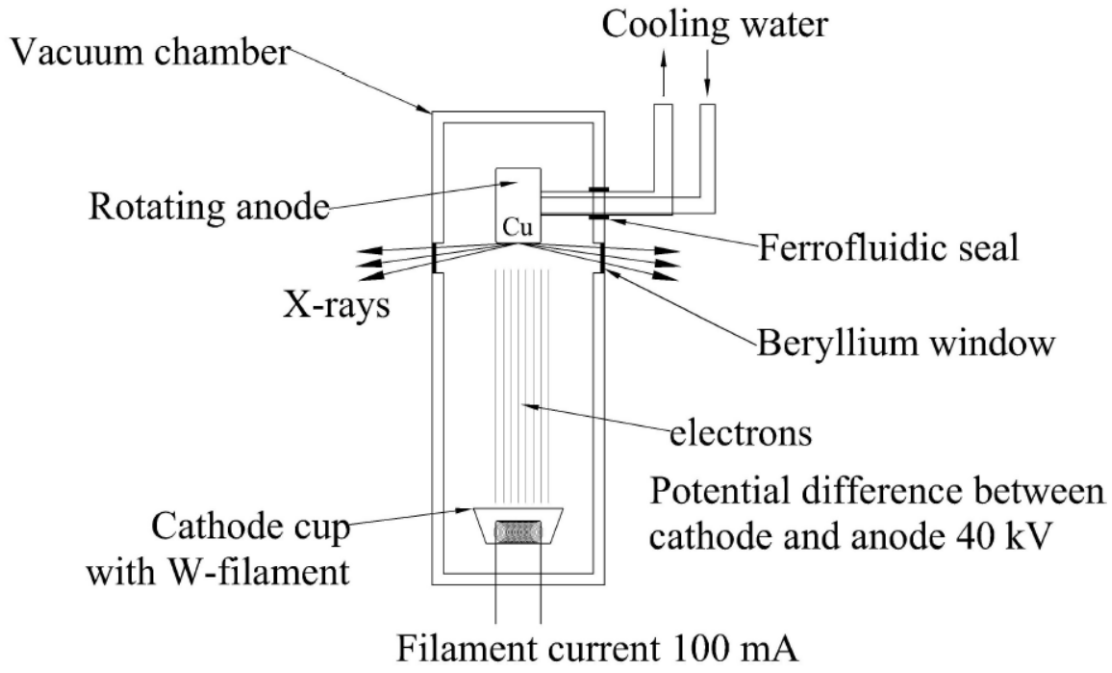

FIGURE 6.3 Schematic of a sealed X-ray tube.

The quality and the kind of X-rays emitted by the anode are largely affected by the accelerating voltage (Suryanarayana & Norton, 1998). The higher the voltage, the more limited will be the range of X-ray wavelengths (i.e. less will be the white light emitted from the source). Hence, the higher the voltage, the larger is the amount of radiation coming from the source and the shorter is the wavelength. Characteristic X-rays result from the source (anode) when the electrons bombard the anode. The electron bombardment not only ejects electrons from various layers of the atom in anode but also induces transition of electrons from upper layers to lower layers. The transition of electrons from higher energy level (outer shell) to lower energy level (inner shell) in the anode causes the emission of characteristic X-rays from the anode. The energies of the X-rays are directly related to the electron transitions involved in the (L-shell to K-shell or M-shell to K-shell) transfer. If E1 and E2 are two energy levels of the electrons then the wavelength of the emitted X-rays can be expressed as

$$\lambda = hc / /E2\text{-}E2/$$

Where h is the Plank's constant, c is the light velocity, E1, and E2 are the energy levels of the electrons that correspond to the respective shells. Furthermore, there will be two distinct wavelengths for the electron transition from the L-shell to the K-shell or from the M-shell to the K-shell. If the X-rays, produced with copper (Cu) as the anode (the most common X-ray source in XRD), are considered, during L to K-shell transition Kα1 and Kα2 with an average of 1.54184 Å (with a wavelength intensity ratio of 2:1) are the two distinguishable wavelengths. Similarly, for M to K-shell transition, again two distinguishable wavelengths (Kβ1 and Kβ2) with an average value of 1.38851 Å (with a wavelength intensity ratio of 2:1) are present. If the Bragg angle is larger (i.e. the scattering is at a higher value), the averaged wavelengths will have to be resolved.

The choice of anode (the proper source of X-ray emission) is very important. The atoms of the material that the X-rays are passing through determine the intensity of the X-rays transmitted (the material with atoms of higher atomic number will have more attenuation and vice versa). Therefore, X-ray transmittance is determined by a coefficient called the linear absorption coefficient of the material (μ) and the thickness of the material (L) through which the X-rays are passing. The linear absorption coefficient of the material changes with the wavelength of X-rays. For any material, the linear absorption coefficient decreases directly proportional to $\lambda^{5/2}$ where, λ is the wavelength. This means that the depth of X-ray penetration will be greater due to the increased energy of the emitted radiation. Consequently, as the wavelength of the X-ray decreases, there will be a point at which the emitted radiation is strong enough to knock down an electron from the atom of a particular energy level (from K, L, or M shell). The linear absorption coefficient rises sharply at this point and is termed an absorption edge or resonance level. A further decrease in wavelength leads to a decrease in the linear absorption coefficient of the material. Then, what does it have to do with the selection of the anode? The practical applicability of the specific radiation will vary based on the informed absorption edge or

resonance level. For instance, the X-rays emitted from copper as an anode cannot be utilized for materials with a greater percentage of iron in them. This happens because the K absorption edge or resonance level for iron is at 1.7433 Å. Thus, the radiation emitted (from Cu) will be molecules of iron and will be given off as a typical K spectrum of iron. Under such circumstances, the anode has to be selected very carefully (Suryanarayana & Norton, 1998). To get the best results, it is very important to have the anode continuously emitting X-rays with the exact same wavelength. The X-rays that are emitted can then be used as a light source to see the crystal structure of the material being studied. This method of analysis can be used with cement-based materials for both qualitative and quantitative phase identification.

6.3.2 Working Principle

Crystalline materials are structured in a certain way. Every single arrangement is identified by the repetitive pattern of the material. The arrangement's smallest part is referred to as a unit cell. A definite arrangement characterizes each unit cell, and when X-rays go through the material according to the position of the unit cell in the material, a typical diffraction pattern can be obtained. These patterns serve to identify different unit cells. When a specimen scatters X-rays from a source, the diffracted rays follow Bragg's law as stated by

$$n\lambda = 2d \sin \theta$$

In the given statement, "n" represents an integer, "λ" denotes the wavelength of the X-rays released by the source, "d" signifies the spacing separating two inter-planes in the crystal, and "θ" indicates the diffraction angle.

When X-rays hit a crystal at certain angles depending on the atomic structure inside the crystal, they can cause the formation of two or more beams that interfere with each other. Interference occurs when two or more waves overlap each other. The resulting effect can be either a constructive interference or a destructive interference depending on the amplitudes of the diffracted waves that are being considered. If the amplitudes of the waves coincide perfectly, then the intensity of the superposition will be the maximum and vice versa. Bragg’s law is the fundamental principle for indexing the X-ray diffraction pattern of any specimen under study. Thus, any crystalline material characterized by the particular spatial arrangement of atoms will cause the diffraction pattern to vary which lets through both constructive and destructive interference. This is accounted for by a parameter named the structure factor, F, which quantifies the impact of crystal structure on the brightness of the diffracted beam.

6.3.3 Apparatus Required and Their Usage

X-ray diffractometer consists of three parts as the most important. They are: (1) X-ray source, (2) Specimen chamber and (3) X-ray detector, and these three components are arranged in such a way that they form a circle. This arrangement is also referred to as the focusing circle. Additionally, a circle can be created with the sample at the center and having a radius equal to that of the X-ray source or the X-ray detector. This circle is known as the goniometer circle.

The source of X-rays is made up of an X-ray tube, which is illustrated in Figure 6.3. The tungsten (W) filament, when heated, releases electrons which are then directed to the anode situated on a turning table. The anode produces characteristic X-rays depending on the electron transition from outer layer to inner layer of energy. The entire assembly within the X-ray tube is surrounded by a high vacuum. The sample that is to be analyzed is put on the sample-holder table inside the goniometer circle. Typically, a non-diffracting material is utilized for mounting the sample. Usually, the non-diffracting material is a glass slide. The amount of sample (powder) is extremely small (1 mg or slightly more), and the sample size must be less than 50 μm. If the grain size is too large, then one can have preferential orientation. Preferred orientation may result in reflections with relatively high intensity. On the other hand, if the grain size is too small, then the diffraction pattern will be wider and may overlap with other peaks.

The angle at which the source of X-rays hits the sample is identified as the Bragg angle (θ). Consequently, the angle between the source and the detector amounts to 2θ (0°-170°). The diffraction patterns that result from this precise arrangement are referred to as θ–2θ scans. In this specific arrangement, the origin of the electrons is stationary. Only the detector rotates around the circular path at different angles. When the detector's angle becomes larger, the radius of the focusing circle grows smaller and vice versa. The extent of the scan angle is largely determined by the selection of the crystal for examination. To specify the collimation (parallel beams) of the X-ray beam, soller slits are applied. These soller slits consist of materials with high atomic numbers due to their large absorption capacity. Similarly, to limit the divergence of the X-ray beam (width), divergence slits are utilized. Once the X-ray beam has diffracted the specimen, it is filtered through a set of slits before being sent to the detector for processing. The background radiation is decreased by an anti-scatter slit followed by a receiving slit. The X-ray beam is converged while it passes through the receiving slit. Before it goes to the detector, the beam travels through one more soller slit. A monochromatic beam can only be produced if the Kβ X-ray beams are eliminated. This can be done by the use of a filter (monochromator) or, more recently, by a graphite crystal placed after the diffracted beam in front of the detector. If the monochromator is applied then the assembly of soller slits after the specimen might not be required as the width of the diffracted beam can be regulated by the monochromator itself. A contemporary X-ray diffractometer is depicted in Figure 6.4.

6.3.4 Steps Involved in Sample Preparation Specific to Cement-Based Materials

1. According to the need, the specimen is dried by a suitable method. The samples are either placed in the oven at the desired temperature and dried, or organic solvent exchange methods are employed to halt hydration at corresponding days.

FIGURE 6.4 Modern X-ray diffractometer.

2. Each of the aforementioned techniques possesses its own pros and cons. The selection of the technique should depend on the specific needs and the variety of materials that need to be tested.

3. After the sample for analysis has been subjected to one of the aforementioned methods, place the sample into the mold in two layers with the compaction done by a spatula.

4. Next, the lid is placed over the open end and removed from the holder carefully.

5. The mold is turned upside down and the surface now presented is subjected to the investigation. Since this surface has not been subjected to the normal hand leveling, up to 90% of the preferential orientation can be prevented.

6. Mold and holder cleaning should preferably be done with iso-propanol.

7. Preferential orientation occurs primarily because of the crystals such as Ca(OH)2 formed in the hydrated samples and sometimes due to C-S-H crystals.

8. The aspect ratios of Ca (OH)2 and C-S-H are significantly higher compared to those of other crystals which formed during the hydration process.

9. If measurements were made on in-situ hydrating samples, measures should be taken to eliminate carbonation. Carbonation might have a bigger influence on diffracted patterns. To avoid this, a holder with a tight lid can be used to keep a cement sample away from atmospheric CO2.

6.3.5 Experimentation and Interpretation of Obtained Results

Analysis of the X-Ray Pattern: Search-Match Procedure

The analysis was performed by comparing the XRD pattern with those of known components, considering the differences in the position and the relative intensities of the peaks. This comparison can be done using a collection of patterns of pure phases or powder diffraction files of the International Centre for Diffraction Data (ICDD). The automatic suggestions yielded by X'Pert high score plus or any such similar program can be considered as a suggestion. However, in the end, to assess the existence of all phases, a preliminary chemical investigation has to be done by other methods. Moreover, the analysis obtained using different techniques like scanning electron microscopy (SEM) and thermo-gravimetric analysis (TGA) can be used for confirmation. Through the Rietveld method, quantitative analysis, selective dissolution for controlled phase identification, and density or magnetic separation can be very helpful in determining the concentration of trace phases.

The quantitative analysis regarding the composition of multiphase mixtures is based on the correlation between the phase intensity reflection (Sα) in a mixture (m) and its concentration in the mixture (Wα), which is mathematically expressed as follows:

$$S_\alpha = K_e \frac{W_\alpha}{\rho V^2 \mu_m}$$

Here, Ke is the constant that varies according to the diffractometer and the component. α, ρa, and Vα stand for the density and cell volume of the component, respectively, whereas μ_m represents the mass absorption coefficient of the mixture.

The quantification can be performed in two ways: one is based on the extracted intensities of different lines in the XRD pattern; among the different methods in this category are the addition/dilution method, the use of standards, or the direct reference intensity ratio (RIR)

method. The second group of methods is represented by the Rietveld method, which is a full pattern-fitting. The Rietveld approach makes use of the crystal structure data to calculate the diffraction pattern; then, using a parameter as a set, the calculated parameters can be compared with the experimental pattern.

Refinement is calculated as the sum of the weighted square differences between the observed and calculated intensities at each step in the digital powder pattern. This method requires prior knowledge of about ten crystal structures such as space group symmetry, atomic positions and site occupancies, and lattice parameters (Snellings, 2016).

Caution to be Observed while Interpreting the Data from XRD:

1. It is essential to be cautious with the measurements that are taken at low angles. This is due to the fact that at low angles, the source and the detector will be directly facing each other at an angle of 180º, which leads to higher peak intensities as the radiation is directly passing through from the source to the detector. By introducing back slits that cut off the direct radiation path between the source and the detector, this problem can be solved.

2. A significant limitation of the currently used methods is that the elements which can be recognized only at low angle measurements cannot be observed. For instance, they are kaolinite in clay; Friedel salt; bi-carbonates and ettringite.

3. High angle measurements will face similar problems as low angles, albeit with even more intensity.

4. The selection of slit type is primarily determined by the power under investigation. Depending on the analysis requirement, either resolution or sample size has to be adjusted. A fine slit can produce higher resolution, but the process will take more time; on the other hand, a coarse slit is responsible for lower resolution, but it can perform the analysis quicker. A middle-range slit is generally used for all sorts of analyses. In case of homogenization, the application is linked to certain tasks, then finer slits are used.

5. The source type is more important as the same element will provide various kinds of intensities and diffractions for copper (Cu) and cobalt (Co). The type of metal source should be specified while data portraying via XRD.

6. Scanning over 80º is not a general practice. No practically useful information will be obtained from the cementitious system scanned using Rietveld method above 65º. Very weak signal is captured as angle increases. NIST has a collection of files available for analysis of cement-based materials.

6.4 PRACTICE QUESTIONS AND ANSWERS

1. Convergence angle of the electrons passing through the column is controlled by an aperture made up of

a) Copper

b) Cobalt

c) Molybdenum

d) Tungsten

2. During the collision of an electron beam on the surface of the sample, different electrons are emitted from the sample. Backscattered electrons (BSEs) are emitted due to

a) Inelastic collision

b) Elastic collision

c) Partial scattering

d) None of the above

3. Both BSEs and SEs are collected to create SEM images. From where the SEs are emitted

a) From the source electron (thermionic tungsten or lanthanum hexaboride)

b) From the material under investigation

c) Escaped from the shell of material under investigation

d) All the above

4. What type of image is obtained from BSEs?

a) Morphological-based images

b) Composition-based images

c) Combination of a and b

d) None of the above

5. Why petrol or iso-propanol is used as a solvent to aid in polishing of the sample instead of water?

a) It acts as a lubricant

b) It avoids the formation of new hydration products

c) Both a and b

d) None of the above

6. Why is the surface of the sample coated before SEM analysis?

a) To allow the electrons to impinge the surface of the sample

b) To make the surface of the sample conductive

c) Both a and b

d) None of the above

7. During an inelastic collision, which of the following are emitted?

a) BSEs and SEs

b) Characteristic X-rays and BSEs

c) Characteristic X-rays and SEs

d) All the above

8. The probability of emanation of BSEs is higher in which of the following cases?

a) Light elements

b) Heavy elements

c) Hydrogen

d) Water

9. In a compositional image of cement, how will you differentiate a void from other compounds?

a) Location of the void will be dark

b) Location of the void will be bright

c) Location of other compounds will be dark

d) None of the above

10. How is calcium hydroxide identified in SEs image?

a) Tubular structure

b) Hexagonal pyramid

c) Hexagonal prism

d) All the above

11. What is the principle behind thermo-gravimetric analysis (TGA)?

a) Thermal reaction results in a change of weight

b) Thermal reaction results in a change of volume

c) Thermal reaction results in a change of length

d) None of the above

12. How does the rate of heating affect TGA?

a) Shifts the decomposition temperature to higher range

b) Shifts the decomposition temperature to lower range

c) Narrows down the range of peak and shifts the peak to the higher temperature

d) Broadens the range of peak and shifts the peak to the higher temperature

13. A higher flow rate of gas may result in a shift of temperature to a lower magnitude. This is attributed because

a) Increase in flow rate decreases the vapour pressure inside the chamber

b) Increase in flow rate increases the vapour pressure inside the chamber

c) Decrease in flow rate decreases the vapour pressure inside the chamber

d) All the above

14. How does the weight of the sample taken affect the peak values?

a) Increase in weight of the sample increases the peak temperature range.

b) Increase in weight of the sample decreases the peak temperature range.

c) Decrease in weight of the sample increases the peak temperature range.

d) None of the above.

15. Compared to methanol and iso-propanol, which of the following can be used as an alternative solvent and why?

a) Ethanol and high sorptivity

b) Benzene and less sorptivity

c) Nitro-benzene and high sorptivity

d) Diethyl ether and less sorptivity

16. What are the decomposition ranges or temperature of calcium hydroxide, calcite and C-S-H (in °C)?

a) 460, 600–800, 50–600

b) 600–800, 460, 50–600

c) 460, 50–600, 600–800

d) 50–600, 600–800, 460

17. Which of the following method over-estimates portlandite?

a) Tangential method

b) Step-wise method

c) Manual integration method

d) All the above

18. Reactivity of any supplementary cementitious material (SCM) can be identified by knowing the mass of unreacted

a) C-S-H

b) Ca(OH)2

c) AFm

d) CaCO3

19. Decomposition temperature of hydro garnets ……°C

a) 140

b) 270

c) 320

d) 340

20. Usage of freeze-drying method should be practised with caution. Why?

a) It can dehydrate some of the hydration products during the drying process.

b) It decomposes most of the hydration products.

c) It can vigorously destabilize ettringite and AFm phases.

d) None of the above.

21. How are X-rays emitted?

a) An elastic collision of source electrons

b) An inelastic collision of source electrons

c) Both a and b

d) None of the above

22. Why X-rays radiated from copper cannot be used for investigation of material with higher percentage of iron in it?

a) K absorption edge of copper and iron are similar.

b) Their resonance levels are similar.

c) Their linear absorption coefficients are similar.

d) All the above.

23. What will happen if the size of the specimen is too large?

a) Preferential orientation may take place.

b) Diffraction pattern may overlap.

c) Both a and b.

d) None of the above.

24. Characteristic X-rays emitted from anode highly depend upon the applied voltage. If the applied voltage is less, what will happen?

a) Wavelength of X-rays will be unique and short.

b) Wavelength of X-rays will be continuous and short.

c) Wavelength of X-rays will be continuous and large.

d) Wavelength of X-rays will be unique and large.

25. X-rays are collimated by allowing the X-ray beams to pass through

a) Soller slits

b) Anti-scatter slits

c) Receiving slits

d) Monochromator

26. Monochromator is used to

a) Collimate the beam

b) Receive the beam for processing

c) Convert the beam to a single wavelength

d) None of the above

27. What is the crystal structure of calcium carbonate?

a) Hexagonal

b) Trigonal

c) Cubical

d) Tetragonal

6.5 ANSWERS OF THE QUESTIONS

1.	c	2.	b	3.	c	4.	b	5.	b	6.	c	7.	c	8.	b	9.	a	10.	c
11.	a	12.	c	13.	a	14.	a	15.	d	16.	a	17.	b	18.	b	19.	d	20.	a
21.	b	22.	d	23.	a	24.	c	25.	a	26.	c	27.	b						

Test Your Knowledge

1. What is the significance of the microstructure of a material? How do you define microstructure?

2. Describe some of the unique features of the concrete microstructure that make it difficult to predict the behavior of the material from its microstructure.

3. Discuss the physical-chemical characteristics of the C-S-H, calcium hydroxide, and calcium sufflaminates present in a well-hydrated Portland cement paste.

4. How many types of voids are present in a hydrated cement paste? What are their typical dimensions? Discuss the significance of the C-S-H interlayer space with respect to properties of the hydrated cement paste.

5. How many types of water are associated with a saturated cement paste? Discuss the significance of each. Why is it desirable to distinguish between the free water in large capillaries and the water held in small capillaries?

6. What would be the volume of capillary voids in an 0.2-water-cement ratio paste that is only 50 percent hydrated? Also calculate the water-cement ratio needed to obtain zero porosity in a fully hydrated cement paste.

7. When a saturated cement paste is dried, the loss of water is not directly proportional to the drying shrinkage. Explain why.

8. In a hydrating cement paste the relationship between porosity and impermeability is exponential. Explain why.

9. Draw a typical sketch showing how the microstructure of hydration products in the aggregate-cement paste interfacial transition zone is different from the bulk cement paste in concrete.

10. Discuss why the strength of the interfacial transition zone is generally lower than the strength of the bulk hydrated cement paste. Explain why concrete fails in a brittle manner in tension but not in compression.

11. Everything else remaining the same, the strength and impermeability of a mortar will decrease as coarse aggregate of increasing size is introduced. Explain why.

12. When concrete is exposed to fire, why the elastic modulus shows a relatively higher drop than the compressive strength?

13. Why is strength the property most valued in concrete by designers and quality control engineers?

14. In general, discuss how strength and porosity are related to each other.

15. One of the early hydration products formed is Ca $(OH)_2$, which of the following statement (s) is/are correct?

1. It is a crystalline phase which gives very high cohesion and bonding strength.
2. It is an amorphous phase and has very low strength.
3. It is a crystalline phase with very poor strength.
4. It acts as an entry point for the deterioration.

a) All the statements are correct
b) 1 and 2 are correct
c) 2 and 3 are correct
d) 3 and 4 are correct

16. Aft (ettringite) phases are formed during the hydration of cement. What are the compounds involved in the formation of ettringite?

a) C_3S, gypsum and water
b) C_3A, gypsum and water
c) C_3S, C_3A and water
d) All the above

17. During the process of hydration of cement, due to increase in dicalcium silicate (C_2S) content in the cement clinker, the heat of hydration

a) Increases
b) Decreases
c) Initially decreases and then increases
d) Does not change

For complete hydration of cement the water–cement ratio needed is

a) Less than 0.25
b) More than 0.25 but less than 0.35
c) More than 0.35 but less than 0.45
d) More than 0.45 but less than 0.60

18. Assertion (A): The higher percentage of tri-calcium silicate in cement results in rapid hardening with an early gain in strength at a higher heat of hydration.

Reason (R): A higher percentage of dicalcium silicate in cement results in slow hardening and less heat of hydration and greater resistance to chemical attack.

a) Both A and R are true and R is the correct explanation of A.
b) Both A and R are true and R is not the correct explanation of A.
c) A is true but R is false.
d) A is false but R is true.

19. What happens during the hydration of cement if no gypsum is available in cement?

a) Flash set

b) False set

c) Perfect set

d) All the above

20. In which of the following condition false set occurs

a) Excess presence of gypsum

b) Gypsum in un-hydrated form

c) Gypsum in hydrated form

d) All the above

21. When fineness of cement is higher, what characteristics does the cement possess?

a) Higher heat of hydration

b) Lower heat of hydration and higher strength

c) Higher heat of hydration and high soundness

d) None of the above

22. One of the early hydration products formed is Ca $(OH)_2$, which of the following statement (s) is/are correct?

1. It is a crystalline phase which gives very high cohesion and bonding strength.

2. It is an amorphous phase and has very low strength.

3. It is a crystalline phase with very poor strength.

4. It acts as an entry point for the deterioration.

a) All the statements are correct

b) 1 and 2 are correct

c) 2 and 3 are correct

d) 3 and 4 are correct

23. Aft (ettringite) phases are formed during the hydration of cement. What are the compounds involved in the formation of ettringite?

a) C_3S, gypsum and water

b) C_3A, gypsum and water

c) C_3S, C_3A and water

d) All the above

24. The compound which is mainly responsible for initial setting and early strength gain of ordinary Portland cement is

a) C_3A
b) C_3S
c) C_2S
d) C_4AF

25. During the process of hydration of cement, due to increase in dicalcium silicate (C_2S) content in the cement clinker, the heat of hydration

a) Increases

b) Decreases

c) Initially decreases and then increases

d) Does not change

26. For complete hydration of cement the water–cement ratio needed is

a) Less than 0.25

b) More than 0.25 but less than 0.35

c) More than 0.35 but less than 0.45

d) More than 0.45 but less than 0.60

27. Gypsum is used as an admixture in cement grouts for

a) Accelerating the setting time

b) Retarding the setting time

c) Increasing the plasticity

d) Reducing the grout shrinkage

28. Assertion (A): Flash set is the stiffening of the cement paste within a few minutes after mixing.

Reason (R): Flash set occurs due to insufficient gypsum to control the rapid reaction of C_3A with water.

a) Both A and R are true and R is the correct explanation of A.

b) Both A and R are true and R is not the correct explanation of A.

c) A is true but R is false.

d) A is false but R is true.

29. Assertion (A): The higher percentage of tri-calcium silicate in cement results in rapid hardening with an early gain in strength at a higher heat of hydration.

Reason (R): A higher percentage of dicalcium silicate in cement results in slow hardening and less heat of hydration and greater resistance to chemical attack.

a) Both A and R are true and R is the correct explanation of A.
b) Both A and R are true and R is not the correct explanation of A.
c) A is true but R is false.
d) A is false but R is true.

30. Assertion (A): For a given composition, finer cement will develop strength and generate heat more quickly than a coarse cement.

Reason(R): The reaction between water and cement starts on the surface of the cement particles and in consequence the greater the surface area of a given volume of cement, the greater the hydration.

a) Both A and R are true and R is the correct explanation of A.
b) Both A and R are true and R is not the correct explanation of A.
c) A is true but R is false.

d) A is false but R is true.

31. Four main oxides present in ordinary Portland cement are: CaO, Al_2O_3, SiO_2 and Fe_2O_3. Identify the correct ascending order of their proportions in a typical composition of OPC.

a) Al_2O_3, Fe_2O_3, CaO, SiO_2
b) Al_2O_3, CaO, Fe_2O_3, SiO_2
c) Fe_2O_3, Al_2O_3, SiO_2, CaO
d) Fe_2O_3, SiO_2, Al_2O_3, CaO

32. Assertion (A) : The greater the surface area of a given volume of cement the greater the hydration.

Reason (R): The reaction between the water and cement starts from the surface of the cement particles.

a) Both A and R are true and R is the correct explanation of A.

b) Both A and R are true and R is not the correct explanation of A.

c) A is true but R is false.

d) A is false but R is true.

33. Consider the following statements:
Low percentage of C_3S and high percentage of C_2S in cement will result in
1. Higher ultimate strength with less heat generation
2. Rapid hardening
3. Better resistance to chemical attack

Which of these statements are correct?

a) 1 and 2

b) 2 and 3

c) 1 and 3

d) 1, 2 and 3

34. In cements, generally, the increase in strength during a period of 14 –28 days is primarily due to

a) C_3A

b) C_2S

c) C_3S

d) C_4AF

35. The ultimate strength of cement is influenced by which one of the following ?

a) Tri-calcium silicate

b) Di-calcium silicate

c) Tri-calcium aluminate

d) Tetra-calcium alumino-ferrite

36. Consider the following statements :

1. Setting and hardening of cement takes place after the addition of water.

2. Water causes hydration and hydrolysis of the constituent compounds of cement which Act as binders.

Which of these statements is/are correct?

a) 1 only

b) 2 only

c) Both 1 and 2

d) Neither 1 nor 2

37. Assertion (A): The rate of hydration is faster in finer cements.
Reason (R): The surface area is more in case of finer cement.
a) Both A and R are true and R is the correct explanation of A.
b) Both A and R are true and R is not the correct explanation of A.
c) A is true but R is false.
d) A is false but R is true.

38. What is the requirement of water (expressed as % of cement w/c) for the completion of chemical reactions in the process of hydration of OPC ?
a) 10–15%
b) 15–20%
c) 20–25%
d) 25–30%

39. Fineness of cement is measured in the units of

a) Volume/mass

b) Mass/volume

c) Area/mass

d) Mass/area

40. he initial setting time of cement depends most on The initial setting time of cement depends most on

a) Tri-calcium aluminate

b) Tri-calcium silicate

c) Tri-calcium alumino-ferrite

d) Di-calcium silicate

41. Which compound of cement is responsible for the strength of cement ?

a) Magnesium oxide

b) Silica

c) Alumina

d) Calcium sulphate

42. Consider the following forms of water in a hydrated cement paste :

1. Capillary water

2. Chemically combined water

3. Interlayer water

4. Adsorbed water

Which of the above forms of water will, on their removal, cause shrinkage of the paste?

a) 1, 2 and 3

b) 1, 2 and 4

c) 2, 3 and 4

d) 1, 3 and 4

43. Consider the following statements:
High early strength of cement is obtained as a result of
1. Fine grinding
2. Decreasing the lime content
3. Burning at higher temperature
4. Increasing the quantity of gypsum

Which of the above statements are correct?
a) 1 and 2

b) 1 and 3

c) 2 and 3

d) 3 and 4

44. The constituent compound in Portland cement which reacts immediately with water and also sets earliest is
a) Tri-calcium silicate
b) Di-calcium silicate
c) Tri-calcium aluminate
d) Tetra-calcium alumino-ferrite

45. Statement (I): the finer the cement, the greater is the need for water for hydration and workability.
Statement (II): Bleeding of a mix occurs due to low water–cement ratio.
a) Both statement (I) and statement (II) are individually true and statement (II) is the correct explanation of statement (I).
b) Both statement (I) and statement (II) are individually true and statement (II) is not the correct explanation of statement (I).
c) Statement (I) is true but statement (II) is false.
d) Statement (I) is false but statement (II) is true.

46. Hydration of which compound is responsible for an increase in the strength of cement in later age?

a) Tri-calcium aluminate

b) Tetra-calcium alumina ferrite

c) Tri-calcium silicate

d) Di-calcium silicate

47. Statement (I): Finer grinding of cement results in early development of strength.

Statement (II): Finer the cement, higher is the rate of hydration.

a) Both statement (I) and statement (II) are individually true and statement (II) is the correct explanation of statement (I).

b) Both statement (I) and statement (II) are individually true and statement (II) is not the correct explanation of statement (I).

c) Statement (I) is true but statement (II) is false.

d) Statement (I) is false but statement (II) is true.

48. Statement (I): Pozzolana is added to cement to increase early strength.

Statement (II): It reduces the heat of hydration.

a) Both statement (I) and statement (II) are individually true and statement (II) is the correct explanation of statement (I).

b) Both statement (I) and statement (II) are individually true and statement (II) is not the correct explanation of statement (I).

c) Statement (I) is true but statement (II) is false.

d) Statement (I) is false but statement (II) is true.

49. Compound of cement which reacts immediately with water and sets first is
a) Tri-calcium silicate
b) Tri-calcium aluminate
c) Di-calcium silicate
d) All of the above

50. Specific gravity of OPC is generally
a) 4.92
b) 3.15
c) 2.10
d) 1.75

51. The main ingredients of Portland cement are

a) Lime and silica

b) Lime and alumina

c) Silica and alumina

d) All the above

52. In ordinary Portland cement, the first one to react with water is:
a) C_3A
b) C_2S
c) C_3S
d) C_4AF

53. Out of the constituents of cement, namely, tri-calcium silicate (C_3S), di-calcium silicate (C_2S), tri-calcium aluminate (C_3A) and tetra-calcium aluminoferrite (C_4AF), the first one to set and harden is

a) C_3A

b) C_4AF

c) C_3S

d) C_2S

54. Which of the following Bogue's compounds of cement liberates maximum heat of hydration ?

a) C_3S

b) C_4AF

c) C_3A

d) C_2S

55. The most important constituents of cement are
a) C_3A and C_2S
b) C_3S and C_3A
c) C_3S and C_2S
d) C_3A and C_4AF

56. The development of strength of cement and its fineness are

a) Directly proportional

b) Inversely proportional

c) Not related

d) Randomly related

57. Hardening of cement occurs at a

a) Rapid rate during the first few days and afterwards it continues to increase at a decreased rate

b) Slow rate during the first few days and afterwards it continues to increase at a rapid rate

c) Uniform rate throughout its age

d) None of these

58. To obtain cement dry powder, limestones and shales or their slurry is burnt in a rotary kiln at a temperature between

a) 1100°C and 1200°C
b) 1200°C and 1300°C
c) 1300°C and 1400°C
d) 1400°C and 1500°C

59. The cementing property of cement is mainly due to

a) Lime
b) Alumina
c) Silica
d) Gypsum

60. When water is added to cement

a) Heat is generated

b) Heat is absorbed

c) Chemical reaction is initiated

d) Both heat is generated and chemical reaction is initiated

61. Efflorescence in cement is caused due to an excess of

a) Alumina

b) Iron oxide

c) Silica

d) Alkalis

62. Pick up the correct statement from the following.

a) Lime in excess causes the cement to expand and disintegrate.

b) Silica in excess causes the cement to set slowly.

c) Alumina in excess reduces the strength of the cement.

d) All options are correct.

63. Which of the following is an important factor that affects the shrinkage of cement concrete ?

a) Quantity of cement
b) Size of coarse aggregate
c) Size of fine aggregate
d) Amount of water added during mixing of concrete

64. Which of the following shows the correct decreasing order of rate of hydration of Portland cement compounds?

a) $C_3A>C_4AF>C_3S>C_2S$

b) $C_3A>C_4AF>C_2S>C_3S$

c) $C_3A>C_3S>C_2S>C_4AF$

d) $C_4AF>C_3A>C_3S>C_2S$

65. Increase in fineness of cement

a) Reduces the rate of strength development and leads to higher shrinkage

b) Increases the rate of strength development and reduces the rate of deterioration

c) Decreases the rate of strength development and increase the bleeding of cement

d) Increases the rate of strength development and leads to higher shrinkage

66. In optical microscopy of cement, large crystals are …… and small rounded crystals are ……., respectively.

a) C_3S and C_2S
b) C_3A and C_2S
c) C_3A and C_3S
d) C_3A and C_2AF

Examination Questions on Hydration and Structuring of Cement Pastes

1. What are the consequences of the following phenomena:

a- Excess sulfates in cement or mixing water.

b- Wet curing of concrete at an early age.

c- The concentration of Ca^{2+} and OH^- ions in the interstitial solution becomes significant.
d- the simultaneous existence of sufficient quantities of C_3A and the absence of gypsum in the cement composition

2. Complete the following table

Composition	Chemical formula
.....	$3CaO.Al_2O_3.3CaSO_4.32H_2O$
Gypsum	.....
Tricalcium aluminate	.....
.....	$3CaO.2SiO_2.3H_2O$
Monosulfoaluminate	.....

3. Compare the heat of hydration released by C_3S and C_3A.

4. Give the geometric shape on a micrometer scale (morphology) of the following hydration products:

- *Éttringite*.....

- *portlandite*.....

- tobermorite gel *(CSH)*.....

- *monosulfoaluminate* .....

5. What is interlayer water?

6. Complete the following equations:

$2(CaO.SiO_2) + 4H_2O \longrightarrow$ ..... + $Ca(OH)_2$

$C_3A.3CaSO_4.32H_2O + 2C_3A + 4H_2O \longrightarrow$ .....

In what case does the chemical reaction in equation 2 take place?

7.What do the following abbreviations represent in cement technology? C- A- S- F.

8- a. What oxides make up anhydrous cement?

b. In which rocks can these oxides be found?

9- a. Clinker is generally composed of four minerals. Which ones?

b. Give the chemical formula of each constituent mineral.

10- a. List the components of the microstructure of concrete.

11- Hydration of C_3A causes rapid setting.

a. What material can be added to regulate setting or slow down this hydration?

b. Give the name of the hydration product resulting from the reaction of this material with C_3A.

c. If this material is consumed before all the C_3A has hydrated, what hydration product is formed in this case? Justify your answer.

12- What parameters can influence the strength of the interfacial transition zone and the presence of microcracks?

13- The hydration of Portland cement is affected by a number of factors. Which ones?

14- What types of voids are present in hydrated cement paste? What are their typical dimensions?

15- Why is it desirable to distinguish between free water in large capillary pores and water retained in small capillary pores (between C-S-H sheets)?

16- List the different components of hydrated cement paste.

17- Give this graph a title and explain its content.

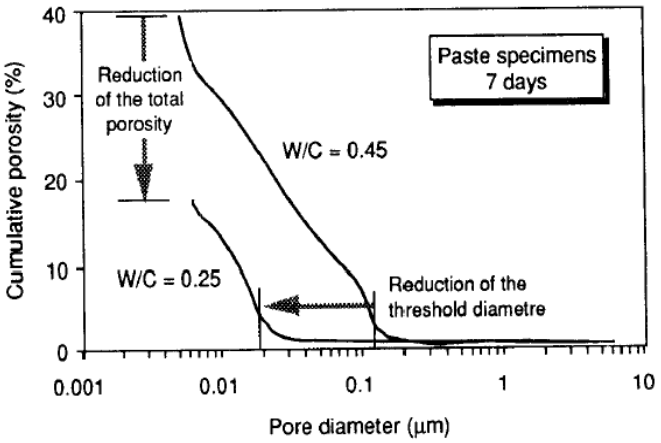

18 . The complexity of cement hydration does not come from the complexity of the elementary processes themselves, but from the complexity of the cement paste. Explain?

19. What does the following abbreviations indicate: C, A, S and H. What is the natural source of each of them?

20. What are the types of voids that are present in hydrated cement paste? What are their typical dimensions?

Discuss the influence of W/C on hair porosity?

21. How many types of water are associated with saturated cement paste? Why is it desirable to distinguish between free water in large capillary pores and water held in small capillary pores (between C-S-H sheets)?

22. Cite the different components of hydrated cement paste.

23. Give the chemical equation that describes the reaction of C_3A with Gypsum. If the gypsum is consumed before all the C_3A has hydrated. What hydration product formed in this case. justify.

24. Abrams established a rule that relates the water-cement ratio to strength of concrete. List two additional factors that have a significant influence on the concrete strength.

25. Explain how water-cement ratio influences the strength of the cement paste matrix and the interfacial transition zone in concrete.

26. Why does air entrainment reduce the strength of moderate- and high-strength concrete mixtures but may increase the strength of low-strength concrete mixtures?

27. In regard to concrete strength, discuss the two opposing effects that are caused by an increase in the maximum size of aggregate in a concrete mixture.

28. At a given water-cement ratio, either a change in the cement content or aggregate grading can be made to increase the consistency of a concrete mixture. Which one of the two options would you recommend? Why is it not desirable to produce concrete mixtures of a higher consistency than necessary?

29. Can we use recycled water from industrial operations as mixing water in concrete? What about the use of seawater for this purpose?

30. What do you understand by the term *curing of concrete*? What is the significance of curing?

31. From the standpoint of concrete strength, which of the two options is undesirable, and why?
(*a*) Concrete cast at 5°C and cured at 21°C.
(b) Concrete cast at 21°C and cured at 5°C.

32. Many factors have an influence on the compressive strength of concrete. Briefly explain which one of the two options listed below will result in higher strength at 28 days:
(*a*) Water-cement ratio of 0.5 vs. 0.4.
(*b*) Moist curing temperature of 25°C vs. 10°C.
(*c*) Using test cylinder of size 150 by 300 mm vs. 75 by 150 mm.
(*d*) Using a compression test loading rate of 3 MPa/s vs. 0.3 MPa/s.
(*e*) Testing the specimens in a saturated condition vs. air-dry condition.

33. The temperature during the placement of concrete is known to have an effect on later age strength. What would be the effect on the 6-month strength when a concrete mixture is placed at (a) 10°C and (b) 35°C.

34. In general, how are the compressive and tensile strengths of concrete related? Is this relationship independent of concrete strength? If not, why? Discuss how admixtures and aggregate mineralogy can affect the relationship.

Bibliographical References

1. Baroghel-Bouny, V. (1994). *Characterization of cement pastes and concretes* (Doctoral dissertation). Laboratoire Central des Ponts et Chaussées, Paris, France, pp. 69–134. Feldman, R. F., Sereda, P. J. (1970). A study of cement paste and concrete. *Engineering Journal (Canada)*, 53(8/9).
2. Mehta, P. K., Manmohan, D. (1980). Properties of cement and concrete. In *Proceedings of the Seventh International Congress on Cement Chemistry* (Vol. III). Paris: Editions Septima.
3. Mindess, S., Young, J. F. (1981). *Concrete*. Englewood Cliffs, NJ: Prentice-Hall.
4. Tazawa, E., Miyazawa, S., & Kasai, T. (1995). Chemical shrinkage and autogenous shrinkage of hydrating cement paste. *Cement and Concrete Research*, 25(2), 288–292.
5. Yssorche, M. P. (1995). *Microfissuring and durability of high-performance concrete* (Doctoral dissertation). National Institute of Applied Sciences, France.
6. Struble, L., Livesey, P., del Strother, P., & Bye, G. C. (2011). Portland Cement: Composition, Production and Properties (3rd ed.). Structures and Buildings Series. ICE Publishing. https://doi.org/10.1680/pc.36116.
7. Martirena-Hernandez, J. F., Alujas-Díaz, A., & Amador-Hernandez, M. (Eds.). (2020). Proceedings of the International Conference of Sustainable Production and Use of Cement and Concrete: ICSPCC 2019 (RILEM Bookseries, Vol. 22). Springer. https://doi.org/10.1007/978-3-030-22034-1
8. Bahurudeen, A., & Moorthi, P. V. P. (2021). Testing of construction materials (1st ed.). CRC Press. https://doi.org/10.1201/9781003124825
9. Campbell, D. H. (1999). Microscopical Examination and Interpretation of Portland Cement and Clinker (2nd ed.). Skokie, IL: Portland Cement Association.
10. Hewlett, P. C., & Liska, M. (Eds.). (2019). Lea's Chemistry of Cement and Concrete (5th ed.). Butterworth-Heinemann. https://doi.org/10.1016/C2016-0-01384-0
11. Shetty, M. S. (2005). Concrete Technology: Theory and Practice (5th ed.). New Delhi, India: S. Chand & Company.
12. Chen, X.-T. (2009). Effet du chauffage sur le comportement mécanique et poro-mécanique de matériaux cimentaires : propriétés hydrauliques et changements morphologiques [Thèse de doctorat, École Centrale de Lille]. https://theses.hal.science/tel-00577102
13. Chatterjee, A. K. (2018). Cement production technology: Principles and practice (1st ed.). CRC Press.
14. Roosz, C. (2016). Propriétés thermodynamiques des phases cimentaires hydratées : C-S-H, C-A-S-H et M-S-H [Thèse de doctorat, Terre solide et enveloppes superficielles]. Université de Poitiers. https://theses.fr/2016POIT2352
15. Kurdowski, W. (2014). Cement and concrete chemistry (1st ed.). Springer. https://doi.org/10.1007/978-94-007-7945-7
16. Tokyay, M. (2016). Cement and concrete mineral admixtures (1st ed.). CRC Press. https://doi.org/10.1201/b20046

17. Dhir, R. K. (Ed.). (1994). Euro-Cements: Impact of ENV 197 on concrete construction. E & FN Spon.
18. Barnes, P., & Bensted, J. (Eds.). (2002). Structure and performance of cements (2nd ed.). Spon Press. https://doi.org/10.4324/9780203477786
19. Edison, M. P. (Ed.). (2008). Natural cement (ASTM Special Technical Publication, STP 1494). ASTM International. https://doi.org/10.1520/STP1494-EB
20. Newman, J., & Choo, B. S. (Eds.). (2003). Advanced concrete technology (1st ed.). Butterworth-Heinemann. https://doi.org/10.1016/B978-0-7506-5103-5.X5000-1
21. Soroka, I. (1979). Portland cement paste and concrete (1st ed.). Macmillan Press.
22. Taylor, H. F. W. (1997). Cement chemistry (2nd ed.). Thomas Telford Publishing. https://doi.org/10.1680/cc.25929
23. Chaube, R. P., Maekawa, K., & Kishi, T. (2007). Modelling of concrete performance: Hydration, microstructure and mass transport (1st ed.). CRC Press.
24. Labahn, O., & Kohlhaas, B. (1983). Cement engineers' handbook (4th ed.). Bauverlag GmbH.
25. Mehta, P. K., & Monteiro, P. J. M. (2014). Concrete: Microstructure, properties, and materials (4th ed.). McGraw-Hill Education.
26. Forde, M. C. (Ed.). (2009). ICE manual of construction materials (Vols. 1–2). Thomas Telford Publishing. doi: 10.1680/mocm.35973.0001. ISBN: 978-0-7277-3597-3. 928p.
27. Anwar, U.-H. (2018). A beginners' guide to scanning electron microscopy (1st ed.). Cham. Switzerland: Springer Nature.
28. Deschner, F., Winnefeld, F., Lothenbach, B., Seufert, S., Schwesig, P., Dittrich, S., … Neubauer, J. (2012). Hydration of a Portland cement with high replacement by siliceous fly ash. Cement and Concrete Research, 42, 1389–1400.
29. Hudson-Lamb, D. L., Strydom, C. A., & Potgieter, J. H. (1996). The thermal dehydration of natural gypsum and pure calcium sulphate dihydrate (gypsum). Thermochimica Acta, 282–283, 483–492.
30. Khoshnazar, R., Beaudoin, J. J., Raki, L., & Alizadeh, R. (2013a). Solvent exchange in sulfoaluminate phases; Part II: Monosulfate. Advances in Cement Research, 25, 322–331.
31. Khoshnazar, R., Beaudoin, J. J., Raki, L., & Alizadeh, R. (2013b). Solvent exchange in sulphoaluminate phases; Part I: Ettringite. Advances in Cement Research, 25, 314–321.
32. Lothenbach, B., Durdziński, P., & Weerdt, K. De. (2016). Thermogravimetric analysis. In K. Scrivener, R. Snellings, & B. Lothenbach (Eds.), A practical guide to microstructural analysis of cementitious materials (1st ed., pp. 177–212). Boca Raton, FL: Taylor & Francis.
33. Montes-Morán, M. A., Concheso, A., Canals-Batlle, C., Aguirre, N. V., Ania, C. O., Martín, M. J., & Masaguer, V. (2012). Linz–Donawitz steel slag for the removal of hydrogen sulfide at room temperature. Environmental Science & Technology, 46, 8992–8997.
34. Paulik, F., Paulik, J., & Arnold, M. (1992). Thermal decomposition of gypsum. Thermochimica Acta, 200, 195–204.

35. Schöler, A., Lothenbach, B., Winnefeld, F., & Zajac, M. (2015). Hydrate formation in quaternary Portland cement blends containing blast-furnace slag, siliceous fly ash and limestone powder. Cement and Concrete Composites, 55, 374–382.
36. Snellings, R. (2016). X-ray powder diffraction applied to cement. In K. Scrivener, R. Snellings, & B. Lothenbach (Eds.), A practical guide to microstructural analysis of cementitious materials (1st ed., pp. 107–162). Boca Raton, FL: Taylor & Francis.
37. Suryanarayana, C., & Norton, M. G. (1998). X-ray diffraction a practical approach (1st ed.). New York: Plenum Publishing Corporation.
38. William, J. C. (2006). Under the microscope a brief history of microscopy (1st ed.). Singapore: World Scientific Publishing. Pte. Ltd.
39. Zhang, J., & Scherer, G. W. (2011). Comparison of methods for arresting hydration of cement. Cement and Concrete Research, 41, 1024–1036